

DIGITAL INSTRUMENTATION FOR THE TIME

INTEGRAL-SQUARED OF A VOLTAGE

DIGITAL INSTRUMENTATION FOR THE TIME
INTEGRAL-SQUARED OF A VOLTAGE
AND
ITS ERROR CHARACTERISTICS.

BY
JAYANTILAL MAJITHIA

A Thesis
Submitted to the Faculty of Graduate Studies
in Partial Fulfilment of the Requirements
for the Degree
Master of Engineering

McMaster University

May, 1968

MASTER OF ENGINEERING (1968)
(Electrical Engineering)

McMASTER UNIVERSITY
Hamilton, Ontario.

TITLE: Digital instrumentation for the time integral-squared of a voltage and its error characteristics.

AUTHOR: Jayantilal Majithia. B.Sc. (London University).

SUPERVISOR: Professor R. Kitai

NUMBER OF PAGES: xi, 108

SCOPE AND CONTENTS: A 16-level instrument in which the input voltage is sampled and quantised to yield direct decimal readouts of $\frac{1}{T} \int_0^T v^2 dt$ and T is described. This is an improved version of an instrument previously constructed.² The upper frequency limit has been extended from 5 Hz to about 2 kHz. The readout of the instrument can be in any code, the decimal code being implemented in the instrument described. The original error analysis has been extended. An extensive analysis of the overall error characteristics was carried out theoretically and the results were confirmed experimentally. The instrument is capable of measuring the mean square value of periodic waveform to within 2%. Normal distribution noise of standard deviation between 1V and 3V can be measured with similar accuracy. The accuracy and the upper frequency limit are determined by the 'aperture time' of the sampling process. The errors arising in the sampling instrument depend on the number of levels used.

ACKNOWLEDGMENTS

I wish to thank Professor R. Kitai for his constant encouragement and assistance during the course of this work and also in the preparation of this thesis.

I would also like to express my appreciation of a number of useful discussions and suggestions from Dr. A. S. Gladwin and Dr. S. Chisholm.

The financial assistance provided by the Department of Electrical Engineering is gratefully acknowledged.

Also finally I would like to thank my wife Raj Majithia for typing this thesis.

TABLE OF CONTENTS.

		PAGE
1.	Introduction.	1
2.	Design of a 16-level Instrument.	5
	The equation for the mean square value	5
	The weighted input method to obtain $\sum_{r=1}^{n+1} C_r$	8
	Essential requirements of the instrument	11
	Instrument realisation	12
	Performance Tests	24
3.	Theoretical Error Analysis.	27
	The Error Equation	28
	Error due to quantisation	29
	Error due to finite sampling Rate	32
	Error due to level inaccuracies	36
	Error due to sampling a non-integral number of periodic waves	38
	Error due to finite time of measurement on white noise	41
	The overall error analysis	42
	Effect of finite Aperture time	43
4.	Theoretical Error Analysis for the 16-level Instrument.	45
	Error e_n due to quantisation	45
	Error e_p due to finite sampling rate	48
	Error e_x^p due to a non-integral number of cycles being sampled	54
	Error e_l due to level inaccuracies	60
	The error e_T for normal distribution noise	61
	The overall error analysis	61
5.	Experimental Analysis.	68
	Measurement of error e_n	70
	Measurement of error e_p	71
	Overall error measurements	73
	Amplitude probability distribution	75
6.	Discussion.	85

7.	Appendix.	88
	Details of the D.E.C. Modules	88
	Formulation of error equations	90
	Fortran IV programs	97
	Numerical Convolution	104
	Apparatus	107
	Bibliography	108

LIST OF ILLUSTRATIONS.

<u>FIGURE NO.</u>	<u>TITLE</u>	<u>PAGE</u>
1.	Voltage waveform with Quantising Levels.	7
1a.	Weighted - feed binary counter.	10
2.	Block diagram of a 16-level Instrument.	11a
3.	Rectifier.	13
4.	Level Determination Circuit.	15
5.	Counter Input Logic.	19
6.	Timing pulse generator.	21
7.	Control Circuit.	22
8.	Normal Wave.	30
9.	Input waveform with peak at $(m-1+\epsilon)$	30
10.	Sampling at r^{th} and $(r+1)^{\text{th}}$ levels.	33
11.	Level offset error at r^{th} level.	39
12.	Sampling of a non-integral number of cycles.	39
14.	Triangular Wave Input: Error e_n for a partially filled 16^{-n} level.	46
15.	Triangular Wave Input: Probability dis- tribution of error e_n .	46
16.	Sine Wave Input: Error for a partially filled 16-level.	47
17.	Sine Wave Input: Probability distribution of error e_n .	47
18.	Error e_n for normal distribution noise.	49
19.	Frequency Histogram of e_n : Sine Wave Input peak between 8^{th} - 16^{th} levels.	50

20.	Frequency Histogram of e_n : Sine Wave Input peak between 12^{th} - 16^{th} levels.	51
21.	Frequency Histogram of e_n : Triangular Wave Input peak between 8^{th} - 16^{th} levels.	52
22.	Frequency Histogram of e_n : Triangular Wave Input peak between 12^{th} - 16^{th} levels.	53
23.	Probability distribution of $(e_p \text{ p/f})$: Sine Wave Input.	55
24.	Probability distribution of $(e_p \text{ p/f})$: Triangular Wave Input.	56
25.	Error e_p for normal distribution noise.	57
26.	Probability distribution of e_α : Sine Wave.	58
27.	Probability distribution of e_α : Triangular Wave.	59
28.	Probability distribution of $(e_n + e_p)$: Sine Wave Input.	63
29.	Probability distribution of $(e_n + e_p)$: Triangular Wave Input.	64
30.	Probability distribution of $(e_n + e_p + e_\alpha)$: Sine Wave.	65
31.	Probability distribution of $(e_n + e_p + e_\alpha)$: Triangular Wave.	66
32.	Level offsets for the 16^{th} level Instrument.	69
33.	Measured Error e_n for Sine Wave Inputs.	72
34.	Variation of e_n about a $e_n=0$ point.	72a
35.	Measured Frequency Histogram of $(e_n + e_p + e_\alpha)$: Sine Wave Input peak between 8^{th} - 16^{th} levels.	76
36.	Measured Frequency Histogram of $(e_n + e_p + e_\alpha)$: Sine Wave Input peak between 12^{th} - 16^{th} levels.	77

37.	Measured Frequency Histogram of $(e_n + e_p + e_\alpha)$: Sine Wave Input peak between 15 th - 16 th levels.	78
38.	Measured Frequency Histogram of $(e_n + e_p + e_\alpha)$: Triangular Input peak between 8 th - 16 th levels.	79
39.	Measured Frequency Histogram of $(e_n + e_p + e_\alpha)$: Triangular Input peak between 12 th - 16 th levels.	80
40.	Measured Frequency Histogram of $(e_n + e_p + e_\alpha)$: Triangular Input peak between 15 th - 16 th levels.	81
41.	The total error results for normal distri- bution noise.	82
42.	Circuit for error measurements: Periodic Waves.	83
43.	Circuit for error measurements: Noise Input.	83

LIST OF TABLES.

<u>TABLE NO.</u>		<u>PAGE.</u>
1.	Weighted Inputs.	9
11.	Weighted Inputs and Veitch-Karnaugh Maps.	17
111.	Direct decimal readouts.	26
1V	Sine Wave Amplitude Probability distribution	84
V	Summary of error characteristics.	87

LIST OF SYMBOLS

- s^2 = Variance of a set of observations.
 n = Number of intervals into which samples are grouped.
 V^2 = Mean square value of a input signal.
 V_{mr} = Mid-interval voltage of the r^{th} interval.
 C_{r1} = Number of samples within the r^{th} interval.
 C_0 = Total number of samples collected.
 t_r = Time the voltage waveform spends above the r^{th} level.
 T = Total time of the sampling process.
 b = The sampling rate.
 f = Frequency of the input signal.
 P_r = Probability that the voltage exceeds r^{th} level.
 G_k = Logic expression for the k^{th} gate, $k= 1\text{-----}7$.
 e_1 = Error in the r.m.s. reading due to any one source.
 e_1^* = Error in the mean square value due to any one source.
 e_n = Quantisation error.
 e_p = Error due to finite sampling rate.
 Z_r = Expected number of crossings of the r^{th} level for white noise.
 e_l = Error due to level inaccuracies.
 V_{r1} = Slope of the input waveform at the r^{th} level.
 σ_{Er} = Level inaccuracy at the r^{th} level.
 e_x = Error due to sampling a non-integral number of cycles of
the periodic wave.
 σ = R.m.s. value of white noise.

σ_t = R.m.s. value of white noise measured over a finite time t .

ψ = Error in the measurement of σ

$\Phi(\tau)$ = Autocorrelation function of white noise.

$p(F_i)$ = Probability of F_i .

μ_a = Aperture time.

CHAPTER 1

INTRODUCTION

Conventional methods for measurement of mean square value (and hence the r.m.s. value) of very low frequency waveforms involve use of analogue devices such as a thermocouple and a potentiometer. These methods are tedious in practice and need great care as thermocouples have very limited overload capacity. This thesis describes an instrument, for measuring the mean square value, which is particularly suited to slowly fluctuating voltages whose frequency components do not exceed about 2kHz. The overall errors are within 1% (in r.m.s. value) for the number of quantisation levels used in the process.

The principles of the instrument depend on the basic definition of the variance of a set of data. Thus if X_1, X_2, \dots, X_n denote the set of numerical values of n observations selected from a larger set, then the variance s^2 of the sample of size n is defined as

$$s^2 = \frac{\sum_{i=1}^n (X_i - \bar{X})^2}{n} \quad \text{-----(1)}$$

where \bar{X} is the mean value and when n is large.

If the data are grouped then

$$s^2 = \frac{\sum_{i=1}^n f_i (X_{im} - \bar{X})^2}{n} \quad \text{-----(2)}$$

where f is the frequency and X_{im} is the midinterval value of the i^{th} class.

For a voltage waveform in which samples are classed into intervals, there being n intervals on either side of the mean voltage, the equation (2) for variance (or mean square value V_n^2) becomes

$$V_n^2 = \frac{\sum_{r=1}^n C_{ri} V_{mr}^2}{C_o} \quad \text{-----(3)}$$

where C_{ri} is the number of samples within the r^{th} interval,
 V_{mr} is the midinterval voltage of the r^{th} interval, and
 C_o is the total number of samples collected.

In the instrument described here, the sampling is automatic and the data is processed by digital means to realise the equation (3).

The design is based upon the principles derived in a previous publication in this area¹. Some features of the 16 level instrument constructed are as follows:

1. At the end of the time T both the mean square value and T are immediately available in digital form.
2. The amplitude probability of the input waveform can be readily obtained.
3. There are no low frequency limitations.
4. Although the output readouts are decimal, the code can be changed by changing the counting registers. The entire logic section remains unaltered.
5. The voltage under measurement is sampled systematically and the sampled data are used in the computation of the mean square value. Hence the input voltage is not required to supply any significant energy to the instrument.

For periodic waveforms, only one cycle of the input is

required, to yield the results. Alternatively, for random inputs, measurements may commence on a start signal and proceed for a programmed time.

A substantial part of the thesis is devoted to the investigation of the various errors which occur in the process used in the instrument. The overall error characteristics are analysed theoretically and verified experimentally.

The 16-level instrument described here is an improved version of a binary readout type described in Reference 2. Chapter 2 deals with the theoretical aspect of the process and also includes the complete circuit description of the instrument. The original instrument had an upper frequency limit of 5 Hz. By using FET gates in the rectifier this was extended to about 2 kHz. Furthermore, this binary readout was replaced by decimal readout, details of which are given in Chapter 2.

Chapter 3 and 4 deal with the theoretical error analysis of the sampling process used. The overall error characteristics for the 16 level instrument are evaluated for two modes of operation viz:

1. "One cycle mode" in which the instrument samples one cycle of the input signal,
2. "Self timed mode" in which sampling is started manually and stopped after a fixed time T .

Chapter 5 deals with the experimental determination of the overall errors. Results obtained show good agreement with theoretical results. The experimental data are presented in form of histograms.

The error characteristics and some limitations of the instrument are discussed in Chapter 6.

Fortran programs to evaluate the quantisation error e_n for various waveforms are given in the appendix C.

CHAPTER 2

DESIGN OF A 16-LEVEL INSTRUMENT

In a paper "Digital Transfer Voltmeters: Principles and Error Characteristics" M/S Deist & Kitai investigated the measurement of the mean square value of a fluctuating voltage using sampling techniques. Although the actual system described here differs from that suggested in this paper, the mathematical formulation remains unaltered. This section considers the construction of a 16-level instrument in which the mean-square value of the fluctuating voltage is obtained at the end of a time.

2.1. The equation for the mean square value.

Fig. 1. shows a voltage waveform divided into n quantisation levels, of equal intervals, on both sides of the zero level.

If V_{mr} is the midinterval voltage and t_r is the time, the waveform spends above the positive and negative r^{th} level, then the integral square (IS) value of v is given by

$$\begin{aligned} IS &= \int_0^T v^2 dt \\ &\doteq \sum_{r=0}^{n-1} (t_r - t_{r+1}) V_{mr}^2 \end{aligned} \quad \text{-----(1)}$$

assuming that the n^{th} level is not exceeded .

If voltage at the n^{th} level is taken as unity then the mid-interval values will be

$$\begin{aligned} V_{m0} &= \frac{1}{2n} \\ V_{m1} &= \frac{3}{2n} \quad \text{etc. with } V_{m,n-1} = \frac{2n-1}{2n}. \end{aligned}$$

Note also that $t_0 = T$.

$$\therefore IS = (T - t_1)\left(\frac{1}{2n}\right)^2 + (t_1 - t_2)\left(\frac{3}{2n}\right)^2 + \dots + (t_r - t_{r+1})\left(\frac{2r+1}{2n}\right)^2 + \dots + (t_{n-1} - t_n)\left(\frac{2n-1}{2n}\right)^2$$

Grouping terms in t_r yields,

$$IS = \frac{T}{4n^2} + \frac{2}{n^2} \sum_{r=1}^{n-1} r t_r$$

The mean square value of v is given by

$$V^2 = \frac{1}{T} \int_0^T v^2 dt$$

$$\therefore V^2 = \frac{1}{4n^2} + \frac{2}{n^2 T} \sum_{r=1}^{n-1} r t_r \quad \text{-----(2)}$$

Now if the voltage is sampled systematically at time intervals $\tau = \frac{1}{p}$ then

$$T = \frac{C_0}{p} \quad \text{where } C_0 \text{ is the total number of samples collected.}$$

And $t_r = \frac{C_r}{p}$ where C_r is the number of samples collected in t_r .

The mean square value of v sampled systematically is given by,

$$V^2 = \frac{1}{4n^2} + \frac{2}{n^2 C_0} \sum_{r=1}^{n-1} r C_r \quad \text{-----(3)}$$

In practice the term $\frac{1}{4n^2}$ is small compared to $\sum_{r=1}^{n-1} r C_r$ assuming that most of the available levels are utilised and may be neglected,

$$\therefore V^2 = \frac{2}{n^2 C_0} \sum_{r=1}^{n-1} r C_r \quad \text{-----(4)}$$

As C_0 is increased, $\frac{C_r}{C_0} \rightarrow p_r$ the probability that the voltage exceeds the r^{th} level and $V^2 \rightarrow \frac{2}{n^2} \sum_{r=1}^{n-1} r \cdot p_r$

The errors arising due to the approximations made here, are treated in Chapter 3.

The 16-level instrument described here provides two results viz.

$$C_0 \text{ and } \sum_{r=1}^{n-1} r C_r$$

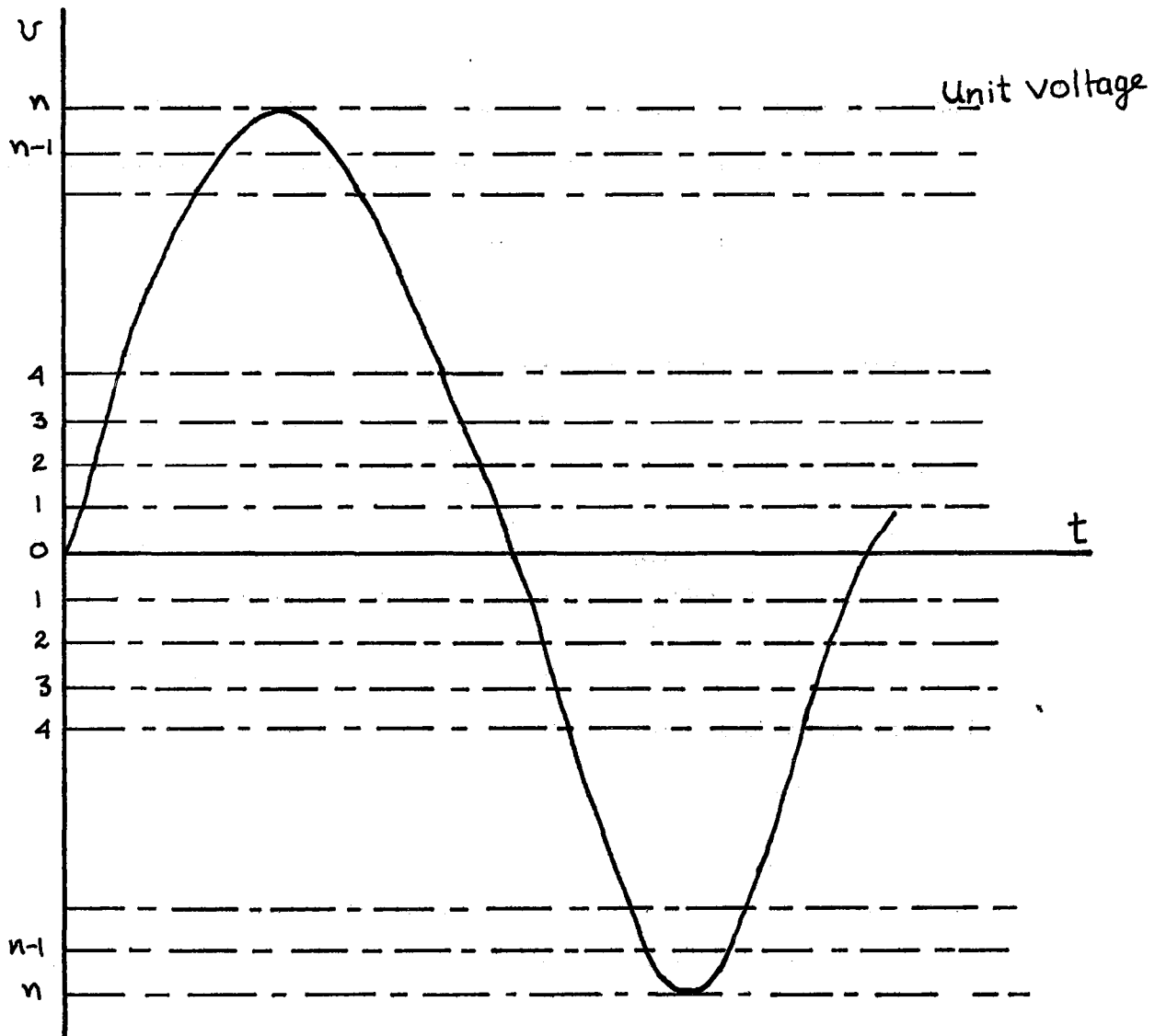


Fig.1. Voltage waveform with Quantising Levels.

2.2 The weighted input method to obtain $\sum_{r=1}^{n-1} r.C_r$.

Consider the term $\sum_{r=1}^{n-1} r.C_r$

The voltage waveform is sampled uniformly. If a sample occurs while the waveform is above the r^{th} level then the sample pulse contributes to C_1 , C_2 --- C_r and also to C_0 . The contribution to $\sum_{r=1}^{n-1} r.C_r$ due to this sample is $\sum_{q=1}^r q$. This quantity is termed the weighting factor for the r^{th} level. Table 1 gives the weighting factors required for a 16-level instrument, in both decimal and binary code.

Thus it can be seen that $\sum_{r=1}^{n-1} r.C_r$ can be realised by determining the highest level exceeded at the sampling instant and adding the corresponding binary weighted input for that level to $\sum_{r=1}^{n-1} r.C_r$ register.

A very simple and economical method to achieve these weightings is to use multiple trigger addition. Fig. 1(a) shows a block diagram of the system to perform this addition for a 16-level instrument. The circuit acts as a binary counter via trigger pulses $\propto \frac{1}{T}$. In addition there are feeds to individual binaries from the gates G1 - G7. These gates are controlled by a logic system, the design of which is described in Section 2. If the voltage v lies above, say, the 6^{th} level then the required addition for this level is 21 or binary 10101. This addition is achieved simply by applying one pulse via G5 to binary B16, a second pulse to B4 and a third to B1 causing the states of these binaries to be complemented. The weighted feeds are applied serially in time, with the most significant bit to be added, being operated first. This is to allow the effects of an addition to propagate along the binaries without interfering with subsequent additions.

T A B L E. I.

Highest level Exceeded	Weighted Input	
	Decimal	Binary
0	0	0
1	1	1
2	3	11
3	6	110
4	10	1010
5	15	1111
6	21	10101
7	28	11100
8	36	100100
9	45	101101
10	55	110111
11	66	1010010
12	78	1001110
13	91	1011011
14	102	1101001
15	120	1111000
16	Never	exceeded

Weighted Inputs.

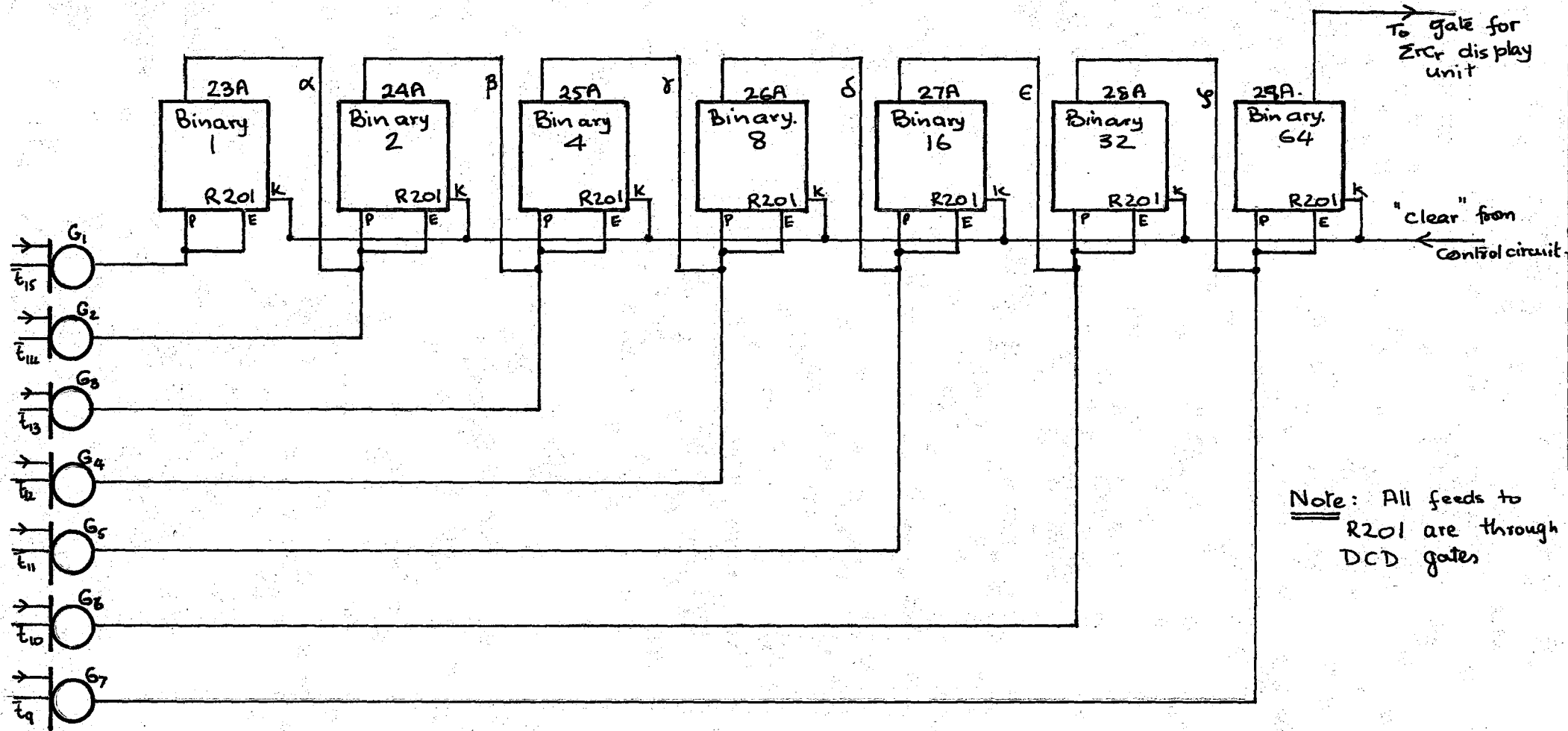


Fig: (a): Weighted-feed binary Counter.

It now remains for division by n^2 to be accomplished. For a 16-level instrument $\frac{2}{n^2} = \frac{1}{128} = \frac{1}{2^7}$. The output of the seventh binary is in fact already the input divided by 2^7 . If a large enough number of samples is collected then the readout of the binaries which provide fractional values of IS will be very small and will not be usually required. A suitable choice of the sampling rate would ensure this. On the basis that the weighted feed method is to be used, the essential requirements of the instrument can be established.

2.3 Essential requirements of the instrument.

Fig. 2 shows a block diagram to illustrate the basic requirements.

These are as follows.

- (a) Since input polarity is an unrequired information, rectification is used so that quantising is in 16-levels on one side only instead of both sides of the zero level.
- (b) A control circuit which allows measurements over one cycle of the input precisely or over an externally fixed period of time.
- (c) A level determination circuit and logic circuits to enable $\sum_{r=1}^{n-1} r C_r$ to be obtained.
- (d) A timing pulse generator for use in (c) and for the base count C_0 .
- (e) Display registers to indicate $\sum_{r=1}^{n-1} r C_r$ (or $\sum_{r=1}^{n-1} r t_r$) and C_0 (i.e T)

Apart from the display registers and an external clock, the entire system is constructed using discrete modules (D.E.C. Ltd). Details of these modules are given in the Appendix A. For the sample-rate clock and C_0 readout counter, a complete timer unit is used consisting of a 100 kHz crystal clock with decimal countdown to 0.1 sec. and a 6 decimal

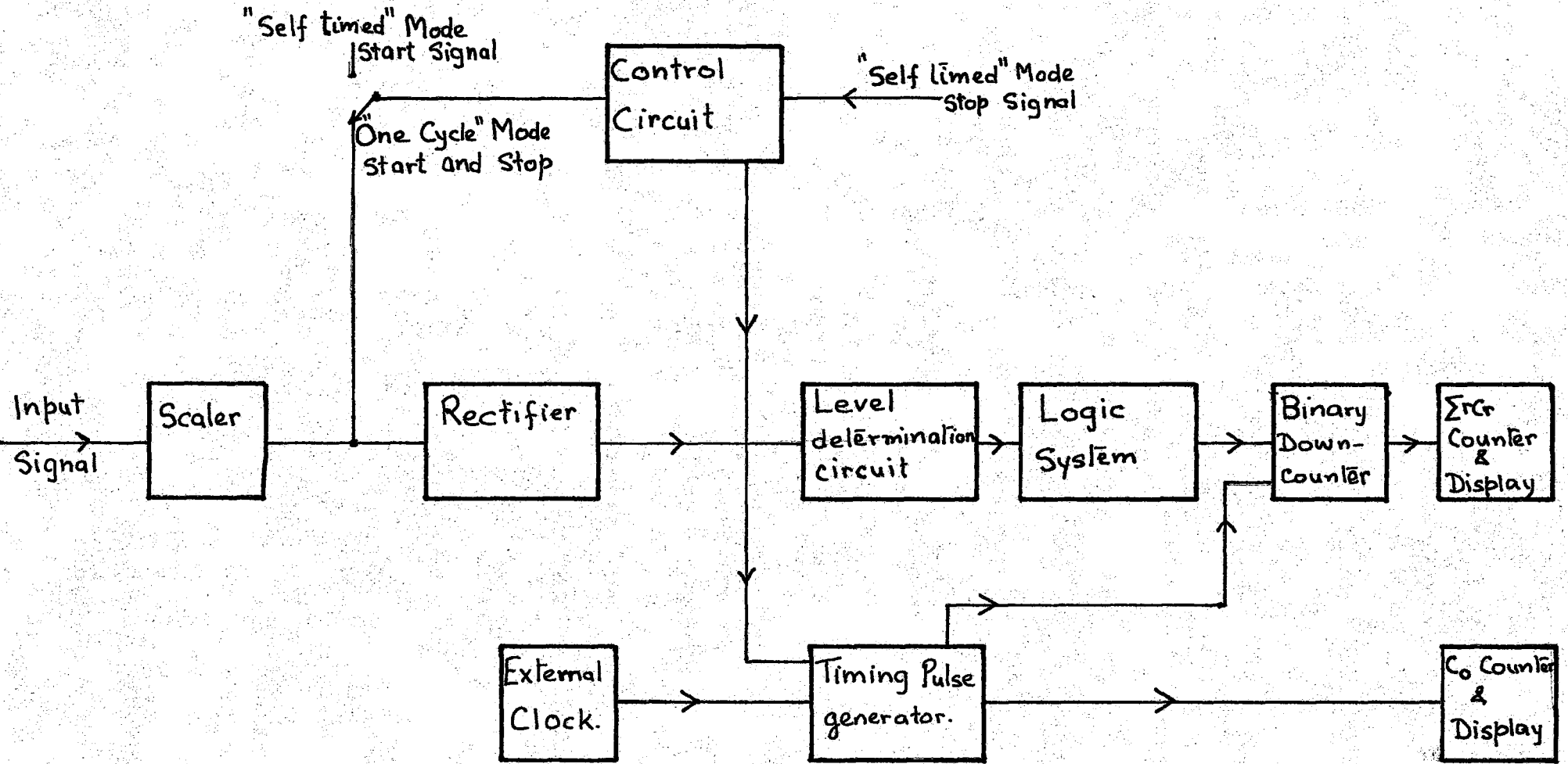


Fig. 2. : Block diagram of a 16-level Instrument.

counter with readout. A similar counter is used for $\sum_{r=1}^{n-1} r C_r$ readout.

2.4 Instrument Realisation.

1. Rectification.

The use of sixteen levels on either side of the zero level has several disadvantages viz:

- (i) for a fixed upper reference of $-10V$ (n^{th} level), the level width is halved, doubling the inaccuracy due to level setup.
- (ii) the switching logic to achieve the $\sum_{r=1}^{n-1} r C_r$ becomes extremely complicated as now a five bit level register is required in the level determination circuit.
- (iii) it is difficult to obtain identical 4 - bit expressions for the r^{th} level on either side of zero level.

As input polarity is a redundant information, the above difficulties can be easily overcome by rectifying the input waveform.

Since no addition is made to $\sum_{r=1}^{n-1} r C_r$ count for voltages not exceeding the 1st level, rectification need not be performed precisely at zero volts.

However conventional rectifiers can cause considerable distortion of the input waveform and hence cannot be used here. Rectification is performed using an operational amplifier inverter, a Schmitt trigger circuit, a digital inverter and two FET gates. Fig.3, shows the diagram of the rectifier circuit.

The FET switch is turned on when both the control inputs are at $-3V$. When input is negative, there is a $-3V$ signal at both the control terminals of the upper switch which is therefore turned on. The input appears at the output of the switch. When the input is positive, the input to the digital inverter is $0V$ and hence a $-3V$ signal is applied to

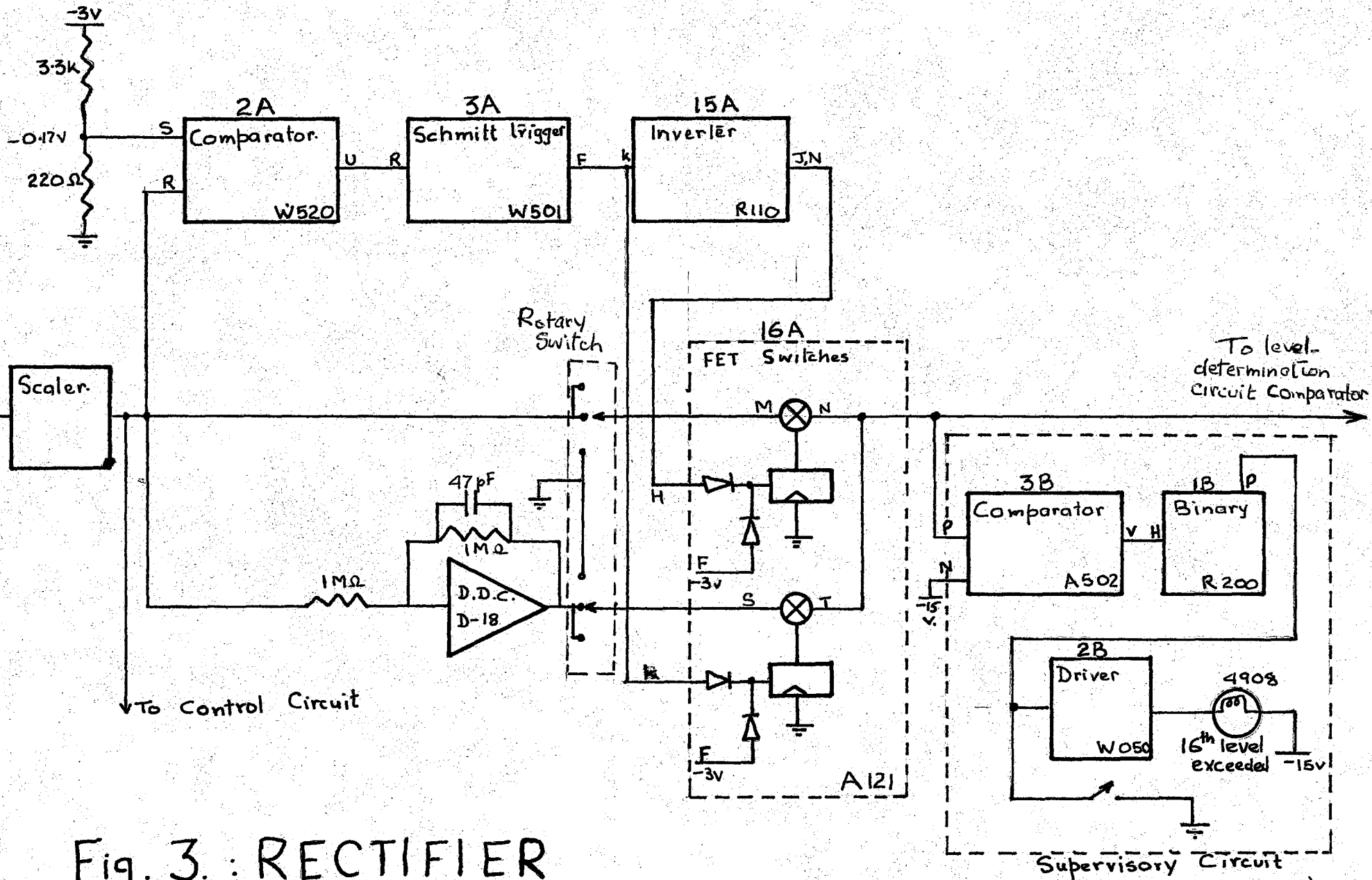


Fig. 3. : RECTIFIER

the control terminals of the lower switch. The input, inverted by the operational amplifier, will now appear at the output of the switch. The input is thus rectified, the output being always negative.

The FET switches must have the correct voltage supplies if they are to perform correctly and without distorting the input waveform. The signal voltage must not be more positive than the positive supply and must be at least 10 volts more positive than the negative supply. Furthermore the differential voltage (difference between positive and negative supplies) must not exceed 30V. See Appendix A.

A supervisory circuit is included which ensures that the highest level i.e. the 16th level is not exceeded. A rotary switch enables selection of either positive half or the negative half of the input waveform.

2. Level determination.

For the weighted input method selected, it is necessary to determine the highest level exceeded at each sampling instant. As this number is required in a binary form, it is necessary to use analog-to-digital conversion. This is carried out by a 4-bit A/D converter of the successive approximation type, shown in Fig.4. The operation is controlled by a internal triggered clock operating at 1 MHz. and a timing pulse generator. The latter produces sixteen pulses for every sampling pulse; eight of which are used in the level determination process.

In the 16-level case, the first triggered pulse sets the binaries in state 1000 (half-scale). The analogue conversion of this state is compared with the input. If it exceeds the input, the binaries

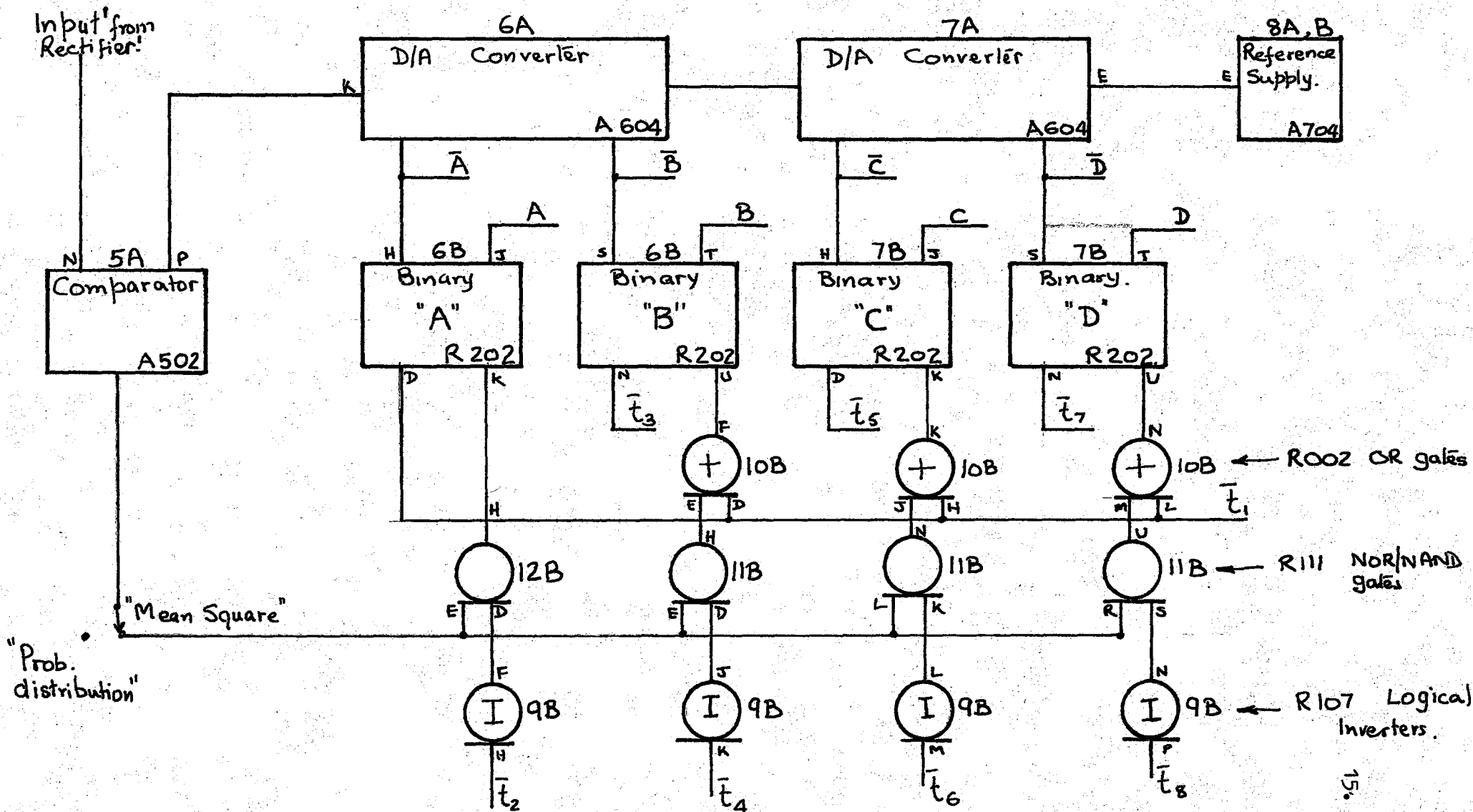


Fig. 4. Level determination circuit.

are reset to 0000. If the approximation is too small the binaries remain at 1000. Next the binaries are set at either 1100 or 0100 depending on first decision. A second decision similar to the first is made. The process is repeated for the $1/8$ and $1/6$ scale and after a total of four approximations, the states of A,B,C, and D give the highest level exceeded. Since sampling is actually initiated by the second pulse and completed by the eighth, the aperture time for each sample is $7 \mu\text{Sec.}$ Sampling should not recommence until the level determination process is completed and the addition to $\sum_{r=1}^{n-1} rC_r$ register carried out.

3. The switching logic circuit.

The gates G1 to G7, controlled by a switching logic system are used to transfer the correctly weighted input information from the level registers of the A/D converter. Table No.II shows the requirements of these gates. Thus gate G1 is required to open for all levels for which there is a 1 in the column corresponding to G1. Similar requirements hold for all the other gates. Using Table No.II Veitch-Karnaugh maps for these gate functions are obtained and are shown in Table No II. Using these maps and DeMorgan's Theorem, these gating functions are realised entirely with NOR gates.

In the 16-level instrument constructed, these gating functions are used to gate a timing pulse i.e. the final expression for a gating function becomes of the form

$$G = F.t = \bar{F} + \bar{t} \quad \text{where } \bar{F} \text{ is the expression realised from maps.}$$

Highest Level Exceeded.		Weighted Inputs										
Decimal	Binary.				Decimal	Binary						
	A	B	C	D		G ₇	G ₆	G ₅	G ₄	G ₃	G ₂	G ₁
1	0	0	0	1	1	0	0	0	0	0	0	1
2	0	0	1	0	3	0	0	0	0	0	1	1
3	0	0	1	1	6	0	0	0	0	1	1	0
4	0	1	0	0	10	0	0	0	1	0	1	0
5	0	1	0	1	15	0	0	0	1	1	1	1
6	0	1	1	0	21	0	0	1	0	1	0	1
7	0	1	1	1	28	0	0	1	1	1	0	0
8	1	0	0	0	36	0	1	0	0	1	0	0
9	1	0	0	1	45	0	1	0	1	1	0	1
10	1	0	1	0	55	0	1	1	0	1	1	1
11	1	0	1	1	66	1	0	0	0	0	1	0
12	1	1	0	0	78	1	0	0	1	1	1	0
13	1	1	0	1	91	1	0	1	1	0	1	1
14	1	1	1	0	105	1	1	0	1	0	0	1
15	1	1	1	1	120	1	1	1	1	0	0	0

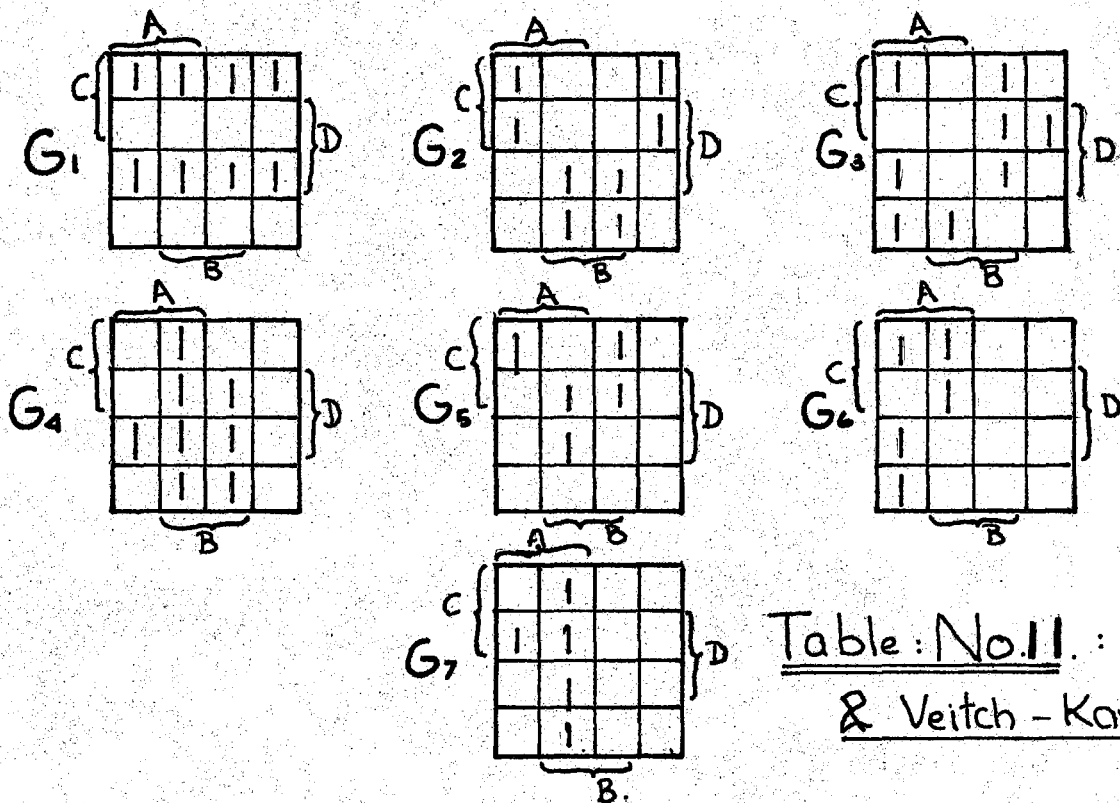


Table: No. 11. : Weighted Inputs & Veitch - Karnaugh Maps.

The final logic expressions for the gates are as follows:

$$G1 = \overline{\overline{C + D}} + \overline{C+D} + \overline{t}_{15}$$

$$G2 = \overline{\overline{C + B}} + \overline{C+B} + \overline{t}_{14}$$

$$G3 = \overline{\overline{\overline{A+B+C}} + \overline{\overline{A+C+D}} + \overline{\overline{A+B+D}} + \overline{A+C+D}} + \overline{A+B+C} + \overline{A+B+D} + \overline{t}_{13}$$

$$G4 = \overline{A + B} + \overline{A+C+D} + \overline{B+D} + \overline{\overline{A+B+C}} + \overline{t}_{12}$$

$$G5 = \overline{\overline{A+B}} + \overline{\overline{A+C}} + \overline{C+D} + \overline{\overline{B+D}} + \overline{\overline{\overline{A+B+D}}} + \overline{t}_{11}$$

$$G6 = \overline{A} + \overline{\overline{B+C}} + \overline{\overline{B+C+D}} + \overline{t}_{10}$$

$$G7 = \overline{A} + \overline{\overline{B+C}} + \overline{\overline{B+D}} + \overline{t}_{9}$$

The timing pulses obtained from a timing pulse generator are applied to the final NOR gates. The A/D converter provides the outputs A, B, C, D as well as their complements. A few terms in the above expressions are common to some gates and can therefore be shared, thereby easing the logic circuit to some extent. The circuit diagrams of the logic circuit is shown in Fig. 5.

4. Timing pulse generator.

For each sampling pulse, eight pulses are required for the level determination process and seven pulses are required for the logic system. The sampling pulse could be used to feed the C_0 register. However, by using two binary to octal decoders, sixteen separate timing pulses can be easily realised. In this case the sixteenth pulse is used for the C_0 register.

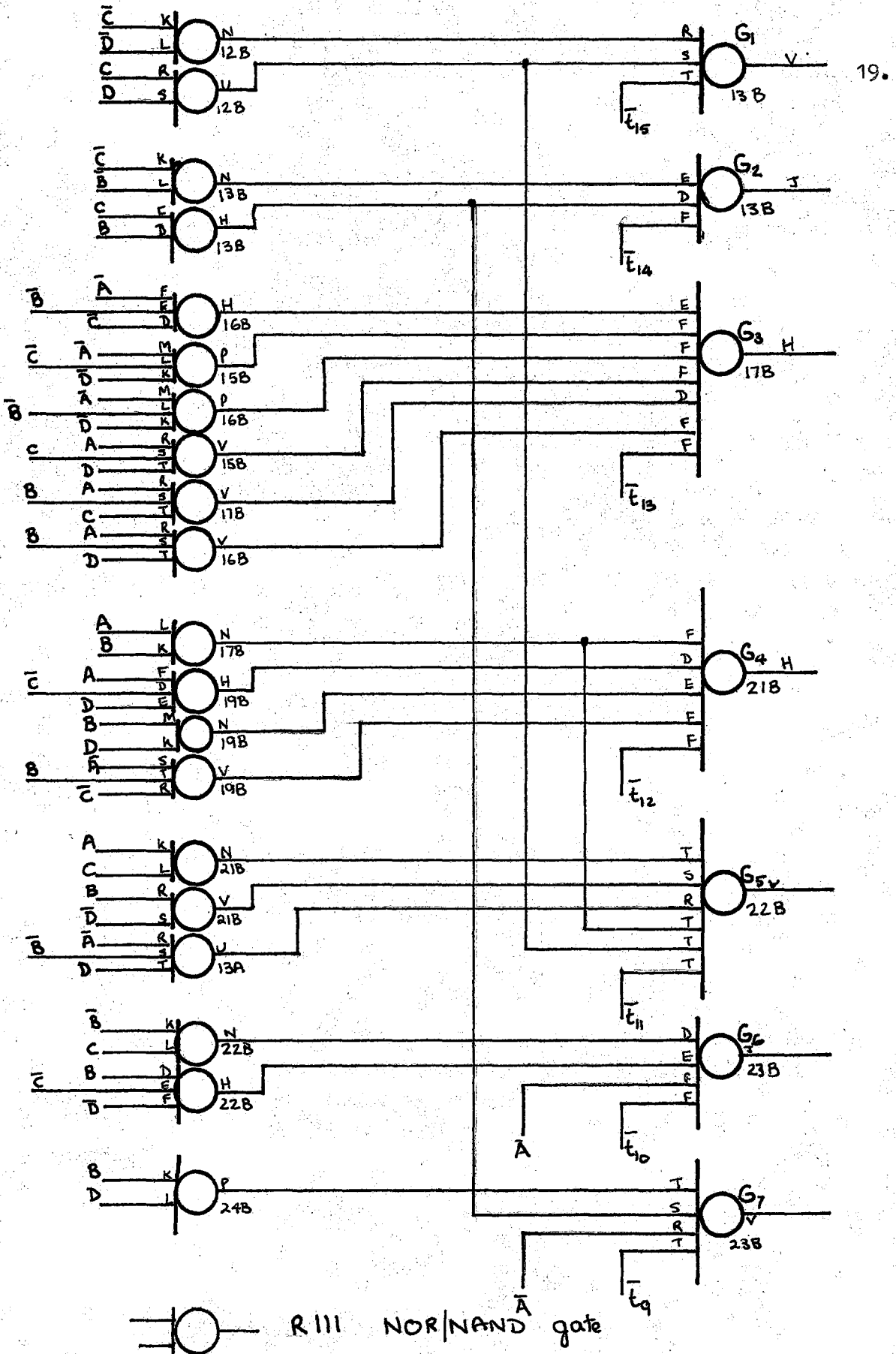


Fig: 5 : Counter Input Logic.

The timing pulse generator circuit is shown in Fig. 6. The internal clock is set at 2 MHz. It is used to drive a binary whose output is the 1 MHz pulse rate. This system is "enabled" for a period of sixteen timing pulses, once for each cycle of the external clock. Thus once every sampling period, sixteen pulses are delivered at 1 MHz. to the B/O converter system. The output of the B/O decoder is sixteen pulses appearing at the sixteen terminals serially in time. The inputs to the B/O converter are obtained using the truth table given. The sixteenth pulse output is used to inhibit the binary, which in turn inhibits the internal clock, until the next sampling pulse occurs when the process is repeated. The "enable" inputs to the B/O decoder are obtained from two NOR gates which are inhibited by the control logic circuit described in the next section.

5. The control logic circuit.

There are two modes of operation to consider. The instrument may be operated in the periodic mode in which only one cycle of the input is used in the measuring process, or in the self-timed mode in which the measurement time is set at will.

The control circuit is shown in Fig. 7. It incorporates a supervisory circuit which indicates the starting and completion of the measurement.

In either mode the start switch is depressed momentarily, setting binaries X and Y. The binary X inhibits the timing pulse generator decoders and therefore also the C_0 register, while binary Y resets the two registers. Measurements commence when the Schmitt trigger circuit

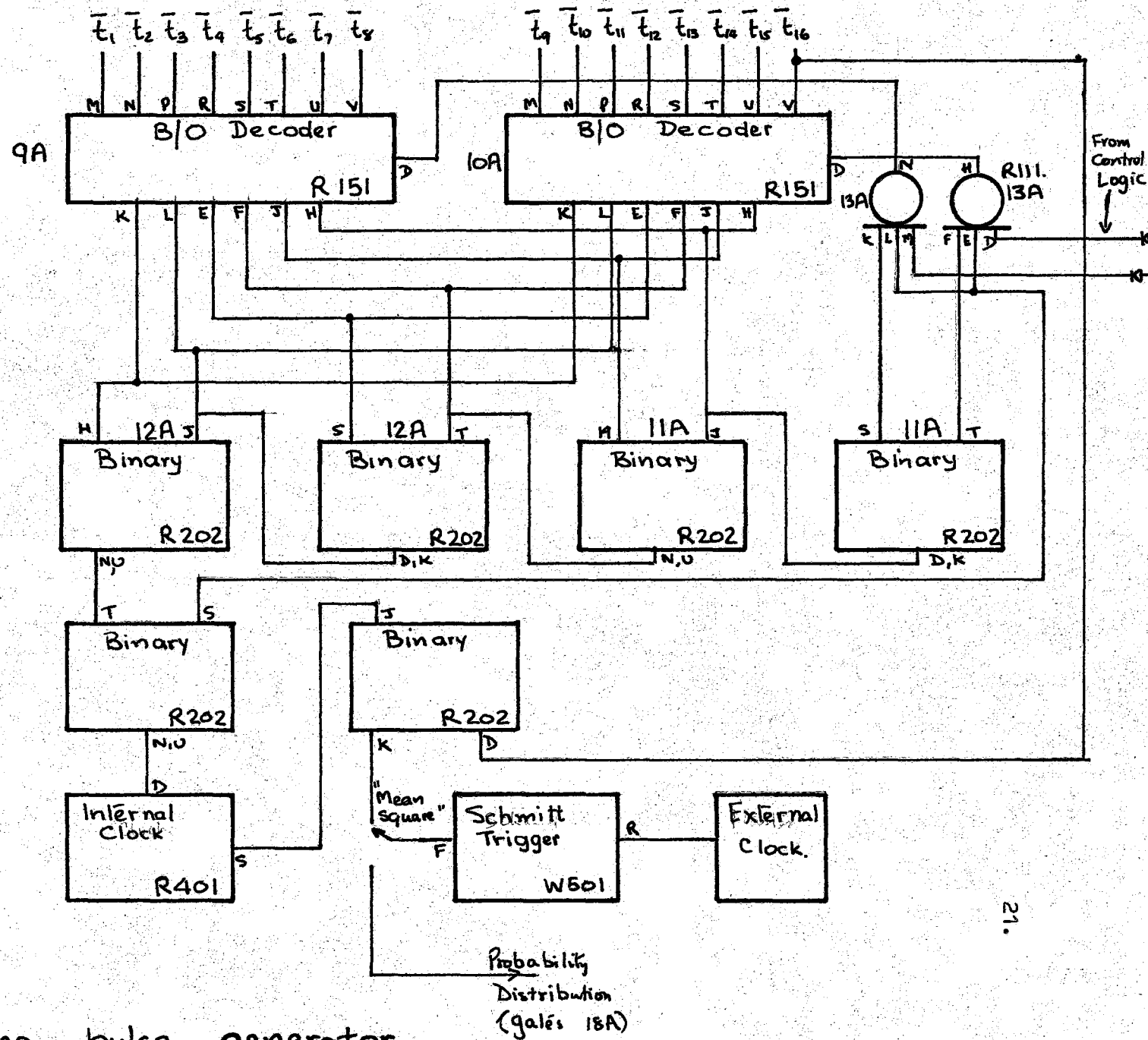


Fig. 6. : Timing pulse generator

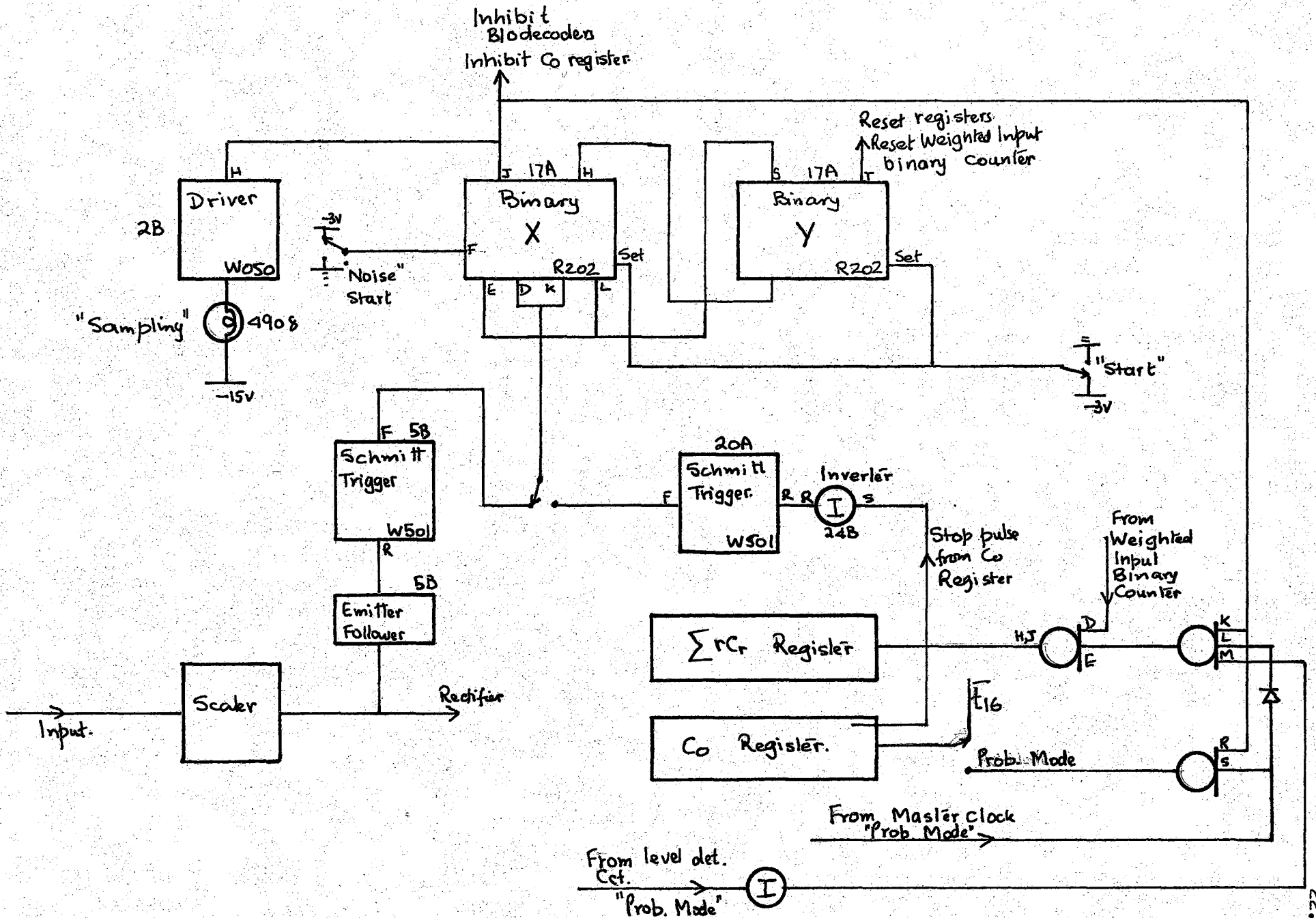


Fig. 7. Control Circuit

produces an output when a negative going zero crossing occurs at its input. The Schmitt trigger output complements binaries X, thereby starting the level determination process and also the C_o count. When the next zero crossing in the same direction occurs, the Schmitt trigger output again complements binary X - thus stopping the measurement process. At this stage binary X is inhibited by binary Y.

In the selftimed mode, measurement commences when the "noise" switch is depressed (the control circuit being in the "noise" position) and ceases when the C_o count reaches 10^3 or some higher power of 10, which may be selected from the C_o counter register circuit. The pulse for the most significant bit chosen is inverted and applied to a second Schmitt trigger circuit whose output is then used to inhibit binary X and stop the measurement process.

6. Additional Facilities.

Two additional facilities are easily incorporated in the instrument.

- (a) By inserting a 2P3T switch in the rectifier circuit, it is possible to investigate either the positive or the negative portion of the input waveform.
- (b) Since the instrument is basically a statistical analyser, an output display of C_r and C_o for a preset level r , can be realised easily. Thus by selecting each of the levels in turn, the amplitude probability distribution (or the time the input waveform spends above the r^{th} level) can be determined.

A rotary switch is used in the level determination circuit which

grounds the appropriate output of the level register to hold it in the binary state corresponding to the level selected. A mode switch when turned from "mean square" mode to "probability" mode makes the following changes in the system:

- (a) the external clock is disconnected from the timing pulse generator and is used to supply clock pulses to two NOR gates N1 and N2.
- (b) the C_0 register input is connected to the output of N2.
- (c) the output of the comparator used in the level determination process is diverted to N1 after inversion.

As the logic system gates G1 - G7 are not supplied with the timing pulses $t_9 - t_{15}$ no weighting factor is involved in the count i.e. both displays have the same weighting.

Both N1 and N2 are inhibited by binary X of the control circuit so that the probability distribution may be measured in either the "periodic" or "self-timed" mode.

2.5. Performance Tests.

The performance of the entire instrument can be readily checked by using a d.c. input. The input is adjusted so that the voltage lies within a certain level interval. The instrument is set in the noise mode so that a fixed $C_0 = 10000$ is obtained. The measured value of $\frac{2}{n^2} \sum_{r=1}^{n-1} r C_r$ should be the same as that given in Table III, for the level chosen. In this manner all the levels are checked.

The formula for V_n expressed as a fraction of the voltage at the n^{th} level is

$$V_n^2 = \frac{1}{4n^2} \left\{ 1 + \frac{8}{C_0} \sum_{r=1}^{n-1} rC_r \right\}$$

The voltage at the n^{th} level is 10V.

$$\therefore V_{in}^2 = \frac{100}{4n^2} \left\{ 1 + \frac{8}{C_0} \sum_{r=1}^{n-1} rC_r \right\}$$

If the input voltage is somewhere between the r^{th} and $(r+1)^{\text{th}}$ level, the readout of the instrument will be that corresponding to the midinterval voltage. This is

$$\left\{ \frac{2r+1}{2n} \right\}^2 \times 100 \text{ volts.}$$

$$\therefore \left\{ \frac{2r+1}{2n} \right\}^2 \times 100 = \frac{100}{4n^2} \left\{ 1 + \frac{8}{C_0} \sum_{r=1}^{n-1} rC_r \right\}$$

$$\therefore \sum_{r=1}^{n-1} rC_r = \frac{r(r+1)C_0}{2}$$

The direct readout of the accumulator register is $\frac{1}{128} \sum_{r=1}^{n-1} rC_r$

\therefore The direct readout for $C_r^1 = \frac{10,000}{2 \times 128} r(r+1)$, for $C_0 = 10,000$

$$\therefore C_r^1 = \frac{r(r+1)}{0.0256}$$

The values of the direct decimal readout for d.c. inputs are given in Table III

T A B L E. N O. III.

D.C. Input Voltage Volts	r	$r(r+1)$	C'_r
0 - 0.625	0	0	0
0.625 - 1.250	1	2	78.125
1.250 - 1.875	2	6	234.375
1.875 - 2.500	3	12	468.750
2.500 - 3.125	4	20	781.250
3.125 - 3.750	5	30	1171.875
3.750 - 4.375	6	42	1640.625
4.375 - 5.000	7	56	2187.500
5.000 - 5.625	8	72	2812.500
5.625 - 6.250	9	90	3515.625
6.250 - 6.875	10	110	4296.875
6.875 - 7.500	11	132	5156.250
7.500 - 8.125	12	156	6093.750
8.125 - 8.750	13	182	7109.375
8.750 - 9.375	14	210	8203.125
9.375 - 10.000	15	240	9375.00

Direct Decimal Readouts.

CHAPTER 3

THEORETICAL ERROR ANALYSIS

The errors arising in an instrument using the sampling technique are considerably different in nature, from those of conventional analogue instruments. The measured mean square value is given by

$$V^2 = \frac{1}{4n^2} + \frac{2}{n^2 C_0} \sum_{r=1}^{n-1} r C_r$$

Errors in the mean square value result from two main sources. These are (i) error due to the assumptions made in deriving the above formula and (ii) errors made in measuring $\sum_{r=1}^{n-1} r C_r$

The first may be regarded as quantisation error, which is inherent in a system in which voltages in any level interval are approximated to the midinterval value for that level, the number of level intervals being finite.

Errors in the measurement of $\sum_{r=1}^{n-1} r C_r$ arise due to

- (a) finite sampling rate.
- (b) incorrect level settings.
- (c) finite time of measurement.

Derivations of the error expressions are often lengthy and involved. Consequently, this Chapter is devoted to descriptions of these errors, the actual derivation being given in the Appendix. B. Since the overall error characteristics are of interest and since the errors are statistical in nature, the overall characteristics are best

described in terms of confidence limits.

The 16-level instrument described before, may be used for measurements on any type of waveform. Therefore it is desirable that waveforms of as wide a range as possible are treated. The error analysis described here is for (1) square wave (2) Sine wave input (3) Triangular wave input and (4) Normal (gaussian) Distribution noise. A theoretical error study is also made for a periodic waveform which has a Gaussian amplitude probability distribution. See Fig. 8.

3. 1. The error equation.

Let the error in the root mean square reading due to any one source be e_1 , so that the instrument reads V_1 (r.m.s.) instead of V (r.m.s.). e_1 is then defined as

$$e_1 = \frac{V_1 - V}{V}$$

Similarly an error e_1^* in the mean square value may be defined as

$$e_1^* = \frac{V_1^2 - V^2}{V^2}$$

Since both e_1 and e_1^* are small in practice, it is possible to express e_1^* in terms of e_1 .

$$\begin{aligned} \therefore V_1^2 &\doteq (1 + 2e_1)V^2 \\ \therefore e_1 &\doteq \frac{1}{2} \left\{ \left(\frac{V_1}{V} \right)^2 - 1 \right\} \\ \therefore e_1^* &= 2e_1 \end{aligned}$$

Thus if e_1 is evaluated in practice, then e_1^* can be easily calculated.

Chapter 4 gives computed values of e_1 for a 16-level instrument due to the different sources. Values of e_1^* and the overall characteristics are derived from those of e_1 . An alternative definition is to consider the error in terms of the full-scale voltages. Since there is no particular advantage in this approach, it has not been used in this analysis.

3.2. Error due to quantisation.

In the instrument described, the voltage waveform is rectified and then quantised into n levels, the square of the mid-interval values being used in computation of the mean square value. This approximation of all voltages within a level interval, to the mid-interval, results in an error in the mean square value. For periodic waveform, the peak may lie anywhere within a given interval i.e. only a fraction ϵ of the m^{th} level is occupied. Thus $\epsilon = 0$ corresponds to the m^{th} level just being entered and $\epsilon = 1$ to this interval just filled. See Fig. 9.

These approximations result in an error e_n produced by use of finite number of intervals. Error expressions for the various waveforms are derived in Appendix B.1. The results are as follows:

(a) Rectangular Wave.

$$e_{nm} = \frac{1 - 2\epsilon}{2(m-1+\epsilon)} \quad \text{where } m-1 \text{ is in the highest level completely filled.} \quad \text{-----(1)}$$

If all n levels are occupied i.e. $m=n$, then a maximum error occurs when $\epsilon = 0$

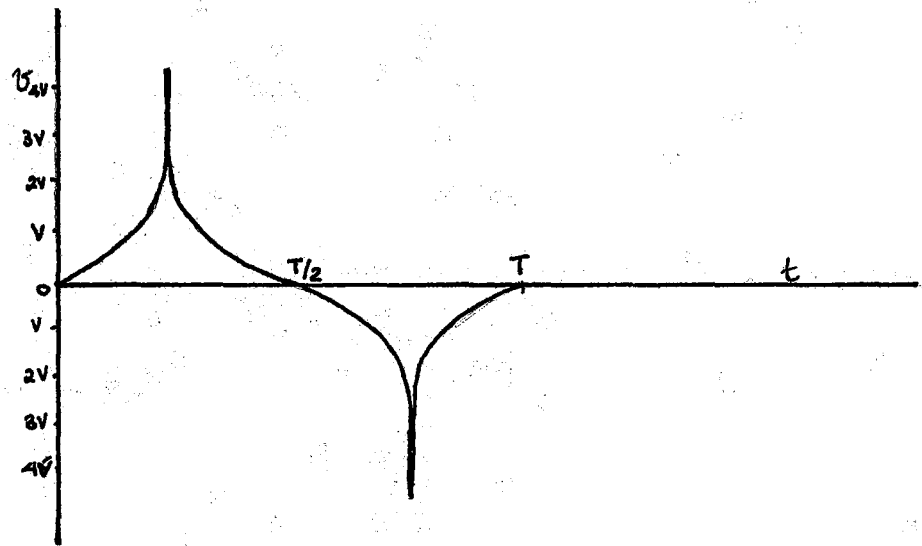


Fig. 8.: Normal Wave.

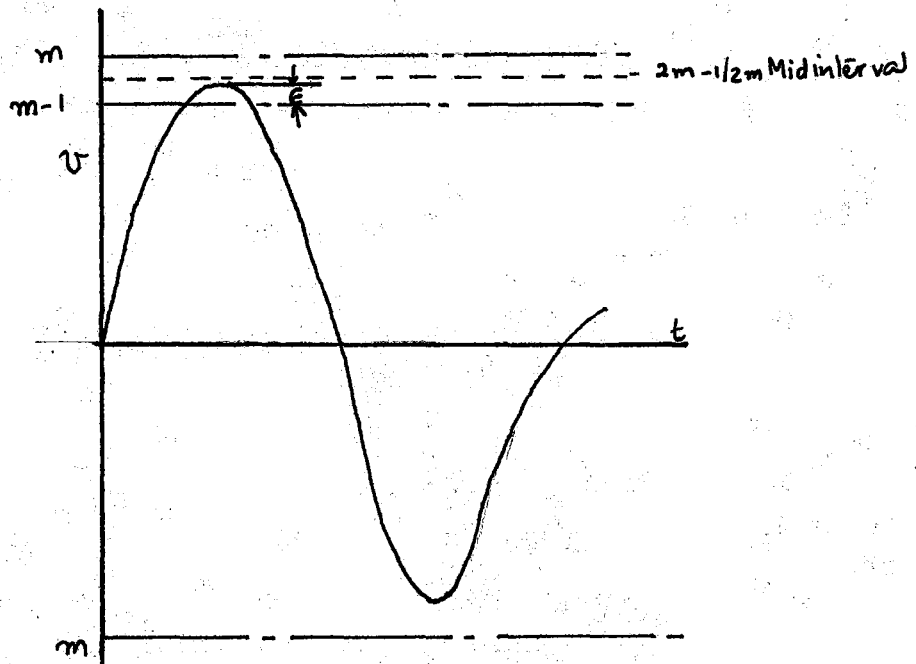


Fig: 9 : Input Waveform with peak at $(m-1+\epsilon)$

$$\therefore e_{nm} = \frac{1}{2(n-1)}$$

$$\therefore e_{n,max}^* = \frac{1}{n-1}$$

(b) Sine Wave

The following general expression is derived

$$e_{nm} = \frac{1}{4(m-1+\epsilon)^2} \left\{ 1 + \frac{16}{\pi} \sum_{r=1}^{n-1} r \cos^{-1} \frac{r}{m-1+\epsilon} \right\} - \frac{1}{2} \quad \text{-----}(2).$$

If all levels are completely filled, there is still an error.

Thus for all filled intervals

$$e_{nm} = \frac{1}{4n^2} \left\{ 2n^2 - 4n + 1 - \frac{16}{\pi} \sum_{r=1}^{n-1} r \sin^{-1} \frac{r}{n} \right\}$$

For large values of n equation (3) may be simplified by approximation methods. Thus it can be shown that for large n

$$e_{nm} \doteq \frac{-0.41}{(n-1)^{1.5}}$$

(c) Triangular Wave

$$e_{nm} = \frac{1 - m + 12m\epsilon(1-\epsilon) - \epsilon(2\epsilon-3)^2}{8(m-1+\epsilon)^3} \quad \text{-----}(3)$$

For all filled intervals and in particular for $n \gg 1$,

equation 4 reduces to

$$e_{nm} = \frac{-1 + 12\epsilon(1-\epsilon)}{8n^2}$$

and $e_{nmax} = \frac{1}{4n^2}$ when $\epsilon = 0.5$

(d) Normal distribution noise and normal wave.

Since both these have the same amplitude probability distribution, the error due to use of finite number of intervals will be the same in both cases. As the voltage is not confined to the n intervals available, two types of errors arise:

- (i) a level limit error, arising because samples beyond the n^{th} level are grouped together. This error is negative.

(ii) an interval error similar to those for the periodic waves.

At the r^{th} level the normalised voltage is $\frac{r}{n}$ so that

$$P_r = 1 - \int_0^v \frac{1}{\sqrt{2\pi}} \exp\left(-\frac{x^2}{2}\right) dx \quad \text{where } v = \frac{r}{nV} \text{ ---(4).}$$

$$e_n = \frac{1}{8n^2V^2} \left\{ 1 + 8 \sum_{r=1}^{n-1} r \left[1 - 2 \int_0^{r/nV} \frac{1}{\sqrt{2\pi}} \exp\left(-\frac{x^2}{2}\right) dx \right] - \frac{1}{2} \right\} \text{ ---(5).}$$

The area under the normal distribution curve for a given V , being known, e_n can be evaluated.

The expressions for e_n for all waveform, except the square wave, are best evaluated using computer programmes. This method has been adopted to calculate e_n for the 16-level instrument for various values of m for ϵ between 0 and 1. (See Appendix C).

3.3. Error due to finite Sampling rate.

(a) Periodic Wave.

The error e_p due to finite sampling rate depends on the sampling process used. The analysis given here is for the above level sampling used in the 16-level instrument.

If during a sample, a level change occurs then an incorrectly weighted input is fed to the $\sum_{r=1}^{n-1} r.C_r$ register. Fig. 10. shows sampling at the r^{th} level, for positive and negative slope waveforms. The timing pulse generator produces sixteen pulses for each external clock pulse.

Of these sixteen pulses, the first eight are used in the level determination process. The next seven pulses are used to feed a correctly weighted input to $\sum_{r=1}^{n-1} r.C_r$ register while the sixteenth is fed to the C_0 .

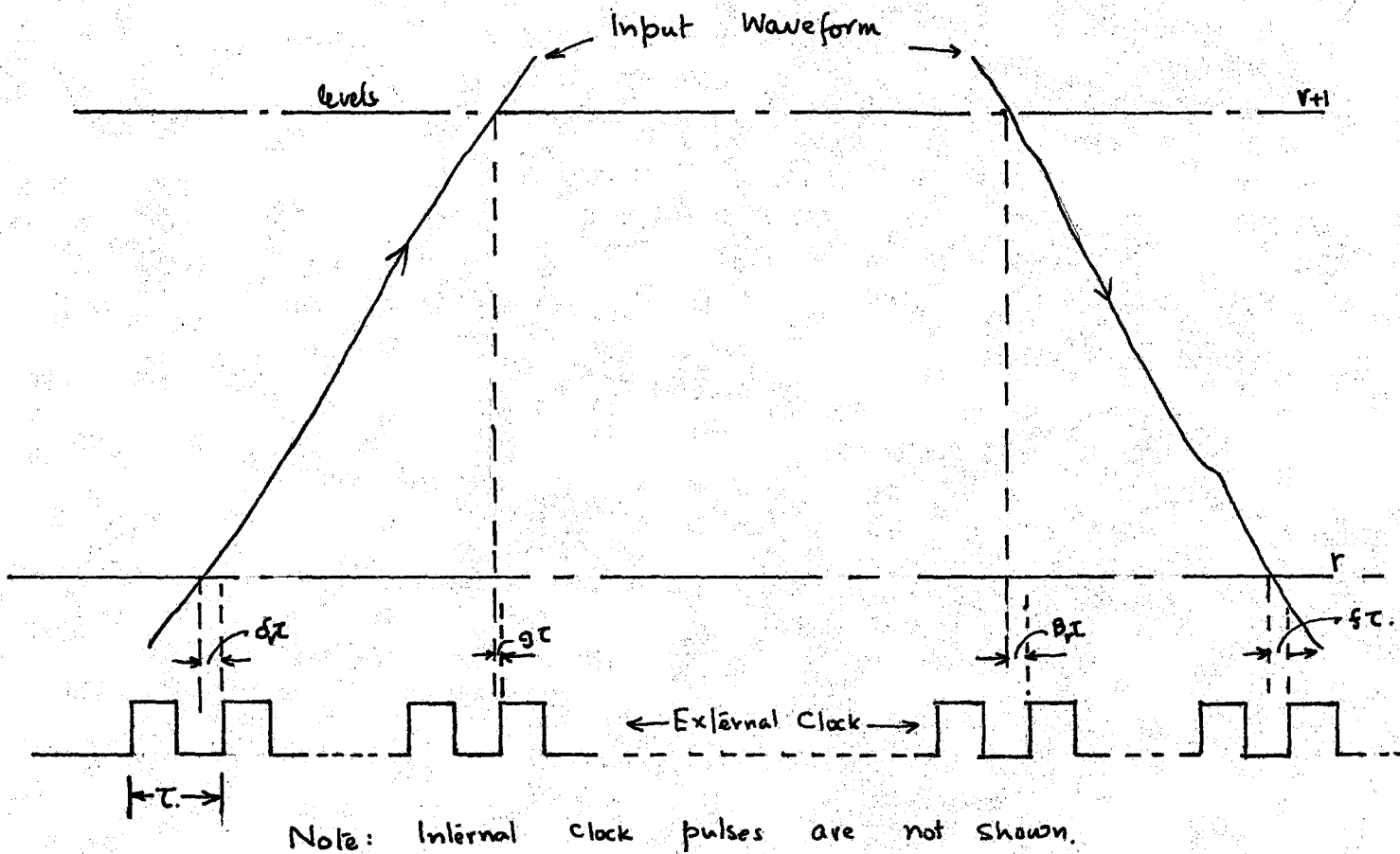


Fig: 10: Sampling at r^{th} and $(r+1)^{\text{th}}$ levels.

register. The weighting factor depends on the states of the binaries in the level determination circuit. Referring to Fig. 10. the portion $g\tau$ of the input waveform is given the correct weighting, whereas the region $f = \delta_r \tau$ has a weighting W_{r-1} , instead of W_r . Similarly, from sampling conditions for the negative-slope waveform, a portion $h = \beta_r \tau$ has a weighting W_{r+1} instead of W_r . Since δ_r and β_r are random for any given level, it is clear that there is a random error due to the finite sampling rate. The exact analysis for e_p , which takes into account the number of crossings of the r^{th} level and the variation of δ_r & β_r from one pair of crossing to another, becomes extremely complicated. However a simpler analysis can be easily made, on the assumption that the total number of level crossing in any measurement is large enough for the central limit theorem to apply (thus even in the "one-cycle" mode there are 32 crossings in the instrument constructed. Derivation of e_p is contained in the Appendix B3, where it is shown that the error in r.m.s. value is given by

$$e_p = \frac{1}{n^2} \frac{1}{\sqrt{2}} \frac{f}{p} \sum \{ \beta_r - r(\delta_r - \beta_r) \} \quad \text{-----}(6).$$

where f = frequency of input waveform

p = sampling clock rate.

Both δ_r and β_r are random variables with all values between 0 and 1 being equally likely. Applying the Central Limit Theorem to the summation term, a probability distribution function for e_p can be obtained. This is shown to be

$$p(e_p) = \frac{1}{n^2} \frac{1}{\sqrt{2}} \frac{f}{p} p(F_1) \quad \text{-----}(7).$$

Where $p(F_i) = \frac{1}{\sqrt{2\pi}\sigma} \exp\left\{-\frac{(x-q)^2}{2\sigma^2}\right\}$ and σ is the

standard deviation, which can be calculated knowing the highest level occupied.

also $e_{p.av.} = \frac{1}{2nV^2} \frac{f}{P}$ if all n levels are occupied

$e_{pmax.} = \pm \frac{1}{2V_n} \frac{f}{P}$ with all levels occupied.

For rectangular, sine and triangular waves $V=1, \frac{1}{\sqrt{2}}$ and $\frac{1}{\sqrt{3}}$ respectively.

In considering the error e_p , it has been assumed that there is no level change during a level determination process. Since the aperture time is finite, this assumption is not strictly true. Errors arising due to finite aperture time are considered in section 3.6.

(b) Normal distribution noise.

Conditions at the r^{th} level are same as for the periodic waves. Every time the voltage crosses the r^{th} level, going more positive, a portion $\delta\tau$ is given incorrect weighting and similarly going negative, on crossing the $(r+1)^{\text{th}}$ level a time error $\beta\tau$ arises.

In measuring over a sufficiently large time T there will be a large number of level crossings. Hence expected values of δ and β can be used to calculate $e_{p.av.}$. Expressions for the expected number of crossings at voltage V have been derived by S. O. Rice⁶. For an ideal low-pass filter with cut off frequency f_c , the expected number of zeros for white noise is

$$Z_0 = \frac{2}{\sqrt{3}} f_c \quad \text{per sec.}$$

The expected error in the IS value is

$$e_{p.av}^* = \frac{\gamma Z_0}{2n^2} \sum_{r=1}^{n-1} \left\{ -r \exp\left(-\frac{r^2}{2n^2 V^2}\right) + (r+1) \exp\left(-\frac{(r+1)^2}{2n^2 V^2}\right) \right\}$$

$$= \frac{\gamma Z_0}{2n^2} \left\{ n \exp\left(-\frac{1}{2V^2}\right) - \exp\left(-\frac{1}{2n^2 V^2}\right) \right\} \text{-----}(8).$$

Whence $e_{p.av} = \frac{1}{2} e_{p.av}^*$.

3.4. Error due to level inaccuracies

The offset at any given level can be due to inaccuracies in the reference supply and due to offset in the comparator used in the D/A converter. There may also ^{be} a voltage drop in the rectifier unit, which may be regarded as a level inaccuracy. Thus let the total level offset at the r^{th} level be δE_r . Conditions at the r^{th} level are given in Fig. 11. An incorrectly weighted input to $\sum_{r=1}^{n-1} \gamma C_r$ register occurs if a sample (i.e. level determination process) occurs within the time the voltage input takes to change from E_r to $E_r + \delta E_r$.

The error e_1 due to level inaccuracies depends on the number of times a level is crossed and the number of samples occurring during the time interval t . For the periodic waveforms considered, a level will be crossed four times per cycle. The frequency of occurrence of samples within interval t is random. However for an external clock rate of $1/T$, the expected number of samples within t will be t/T .

The total time of measurement is $\frac{C_0}{p}$ and the number of crossings at r^{th} level will be $\frac{4C_0 f}{p}$

The expected error in V will be

$$e_{1.av} = \frac{1}{2n^2} \frac{1}{V^2} \frac{1}{C_0} \frac{4C_0}{p} f \sum_{r=1}^{n-1} \frac{\gamma t}{T} \text{-----}(9).$$

$$= \frac{1}{n^2 V^2} \sum_{r=1}^{n-1} \frac{r \cdot \delta E_r}{V_{r1}} \quad \text{where } V_{r1} \text{ is the slope of the waveform at } r^{\text{th}} \text{ level.}$$

(a) Rectangular wave.

$$e_{1.av.} = 0.$$

However the δE_r at the m^{th} level will determine the $(m-1)^{\text{th}}$ or the m^{th} level is the highest exceeded. This will influence the error e_n considered earlier.

(b) Sine Wave.

$$\text{As } V_{r1} = \frac{dv}{dt} = \frac{m}{n} \sqrt{1 - \left(\frac{r}{m}\right)^2}$$

$$e_{1.av.} = \frac{n}{m} \frac{4}{\pi m^2} \sum_{r=1}^{n-1} \frac{r \delta E_r}{\sqrt{1 - \left(\frac{r}{m}\right)^2}} \quad \text{-----(10).}$$

(c) Triangular Wave.

$$e_{1.av.} = \frac{3n}{m^3} \sum_{r=1}^{m-1} r \cdot \delta E_r. \quad \text{-----(11).}$$

(d) Normal wave and normal distribution noise. The slope cannot be calculated for normal distribution noise. Hence a different approach is used to obtain e_1 .

The error in p_r due to a level offset δE_r is

$$\delta p_r = \frac{2 \delta E_r}{\sqrt{2\pi} V} \exp\left(\frac{-r^2}{2n^2 V^2}\right)$$

and the error in V is then given by

$$e_{1.av.} = \frac{1}{2n^2 V^2} \sum_{r=1}^{n-1} r \left\{ \frac{2\delta E_r}{V\sqrt{2\pi}} \exp\left(\frac{-r^2}{2n^2 V^2}\right) \right\} \quad \text{---(12).}$$

If δE_r is same for all levels then the expression for e_1 can be considerably simplified. This is considered in calculating e_1 for the 16-level instrument, where an average value for δE_r is considered.

3.5. Error e_α due to sampling a non-integral number of cycles of periodic waves.

In the "one cycle" mode, the measurement is over one cycle of the input precisely and hence e_α is zero. In the "self timed" mode, however, sampling is started manually and stopped when a certain value of C_0 is obtained. Thus in this mode sampling starts at some instant φ after a zero crossing stops after $(q+\alpha)$ cycles, where q is an integer (see Fig. 12.)

The instrument reads

$$V_\alpha^2 = \frac{1}{2\pi(q+\alpha-\varphi)} \int_0^{2\pi(q+\alpha-\varphi)} v^2 d\theta$$

$$\therefore e_\alpha = \frac{1}{2} \left\{ \left(\frac{V_\alpha}{V} \right)^2 - 1 \right\}$$

$$= \frac{1}{4\pi(q+\alpha-\varphi)} \left\{ -2\pi(\alpha-\varphi) + \frac{1}{V^2} \int_0^{2\pi(\alpha-\varphi)} v^2 d\theta \right\}$$

now $(q+\alpha-\varphi) = \frac{C_0 f}{P}$

$$\therefore e_\alpha = \frac{P}{4\pi C_0 f} \left\{ -2\pi(\alpha-\varphi) + \frac{1}{V^2} \int_0^{2\pi(\alpha-\varphi)} v^2 d\theta \right\} \text{-----(13).}$$

Both α and φ are random variables. Therefore the error e_α is also random. For periodic waveforms $v^2 = k^2 V_f^2(\theta)$ in general. Therefore e_α will be independent of V^2 . This fact is of importance as it simplifies

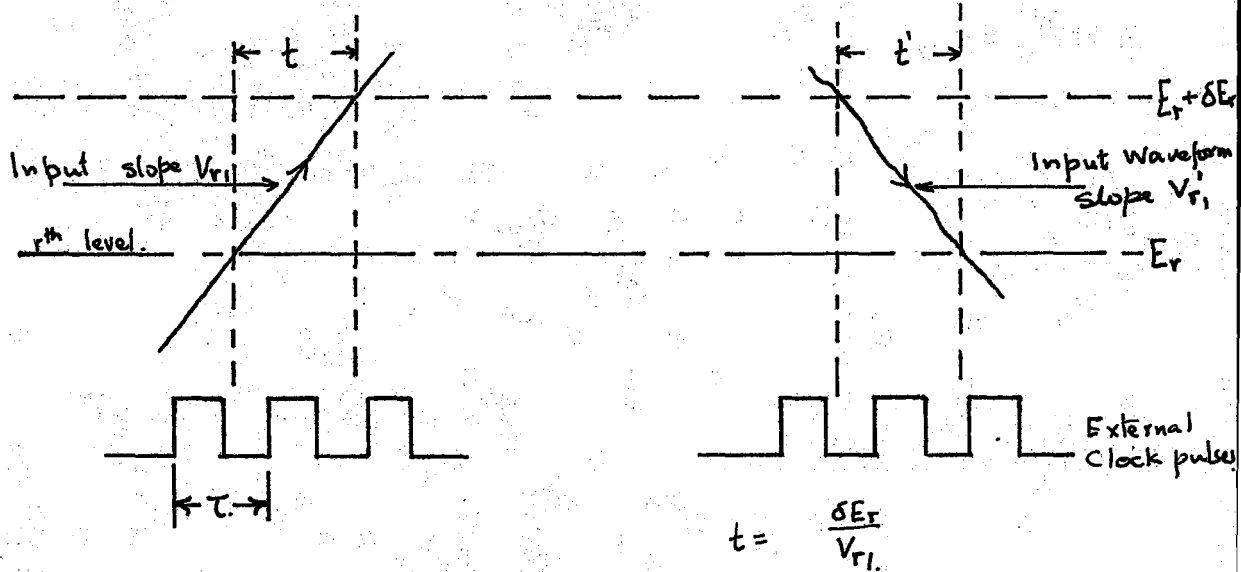


Fig. 11. : Level offset error at r^{th} level

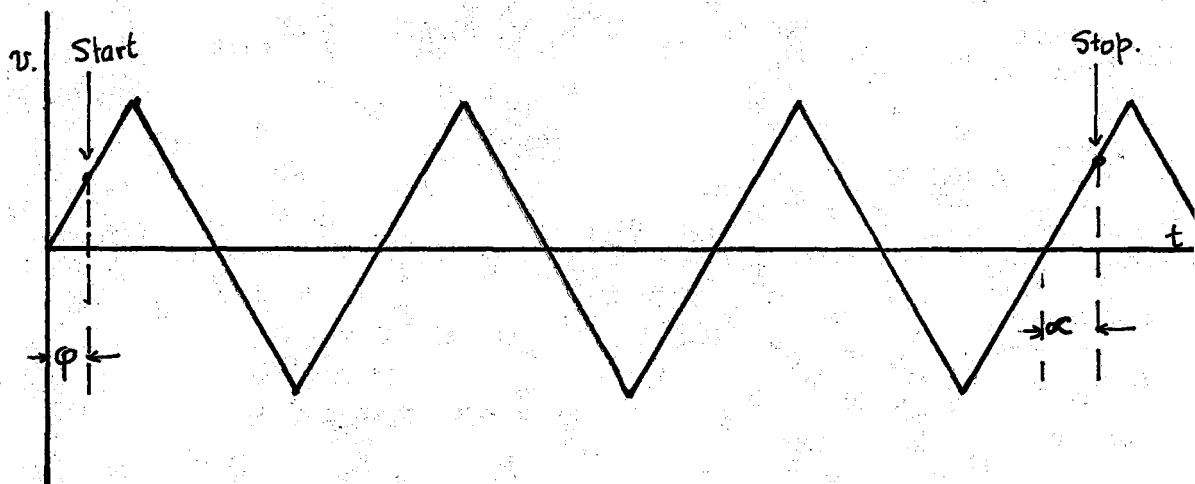


Fig : 12. : Sampling of a non-integral number of cycles.

the evaluation of combined error characteristics.

(a) Rectangular Wave

$$e_{\alpha} = 0.$$

(b) Sine Wave

$$e_{\alpha} = -\frac{1}{8\pi} \frac{p}{C_0 f} \left\{ \text{Sin. } 4\pi (\alpha - \varphi) \right\}$$

$$e_{\alpha \text{ max.}} = \frac{1}{8\pi C_0} \frac{p}{f} \doteq \frac{0.04}{q}$$

As e_{α} is a function of $(\alpha - \varphi)$, an expression for the probability distribution function for e_{α} can be easily derived.

(c) Triangular Wave

Since the triangular wave has discontinuity, a single expression for e_p cannot be obtained. Hence a piecewise analysis is required. Thus

$$(i) \quad 0 \leq (\alpha - \varphi) \leq \frac{1}{4} \quad v = \frac{2\theta}{\pi} \text{ and } v^2 = \frac{1}{3}$$

$$e_{\alpha} = \frac{1}{4\pi q} \left\{ -2\pi(\alpha - \varphi) + 32\pi(\alpha - \varphi)^3 \right\} \text{-----}(14).$$

$$(ii) \quad \frac{1}{4} \leq (\alpha - \varphi) \leq \frac{3}{4} \quad v = 2\left[1 - \frac{\theta}{\pi}\right] \text{ and } v^2 = \frac{1}{3}$$

$$e_{\alpha} = \frac{1}{4\pi q} \left\{ \pi(1 - 2\eta) - 4\pi(1 - 2\eta)^3 \right\} \text{-----}(15).$$

$$\text{where } \eta = (\alpha - \varphi)$$

and finally

$$(iii) \quad \frac{3}{4} \leq (\alpha - \varphi) \leq 1$$

$$e_{\alpha} = \frac{1}{4\pi q} \left\{ 2 - 2\eta + 32(\eta - 1)^3 \right\} \text{ where } \eta = (\alpha - \varphi) \text{---(16).}$$

As for sinewave case, a probability distribution for e_x can be easily obtained from the above expressions. Also $e_{x,max.}$ may be similarly calculated. Thus

$$e_{x,max.} = \pm \frac{0.048}{9}$$

3.6. Error due to finite time of measurement on white noise

The noise voltage is sampled systematically with a sampling clock rate of p pulses/sec. It is assumed that p exceeds the Nyquist sampling rate viz $p \gg 2\Delta f$ where Δf is the bandwidth of the white noise sampled.

If the number of samples taken is C_0 then the measuring time is

$$T = \frac{C_0}{2\Delta f} \quad \text{assuming} \quad p = 2\Delta f$$

The r.m.s. value σ of the white noise is given by

$$\sigma^2 = \lim_{t_i \rightarrow \infty} \frac{1}{t_i} \int_0^{t_i} v^2 dt$$

any measurement conducted over a finite time t_i produces a result

$$\sigma_t^2 = \frac{1}{t_i} \int_0^{t_i} v^2 dt$$

If σ_t is to be taken as a measure of σ with any confidence then t_i must be large. The variance γ^2 of the distribution of σ_t can be considered as a measure of this confidence. Thus

$$\gamma^2 = \frac{(\sigma_t^2 - \sigma^2)^2}{\sigma^4}$$

The error in the measurement of σ will then be γ .

Assuming a normal distribution for the variation of σ_t^2 , the measured value σ_t will be within $\sigma \pm \sqrt{3} \gamma$ with 99.73% confidence.

Van Der Ziel⁵ has shown that

$$\gamma^2 = \frac{4}{t_i} \int_0^{\infty} \frac{\varphi^2(\tau) d\tau}{\varphi^2(0)}$$

where $\varphi(\tau)$ is the auto correlation function of the white noise input.

If an ideal low-pass filter is assumed, this expression can be evaluated (see Appendix B.3.)

$$\text{Thus } \gamma = \frac{1}{\sqrt{\Delta f \cdot t_i}}$$

Hence the 99.73% confidence limit is

$$e_T = \pm \frac{\sqrt{3}}{\sqrt{\Delta f \cdot t_i}} = \pm \frac{1.69}{\sqrt{\Delta f \cdot T}} \text{ -----(17).}$$

3.7. The overall error analysis.

The input waveform peak may be anywhere at $(m-1-\epsilon)$ within the interval between $(m-1)^{\text{th}}$ and m^{th} levels. Thus the error e_n which depends on the position of the peak, will be a random error. This assumes that no prior information regarding the input wave peak is available except that it is, between, say 8^{th} and 16^{th} levels, or between 15^{th} and 16^{th} levels, etc. The errors e_p and e_α will also be random. The probability distributions for e_p and e_α have been obtained. The distribution for e_n can be shown to be proportional to the slope of the e_n versus ϵ curve. To obtain the distribution for $e_n + e_p + e_\alpha$, it is assumed that these errors are statistically independent, and mutually exclusive.

$$\therefore p_m(e_n + e_p + e_\alpha) = p_m(e_n) * p_m(e_p) * p_m(e_\alpha)$$

where $p_m(x)$ is the probability distribution function for x and the symbol '*' denotes convolution.

If the distribution for $(e_n + e_p + e_\alpha)$ is required for a input whose peak can occupy any position between say the i^{th} and n^{th} levels with all positions being equally likely, then the following expression may be used

$$p_{in}(e_n + e_p + e_\alpha) = \frac{1}{n-i} \sum_{m=1}^n p_m(e_n) * p_m(e_p) * p_m(e_\alpha) \text{---(18).}$$

It should be noted that for one cycle mode $e_\alpha = 0$. To obtain the overall error, there remains the error e_1 to be added. As e_1 is evaluated as expected error, this presents no particular problem.

The convolutions mentioned above are difficult to perform analytically because the expression for $p(e_n)$ is intractable. Instead a graphical method can be conveniently used if n is known. The graphical method however has a disadvantage in that the ratio f/p needs to be given, in order that numerical calculations may be performed. This is illustrated in evaluating the overall errors for the 16-level instrument, in the next Chapter.

3.8. Effect of finite aperture time.

The "aperture time" μ_a is defined as the time taken to determine the level at a given instant. In the error analysis it has been assumed that the waveform amplitude changes negligibly during μ_a . If during a level determination process, the input waveform changes its level from

r^{th} to $r + 1^{\text{th}}$ value, then there will be an error in the measured value of V . The aperture time, therefore, restricts the upper frequency of the instrument. Assume that during any level determination process the level should not change from r to $r + 1$. This requires that the input signal should not have a slope which at any time exceeds $\frac{V_a}{\mu_a \tau}$ V/sec.

Even when the frequency of the input is below the upper limit, errors due to finite aperture time will arise, when a sample occurs at the points when the input crosses a level. This error depends on the method of level determination and the probability that a sample occurs at a level crossing. In the successive approximation method of level determination, error due to finite aperture time will be positive or negative depending on whether a "critical decision" lies to the left or right of the level crossing. The "critical decision at the r^{th} level is defined as the comparison of the input waveform with the r^{th} level voltage. Thus, the position of this critical decision must be known before the error due to aperture time can be evaluated.

CHAPTER 4

THEORETICAL ERROR ANALYSIS FOR THE 16-LEVEL INSTRUMENT

The theoretical error analysis can now be performed, using the general results of Chapter 3. As the instrument may be used in either of the two possible modes, two overall analyses for a given input waveform are required. It was noted in Chapter 3 that graphical convolution is more convenient to use in order to obtain the overall characteristics. This method, however, requires that the ratio f/p be given. Hence the overall characteristics are given for one particular value of f/p . Individual errors however may be expressed as functions of f/p .

4.1. Error e_n due to quantisation.

Appendix C. gives computer programmes for calculating e_n and for any level for sine wave and for triangular wave inputs.

The inverse of the derivative is the probability distribution, since for all values of ϵ , between a given level interval, being equally likely, the normalised probability distribution function of e_n is given by

$$p(e_n) = \frac{1}{\left(\frac{de_n}{d\epsilon}\right)}$$

The programmes are used to calculate these two sets of results for all levels from 8 to 16 by inverting appropriate data. Typical results for sine wave and triangular wave inputs are shown in Fig.14, 15, 16 and 17.

Triangular Wave Input.

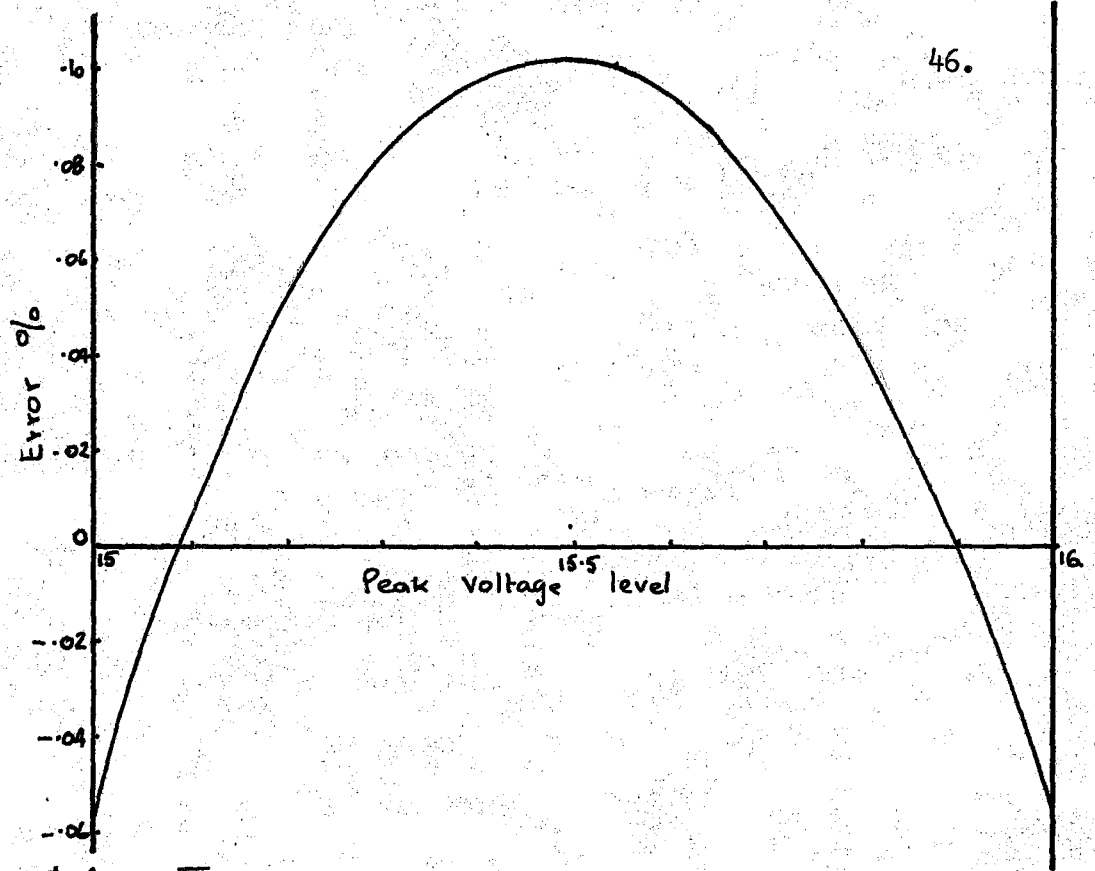


Fig: 14 : Error e_n for partially filled 16th level.

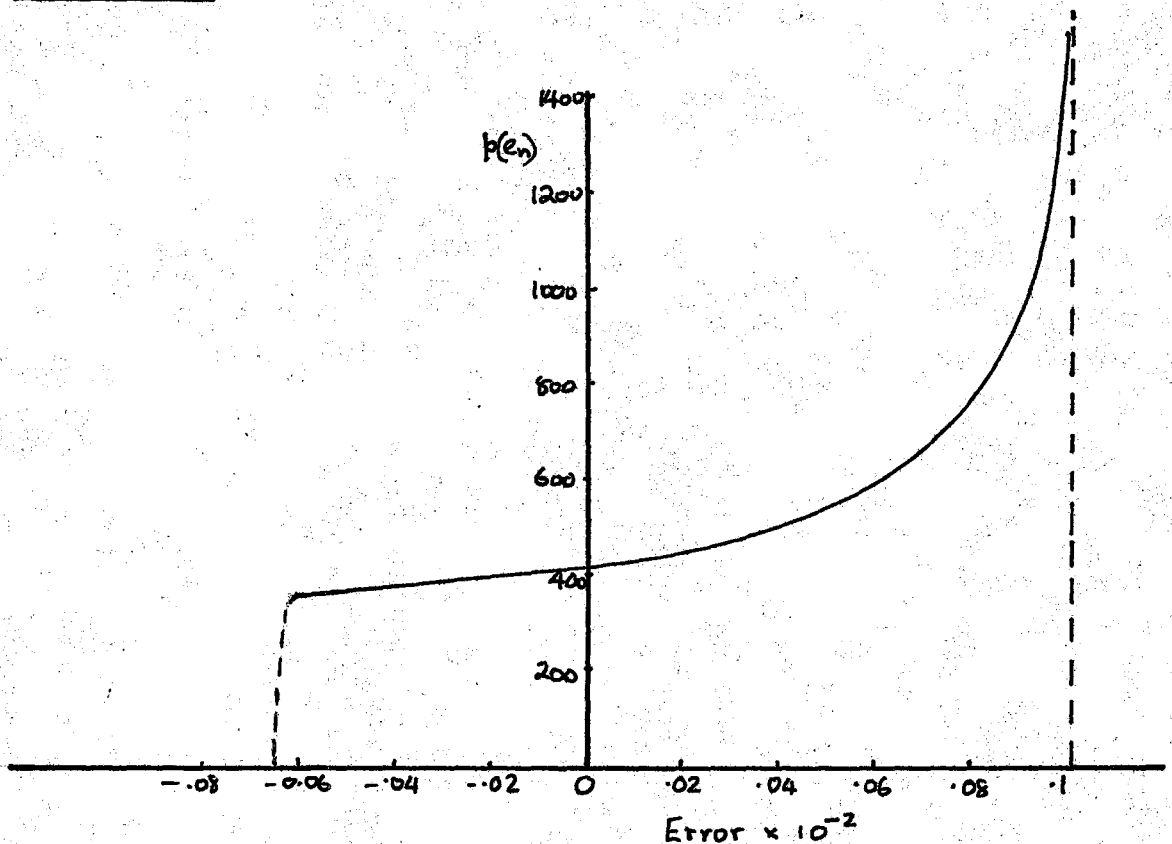


Fig: 15 : Probability distribution of error e_n .

Sine Wave Input.

47.

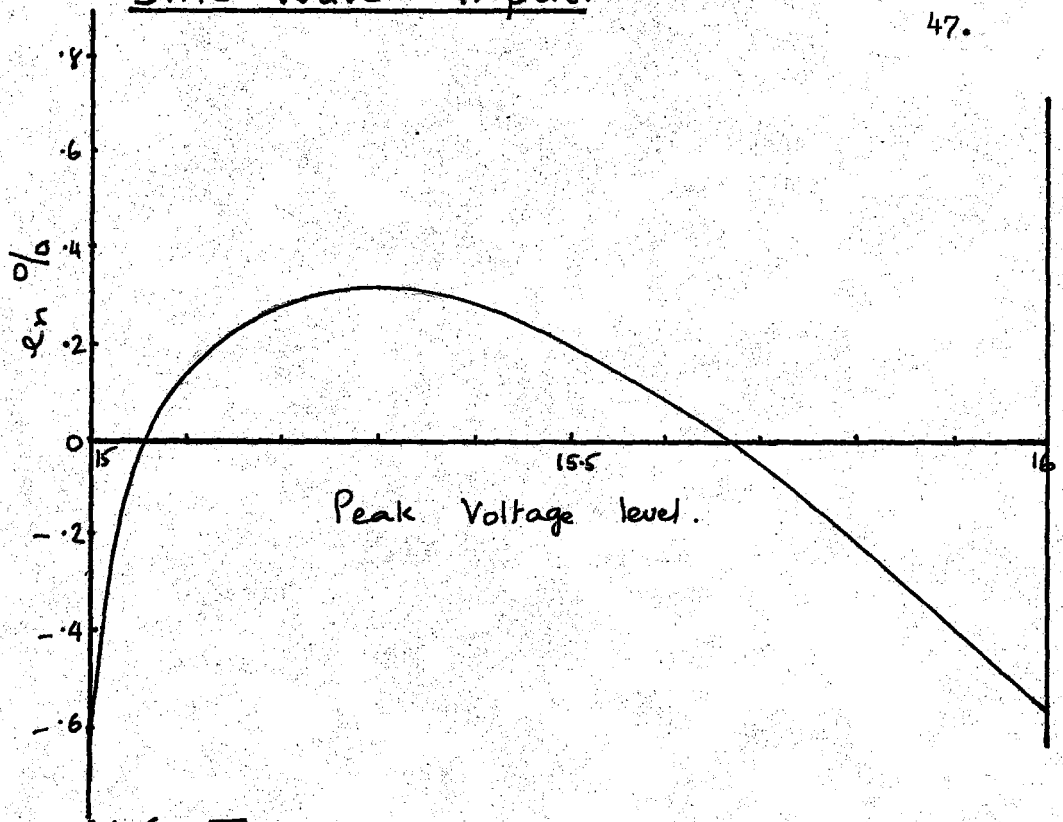


Fig: 16 : Error e_n for partially filled 16th Level.

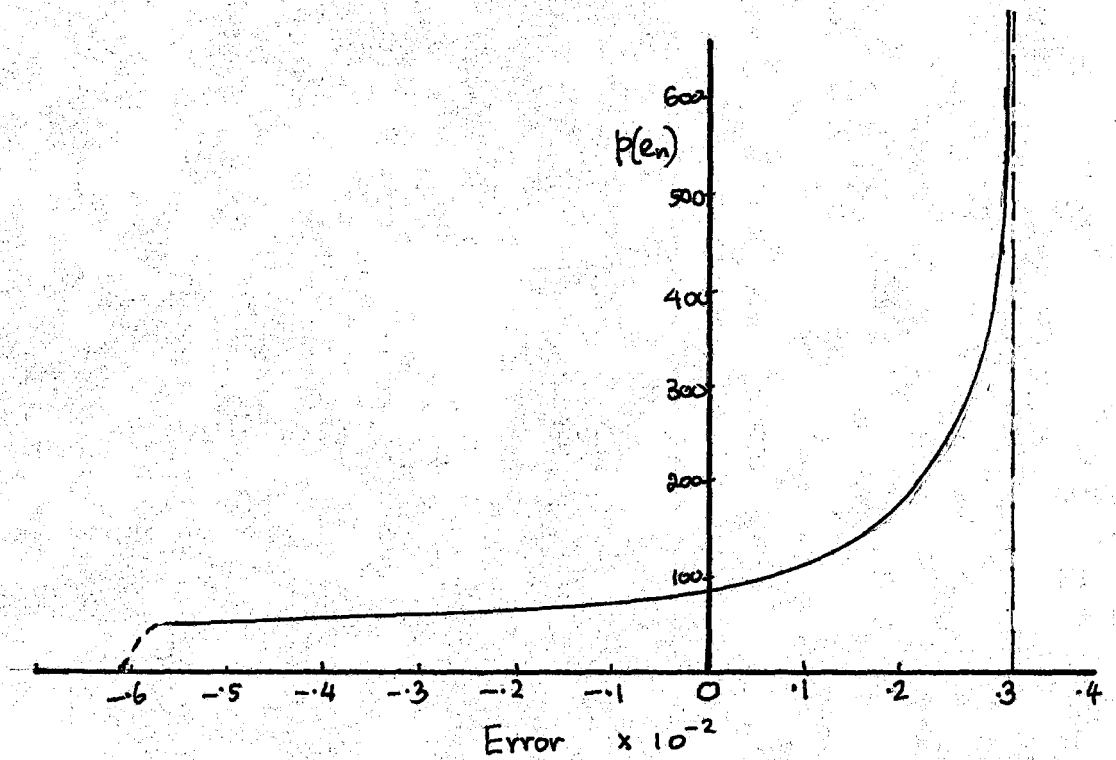


Fig: 17 : Probability distribution of error e_n .

The error e_n for normal distribution noise is similarly calculated using the programme of Appendix C. It is seen from Fig. 18 that for a 16 level instrument, the standard deviation (r.m.s. value) which can be measured within 1% is given by

$$\frac{V_n}{2.58} \geq V \geq \frac{V_n}{7}$$

The precision and range can be improved considerably by using a larger number of levels.

If the ratio f/p is small and the one cycle mode is used then, e_n is the only predominant error. In this case the overall error characteristics are determined by e_n . Error curves for individual level intervals are used to obtain the frequency histograms for e_n when the input waveform peak is anywhere between the 8th and 16th levels or between the 12th and 16th levels. The histograms are shown in Fig. 19, 20, 21, and 22.

4.2. Error e_p due to finite sampling rate.

The application of the central limit theorem to the error formula 6, gives an e_p whose probability distribution function is Gaussian. The accuracy of this Gaussian approximation can be readily established. Thus the worst case error arises if $\beta_r = 1$ and $\delta_r = 0$ for all r or if $\delta_r = 1$ and $\beta_r = 0$ for all r .

$$\therefore e_p \text{ worst case} \quad \doteq \quad -\frac{1}{2V_n^2} \frac{f}{p} \quad \text{if } \beta_r = 1, \delta_r = 0$$

$$\text{and} \quad \doteq \quad +\frac{1}{2V_n^2} \frac{f}{p} \quad \text{if } \delta_r = 1, \beta_r = 0$$

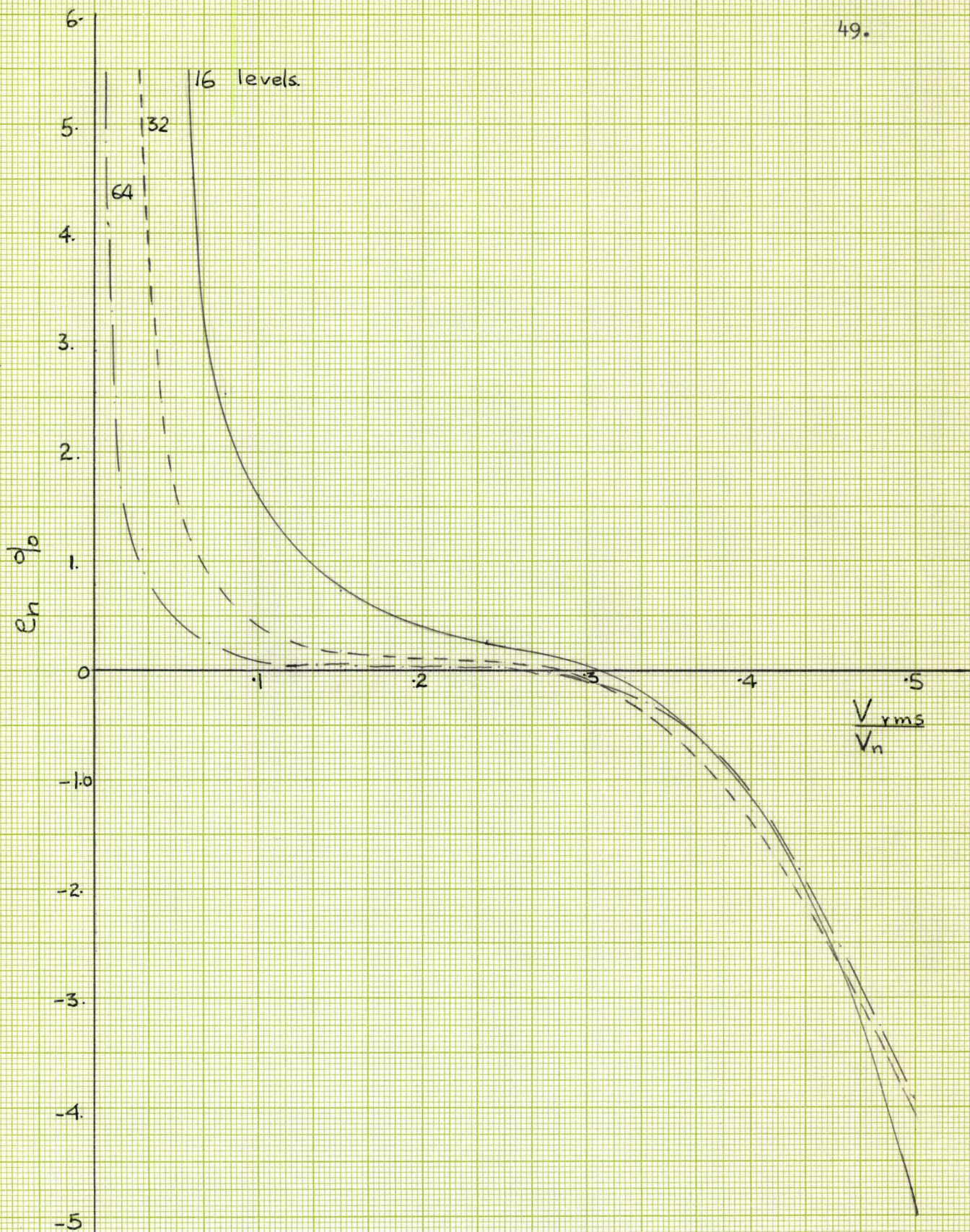


Fig 18 : Error e_n for normal-distribution noise

Normalising Constant = $\sum_{i=1}^n f_i = 750$

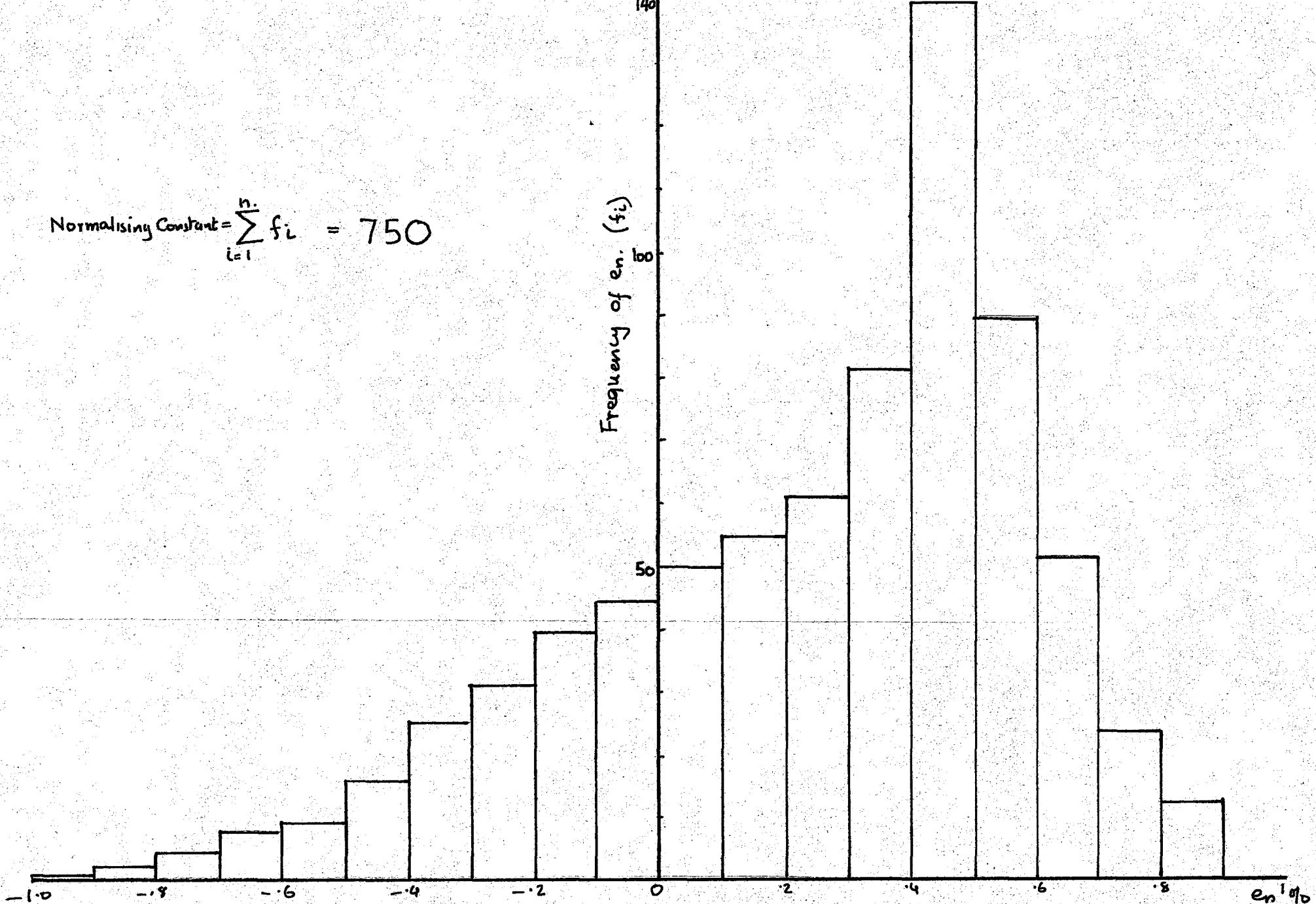


Fig. 19: Frequency histogram of en. Sine Wave Input peak between 8th-16th levels.

Normalising Constant = $\sum_1^7 f_i = 400$

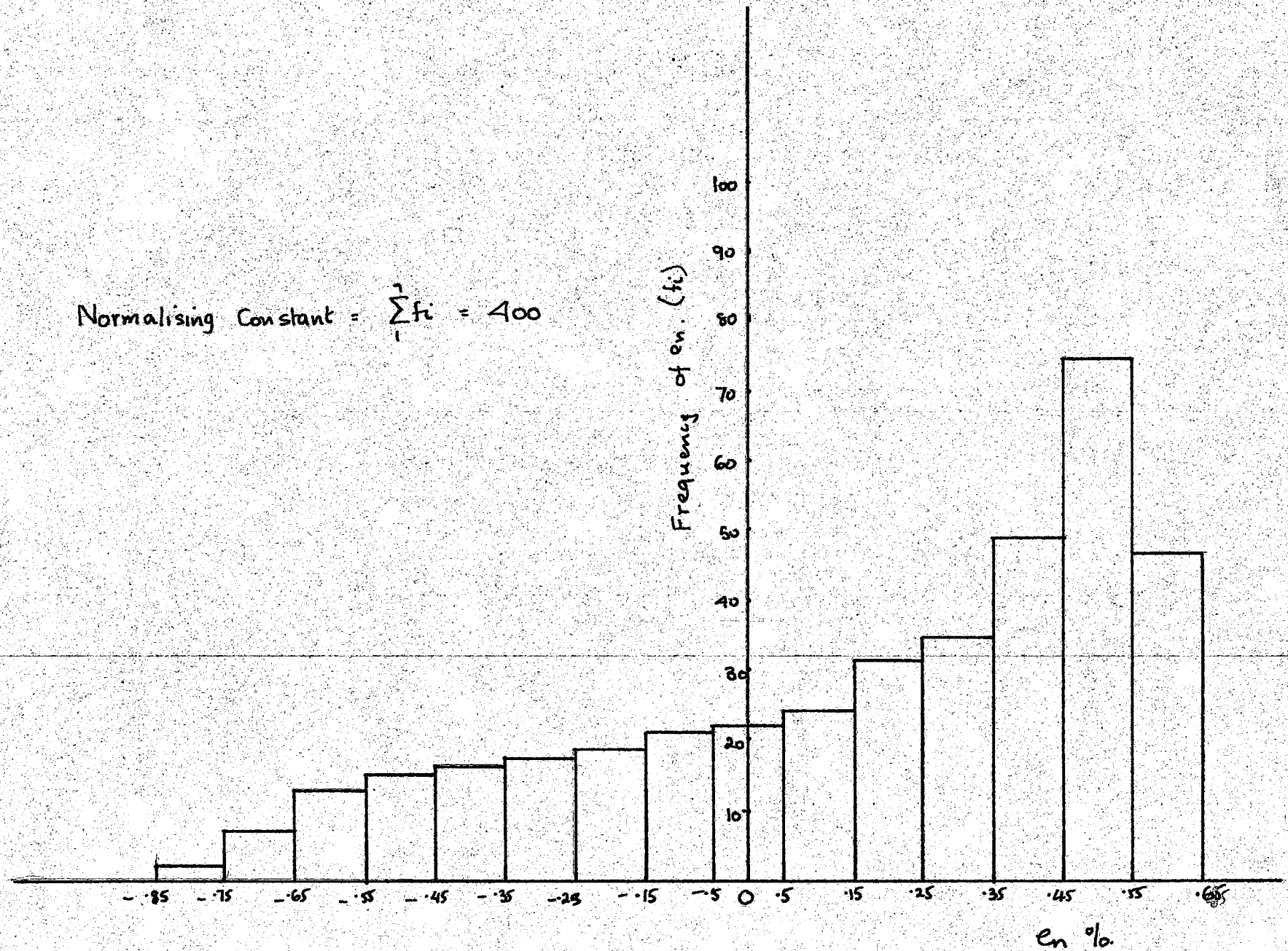


Fig. 20 : Frequency Histogram of e_n . Sine Wave Input peak between 12th - 16th levels

Normalising Constant = $\sum_{i=1}^n f_i = 900$

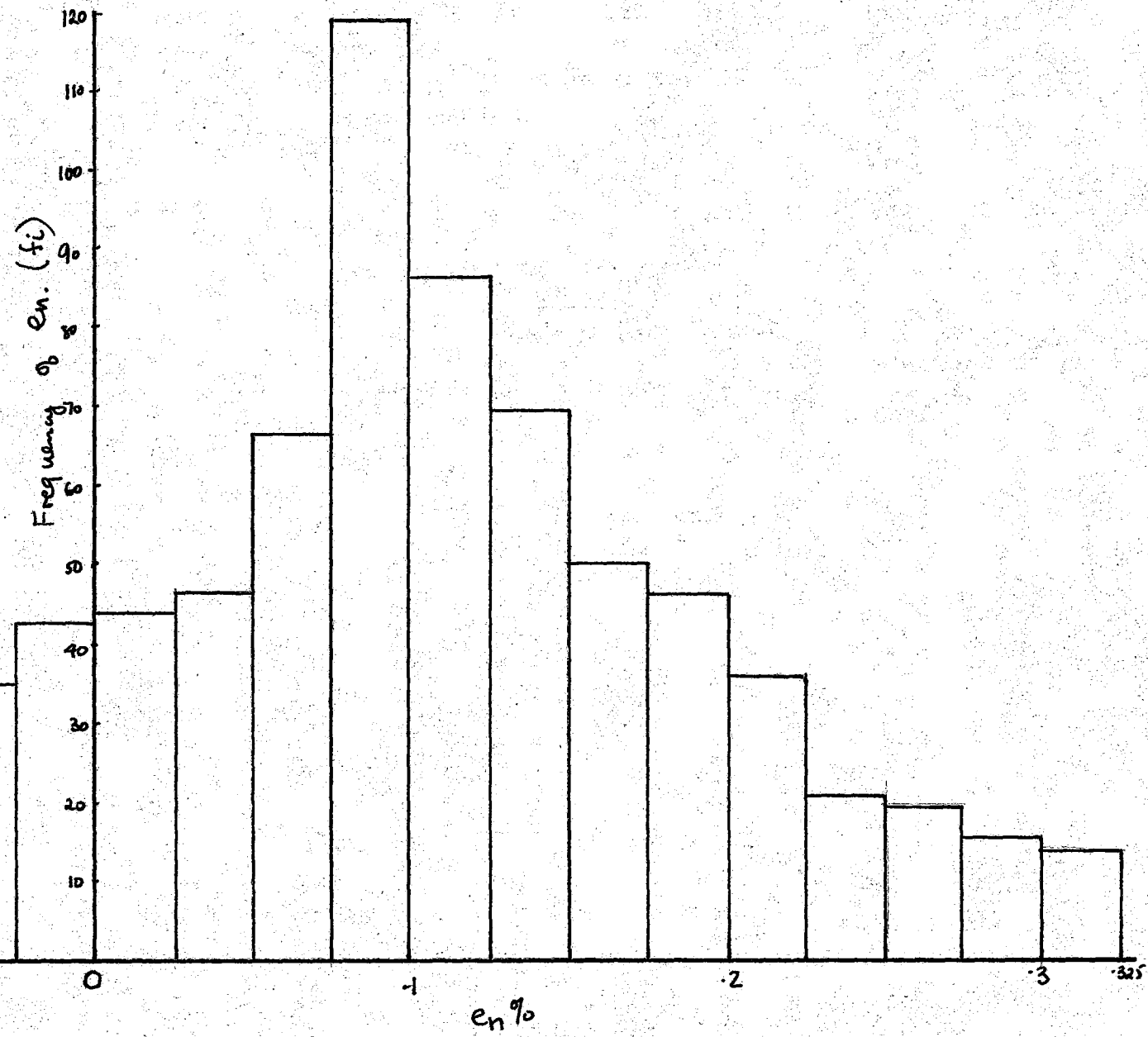


Fig: 21 : Frequency Histogram of en: Triangular Wave Input peak between 8th - 16th levels

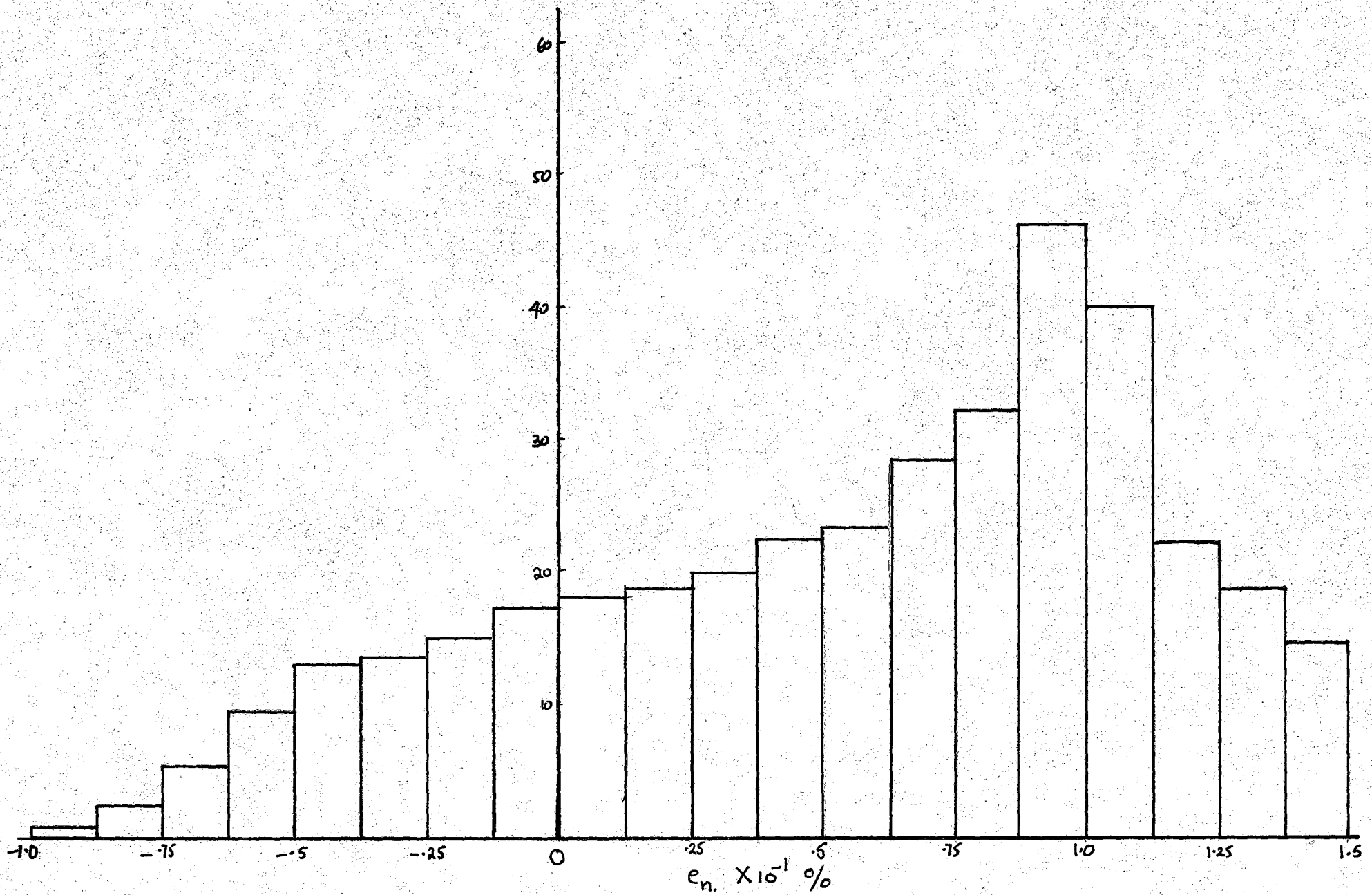


Fig : 22 : Frequency histogram of e_n : Triangular Wave Input peak between 12th - 16th levels

The standard deviation of the Gaussian curve is

$$\sigma = \frac{1}{16V_n^2} \frac{f}{P} \quad \text{for the 16-level case.}$$

For a Gaussian distribution the 99.73% confidence limit is $\pm 3\sigma$ about the mean value. It is seen from above that the worst case errors are well beyond the 99.73% confidence limit. Hence the Gaussian approximation is accurate. Figs 23, 24, shows typical probability distribution curves for e_p for sine wave and triangular wave inputs. The distributions are expressed in terms of f/p . Similar results are obtained for the other levels.

In case of normal distribution noise input, the $e_{p.av.}$ is given by

$$e_{p.av.} = \frac{1}{V^2} \frac{\tau Z_0}{4n^2} \left\{ 16 \exp\left(\frac{-1}{2V^2}\right) - \exp\left(\frac{-1}{512V^2}\right) \right\}$$

for noise passed through a L.P. filter with cut-off at f_c Hz

$$e_{p.av.} = \frac{1}{512\sqrt{3}} \frac{f_c}{P} \frac{1}{V^2} \left\{ 16 \exp \frac{-1}{2V^2} - \exp\left(\frac{-1}{512V^2}\right) \right\}$$

Fig. 25. shows a graph of $e_{p.av.}$ p/f versus V .

4.3. The error e_α due to a non-integral number of cycles being sampled.

For the one cycle sampling mode e_α does not arise. In the self-timed, mode, e_α is a function of p/f . Assuming that α and ϕ have all values between 0 and 1, the distribution for $(\alpha - \phi)$ can be easily obtained. This is then used in the formulae given in Chapter 3, to obtain the probability distribution of e_α . The error e_α is independent of the position of the peak. Hence results given in Fig. 26 and 27 are applicable

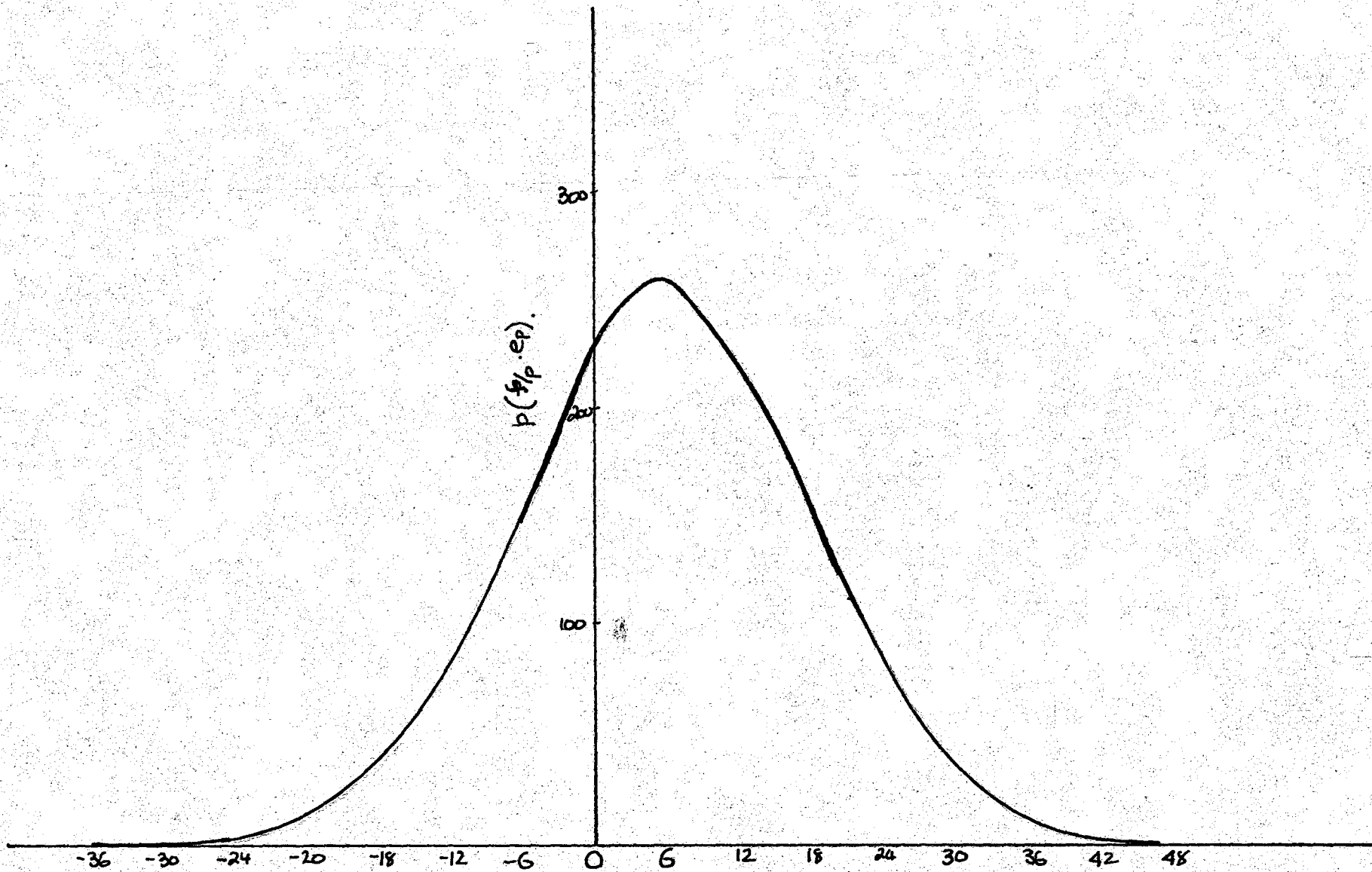


Fig. 23: Probability distribution of $(ep \cdot \frac{p}{4}) \%$ ^{$ep \cdot \frac{p}{5} \%$} Sine Wave Input peak at 16th level

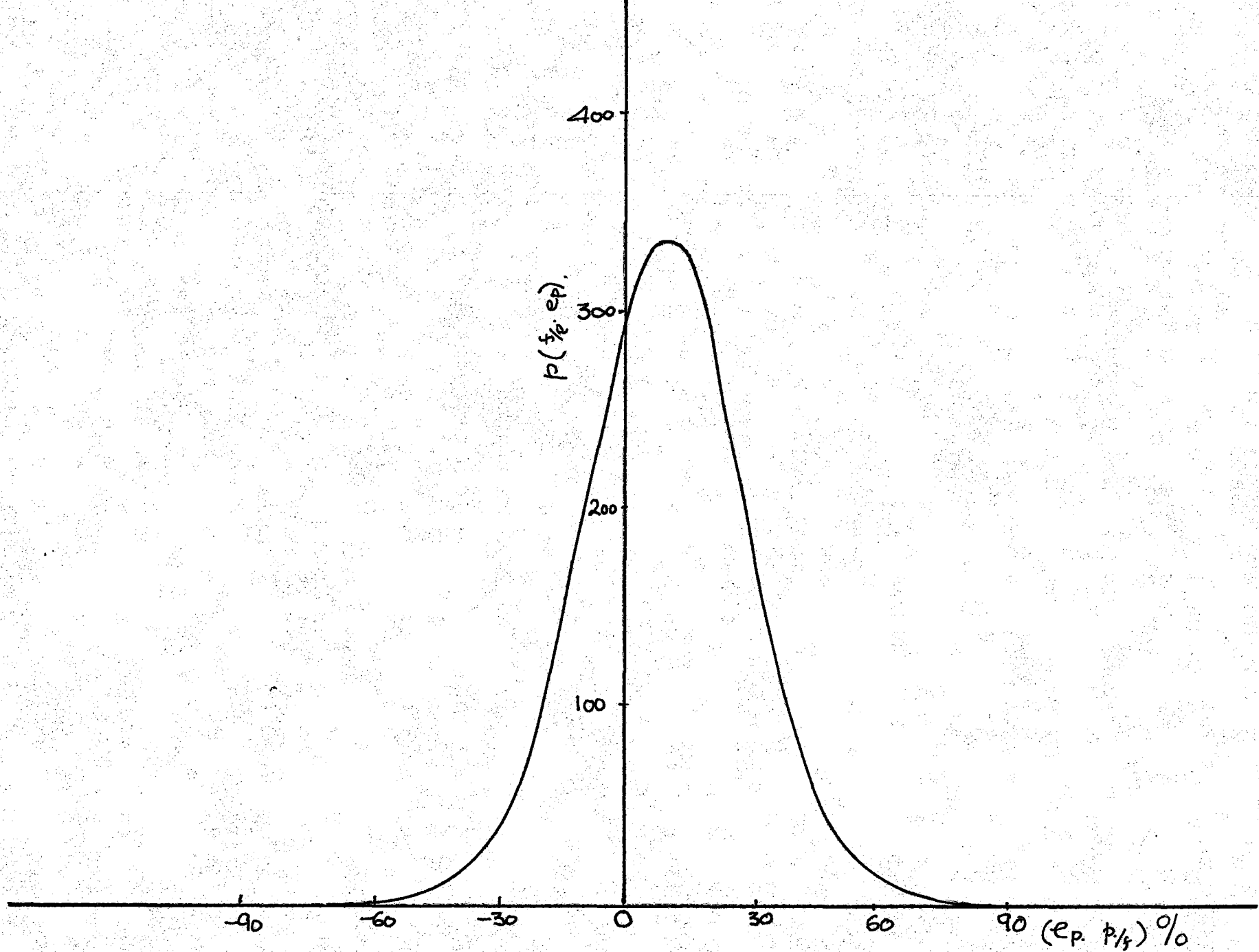


Fig: 24 : Probability distribution of $(ep. P/4)$. Triangular Wave Input peak at 16th level

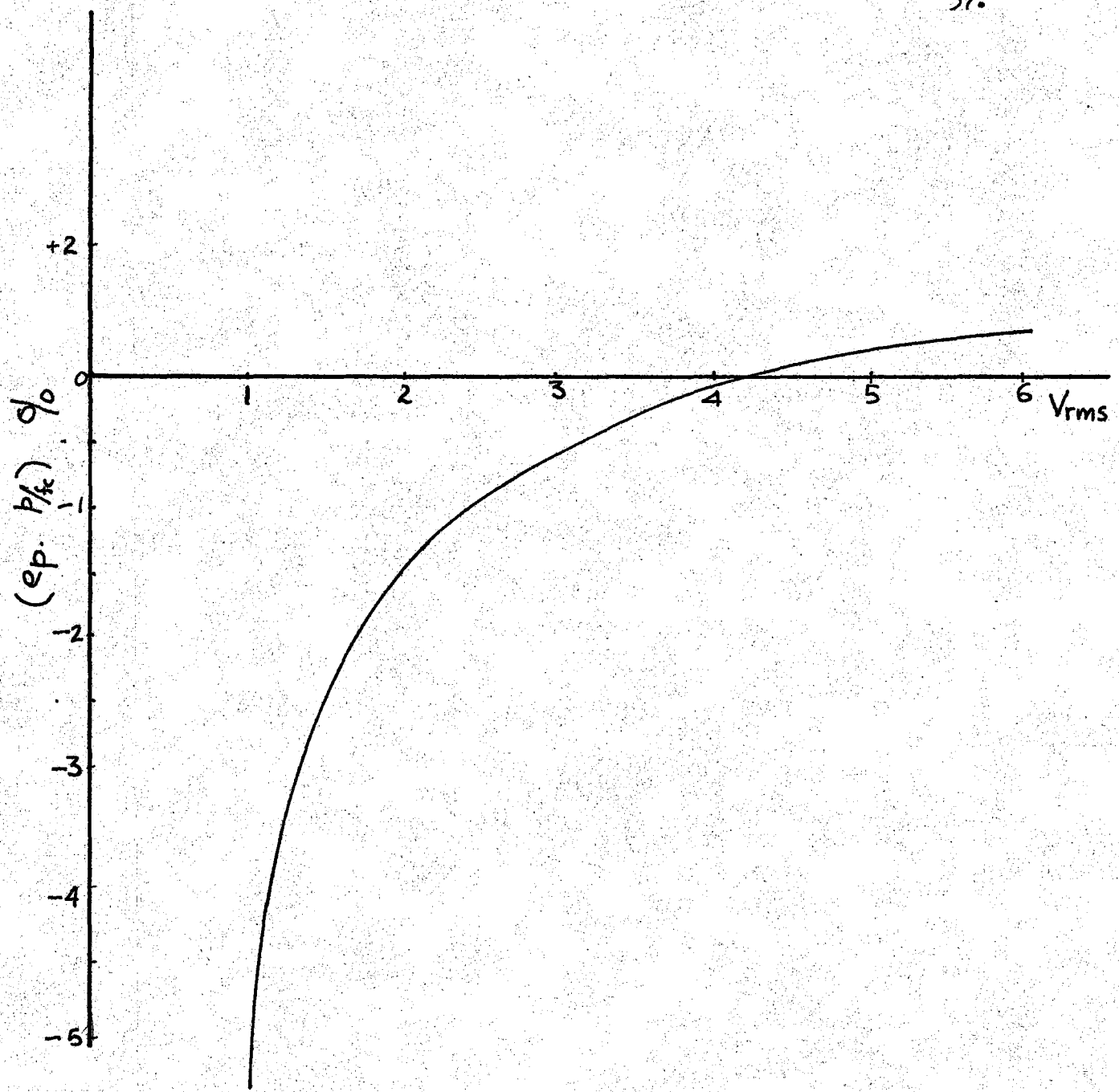


Fig 25 : Error e_p for Normal distribution noise

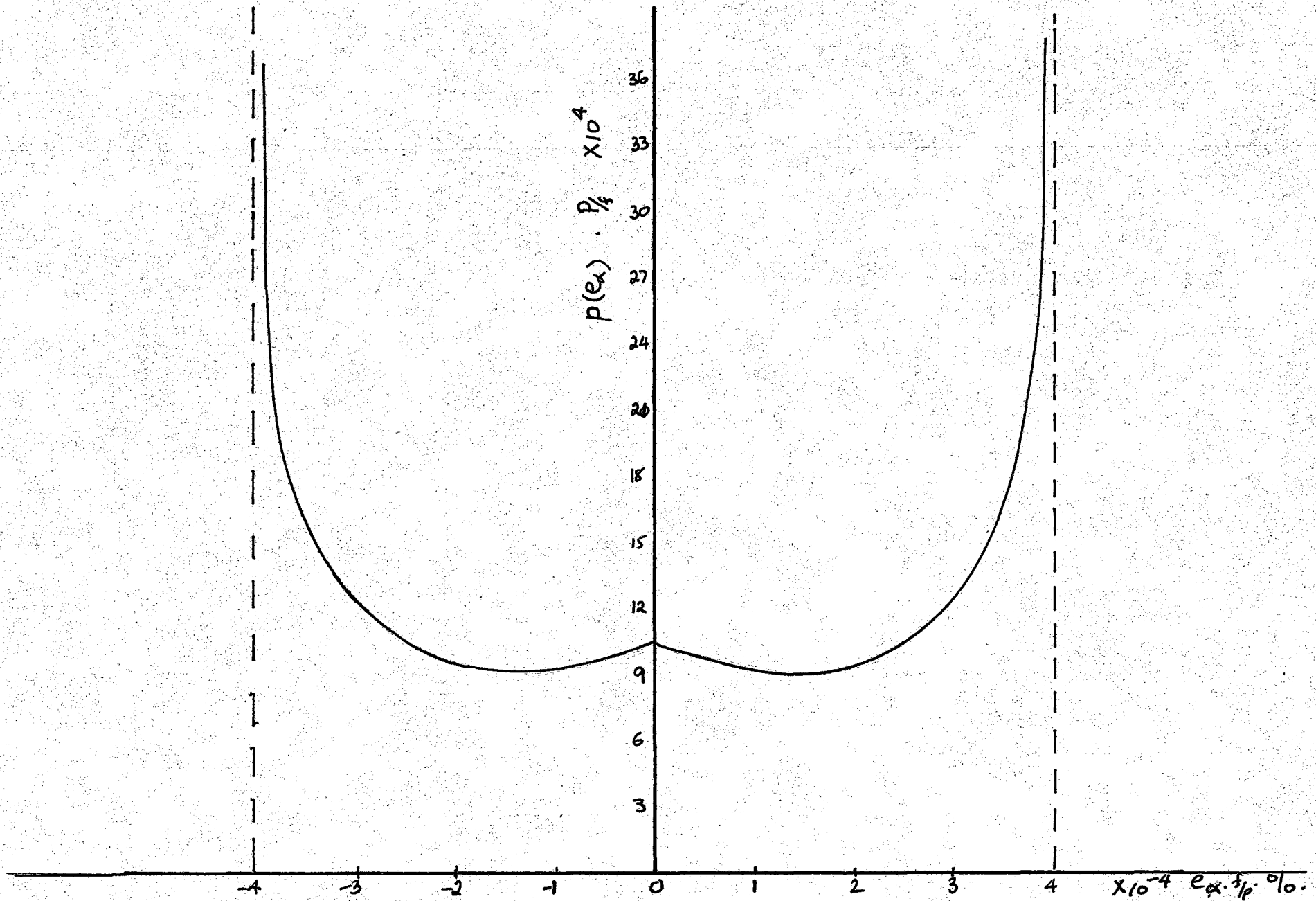


Fig : 26 : Probability distribution of e_α : Sine Wave.

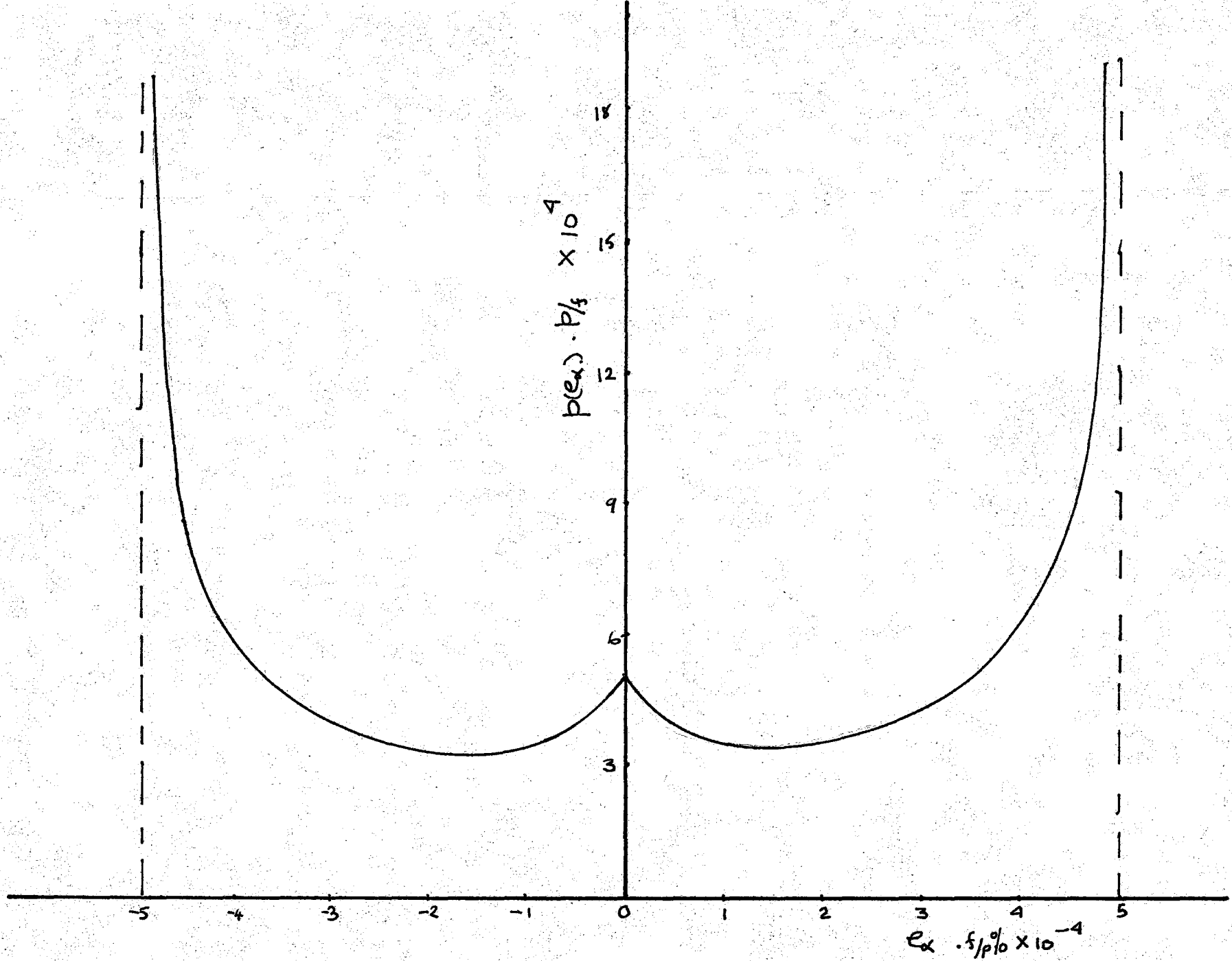


Fig: 27 : Probability distribution of e_α : Triangular Wave.

to any peak position. The error is expressed in terms of p/f.

4.4. The error e_1 due to level inaccuracies.

Calculations of $e_{1.av.}$ can be carried out only if the level offset at each level is known. This method becomes very tedious. Instead an average δE may be assumed to be present for all levels. Thus the following results are obtained.

(i) Sine wave

$$e_{1.av.} = \frac{n}{m} \delta E F_s \text{ where } \delta E \text{ is normalised w.r.t. } V_n = 10V$$

$$\text{and } F_s = \frac{4}{\pi m^2} \sum_{r=1}^m \frac{r}{\sqrt{1 - \left(\frac{r}{m}\right)^2}}$$

Computed values of F_s are as follows:

m	8	9	10	11	12	13	14	15	16
F_s	.813	.839	.861	.880	.896	.910	.924	.936	.946

(ii) Triangular wave.

$$e_{1.av.} = \frac{3 \delta E}{2 m^2} n(m - 1)$$

$$= \frac{n}{m} \delta E F_s \text{ where } F_s \text{ is as follows.}$$

m	8	9	10	11	12	13	14	15	16
F_s	1.31	1.33	1.35	1.36	1.378	1.385	1.395	1.40	1.41

(iii) Normal distribution noise.

$$e_{1.av.} = \frac{\delta E}{V} F_n$$

where
$$F_n = \frac{1}{128V^2} \sum_{r=1}^{n-1} \frac{r}{\sqrt{2\pi}} \exp\left(-\frac{r^2}{512V^2}\right)$$

For $n = 16$ the following values of F_n are obtained ¹

V	.2	.25	.33	.5
F_n	.8	.79	.78	.67

In practice it is possible to make δE small, in which case the error e_1 will be negligible.

4.5. The error e_T for normal distribution noise.

For 99.73% confidence

$$e_T = \frac{1.69}{\sqrt{f_c T}}$$

For $f_c = 1\text{KHz}$, the following values of T are obtained

99.73% confidence e_T	10	1	.1	.01	.54
T	0.3 Sec.	30 Sec.	50 m.	8.33 hrs.	100 sec.

4.6. The overall error analysis

(i) The overall characteristics of importance are the distributions of $(e_n + e_p)$ and $(e_n + e_p + e_{\alpha})$ for periodic wave inputs and of $(e_n + e_{p.av.} + e_T)$ for normal distribution noise. The error e_1 depends on the particular instrument but if care is taken then this error will be negligible. Appendix D. outlines a method of graphical convolution using impulse function approximation. It is reasonable to

expect that some scaling will be used in the instrument so that at least half the available levels will be used. An arbitrary value for f/p is chosen so that some numerical confidence limits may be established theoretically and checked experimentally. Numerical convolutions are performed to obtain $p_m(e_n)^* p_m(e_p)$ for $m=8$ to $m=16$. The method outlined in Section 3.5. is used to obtain the distribution of $e_n + e_p$ when the peak of the input is anywhere between the 8th and 16th levels or anywhere between the 12th and 16th levels. These distributions are shown in Fig. 28 and 29.

To calculate the distribution for $(e_n + e_p + e_\alpha)$, it is realised that e_α is independent of the position of the peak. Hence

$$\begin{aligned} p_{i,n}(e_n + e_p + e_\alpha) &= \frac{1}{n-i} \sum_{m=i}^n \left\{ p_m(e_n)^* p_m(e_p)^* p_m(e_\alpha) \right\} \\ &= \frac{1}{n-i} p(e_\alpha)^* \sum_{m=i}^n \left\{ p_m(e_n)^* p_m(e_p) \right\} \\ &= \frac{p(e_\alpha)^*}{n-i} \sum_{m=1}^n p_m(e_n + e_p) \end{aligned}$$

Thus the result for $e_n + e_p + e_\alpha$ is calculated using the distributions of $(e_n + e_p)$. See Figs. 30 and 31. for $f/p = \frac{1}{300}$.

(ii) For white noise filtered by a 1 KHz Low Pass filter, the Nyquist rate of sampling is 2 KHz. If $C_0 = 10^6$ the time of measurement is

$$T = \frac{10^6}{2 \times 10^3} = 500 \text{ sec.}$$

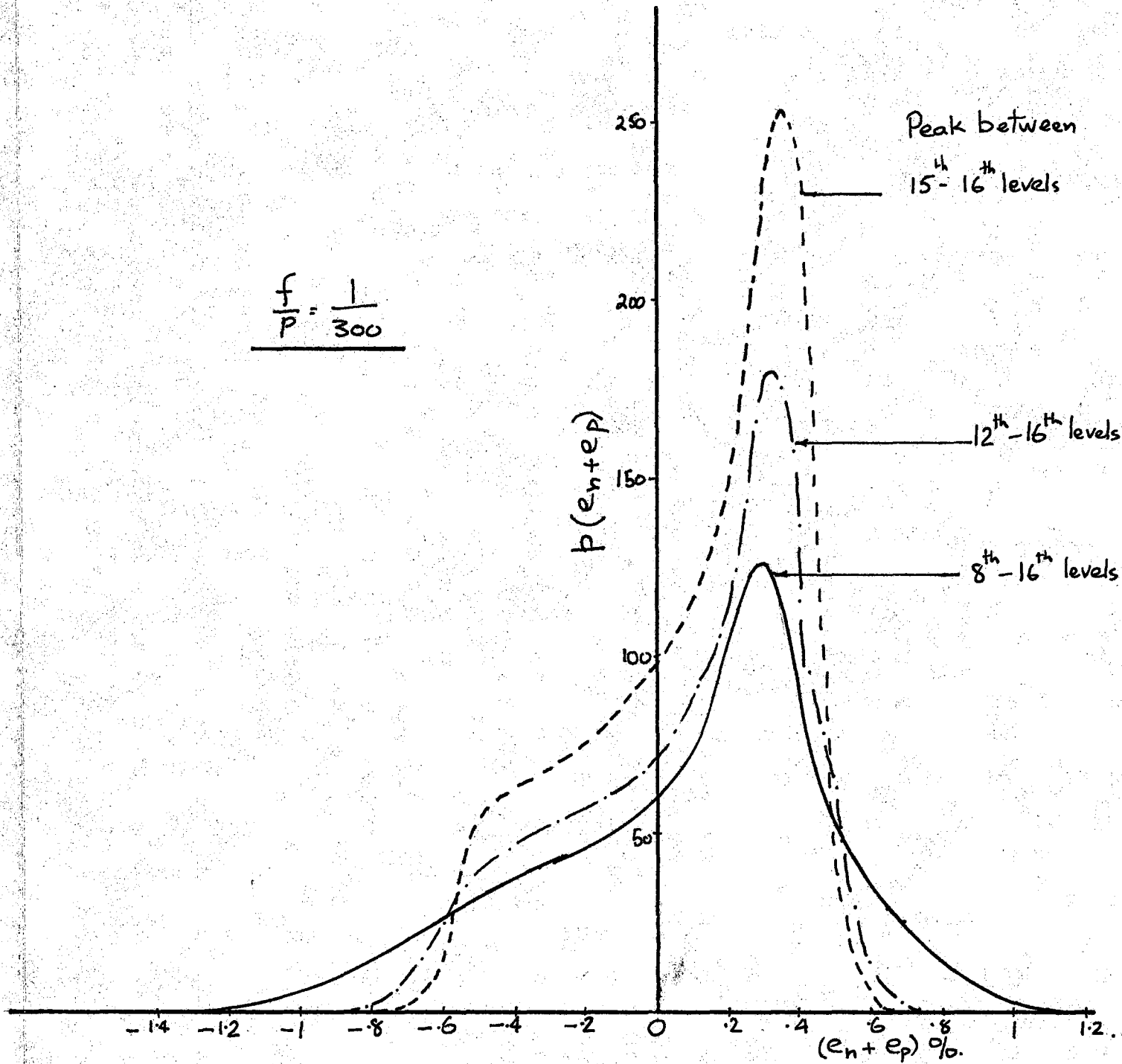


Fig:28: Probability distribution of $(e_n + e_p)$: Sine Wave.

$$\frac{p_i}{p_j} = \frac{1}{300}$$

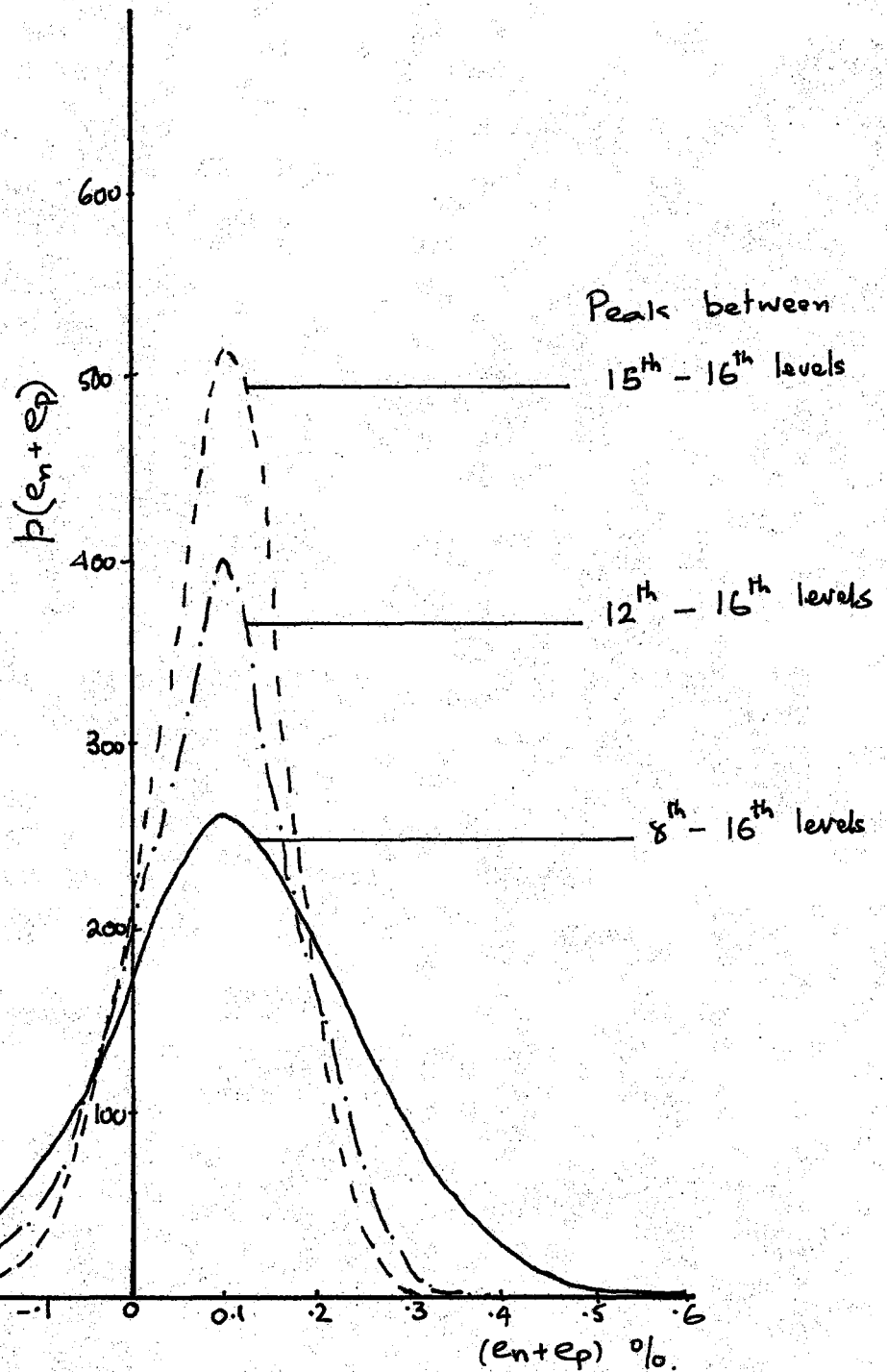


Fig 29.: Probability distribution of $(en+ep)$: Triangular Wave.

$$\frac{f}{P} = \frac{1}{300}$$

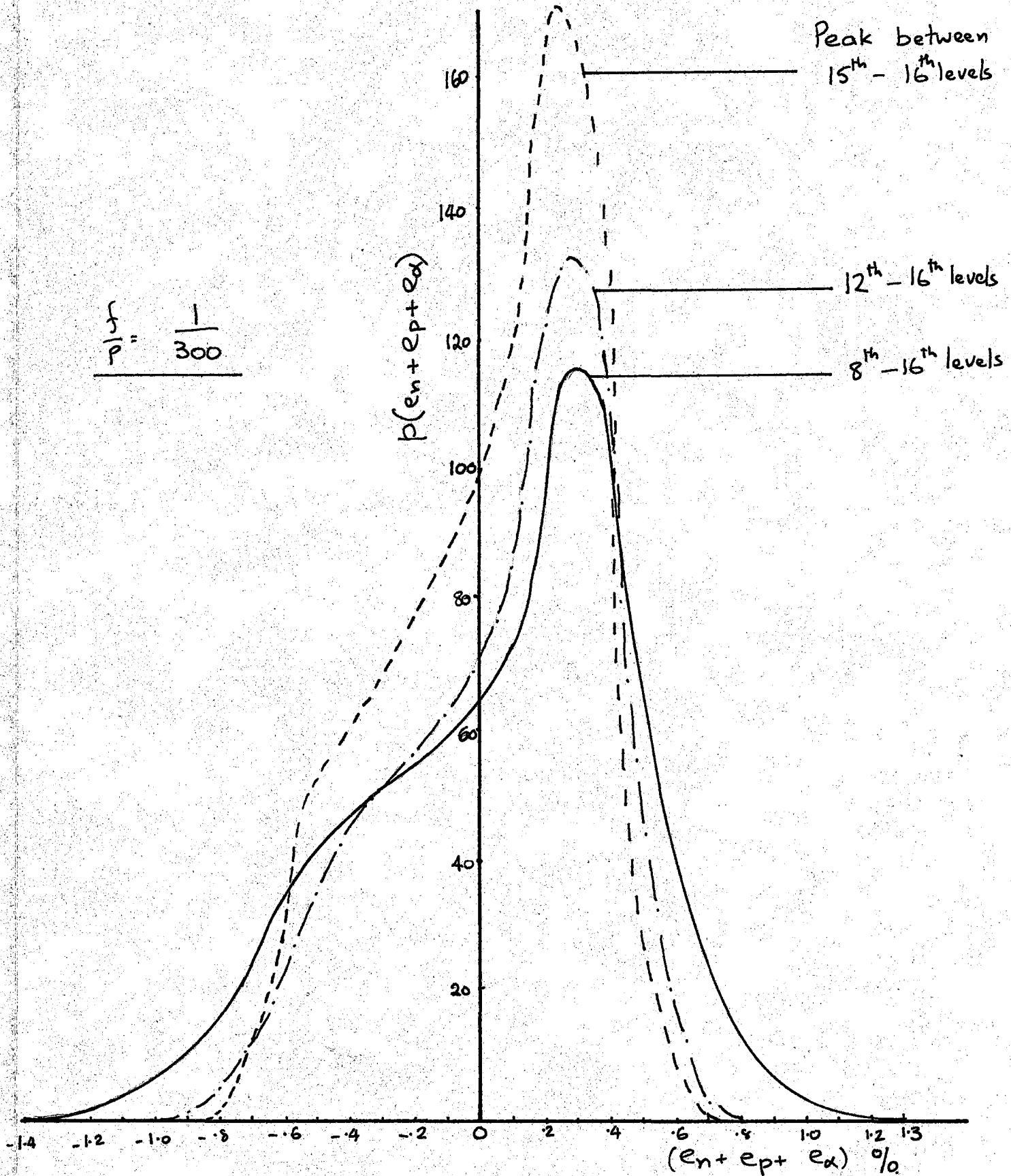


Fig: 30: Probability distribution of $(en+ep+ea)$. Sine Wave.

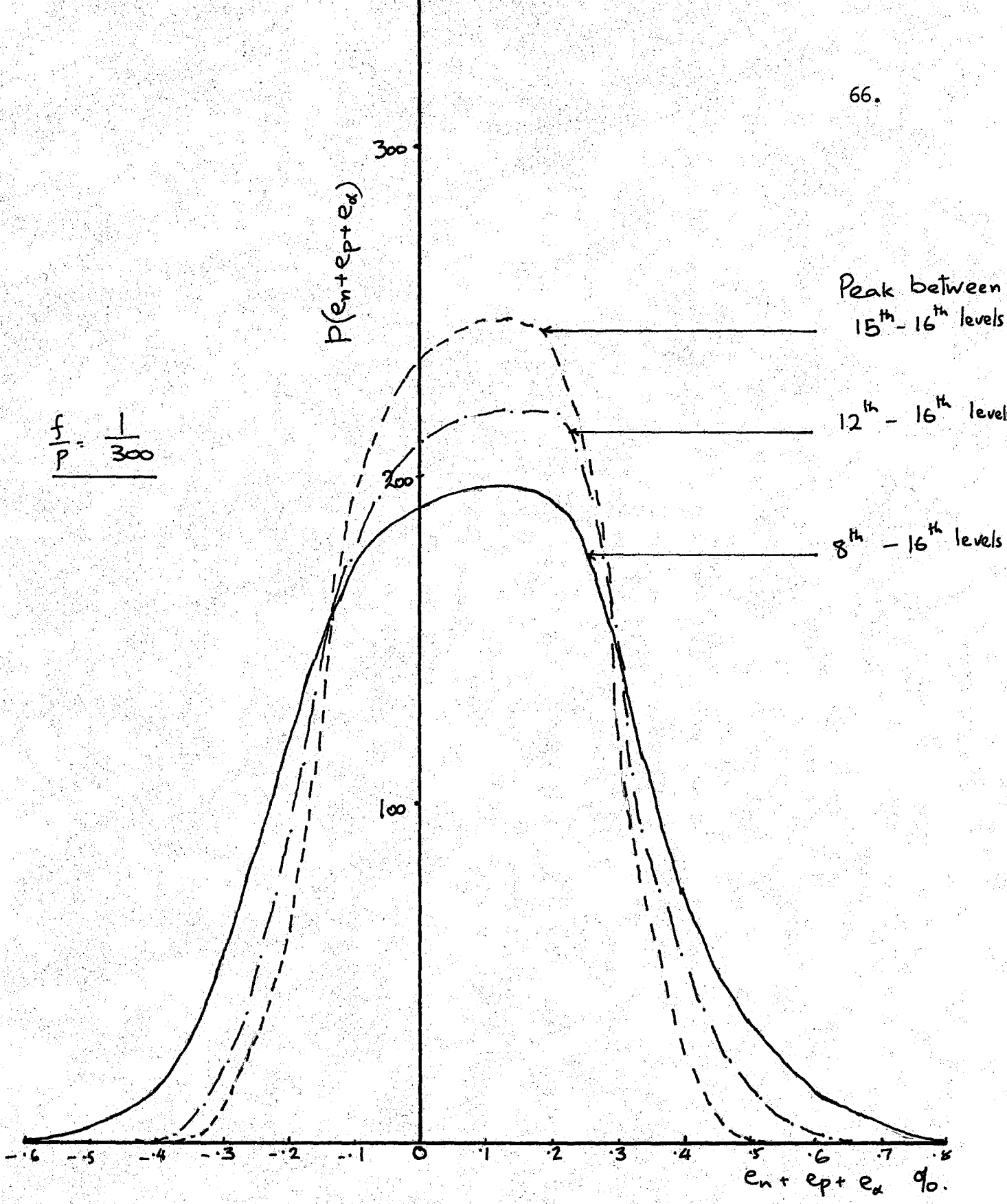


Fig :31: Probability distribution of $(e_n + e_p + e_a)$: Triangular Wave.

In this case $e_T \doteq 0$. Even if $T = 100$ sec., the error e_T will be small. Assuming that $T = 100$ sec. the total error $(e_n + e_p + e_T)$ can be calculated. Fig. 41, gives a graph of $(e_n + e_p + e_T)$ versus V .

CHAPTER 5

EXPERIMENTAL ANALYSIS

5.1. Performance check and level offset measurements

The instrument can be checked by observing the performance of the A/D converter system for d.c. inputs. The same circuit may be used to measure the level offsets. The direct decimal readouts for d.c. inputs were calculated in Chapter 1 and are given in Table III. The d.c. input is adjusted to a value within a level interval to be checked. The instrument is set in the self-timed mode and arranged to stop when $C_0 = 10000$. The sampling clock frequency is $p = 10^4$ Hz. The $\sum_{r=1}^{n-1} rC_r$ reading should agree with the value given in Table III. This was repeated for all levels and for positive and negative inputs. It was found that the $\sum_{r=1}^{n-1} rC_r$ reading did not differ by more than one count for any level, from the theoretical values. To measure the level offsets, a differential voltmeter is connected in the system to measure the d.c. input. The d.c. input is set slightly lower than the voltage corresponding to the level r selected. The $\sum_{r=1}^{n-1} rC_r$ reading is observed and should correspond to the reading for a voltage between $(r - 1)^{\text{th}}$ and r^{th} level. The input voltage is increased by small amounts until the $\sum_{r=1}^{n-1} rC_r$ reading changes to that corresponding to the next level interval. The difference between the measured and theoretical change over voltages gives the level offset. Fig. 32 shows the level offsets at various levels for positive and negative inputs.

The level offset in most cases is small and does not exceed $\pm 8\text{mV}$

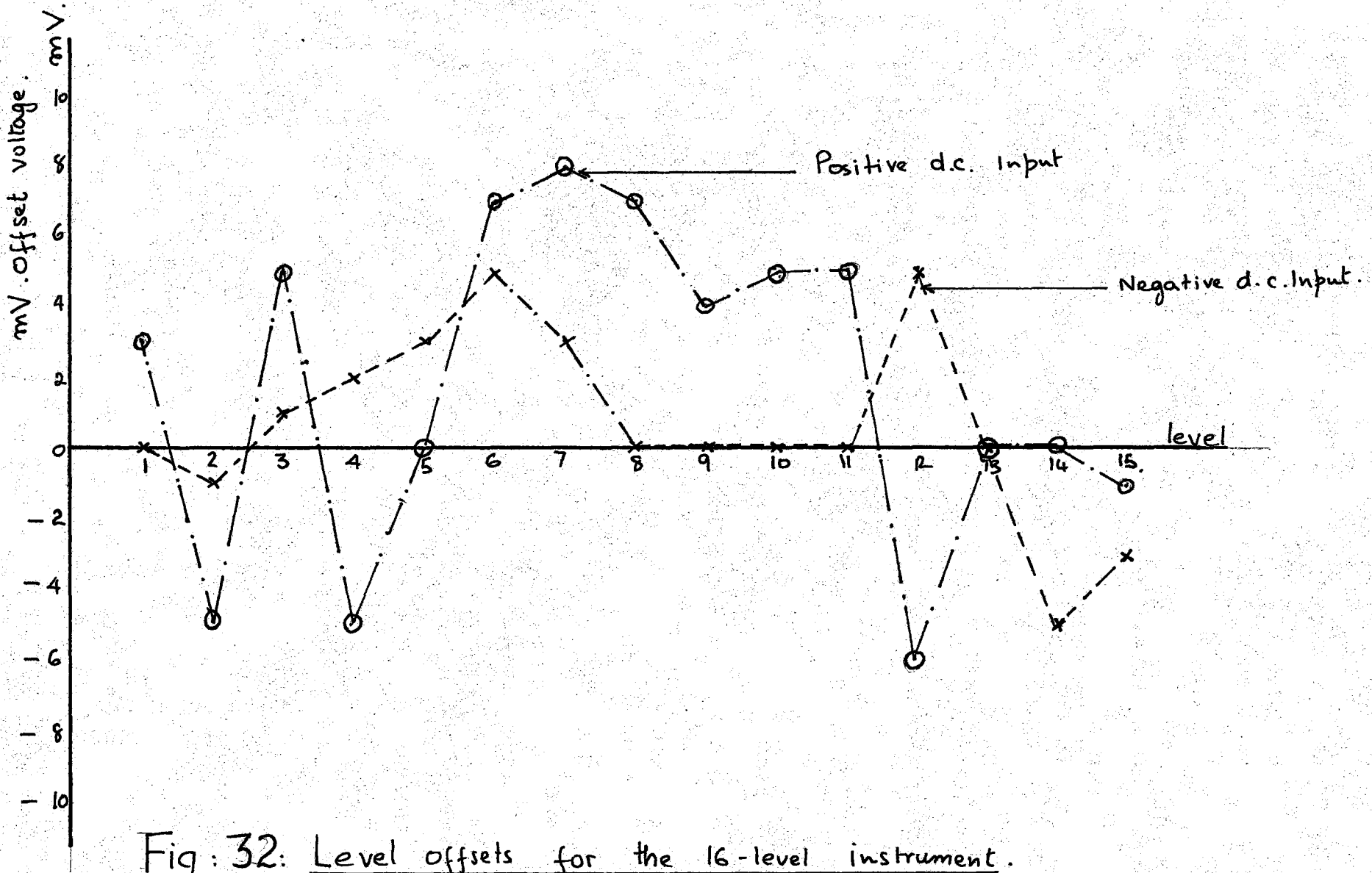


Fig: 32: Level offsets for the 16-level instrument.

at any level. Hence it is justified to assume that the error e_1 due to level offsets is small in practice.

5.2. Error measurements for periodic inputs

For accurate measurements of the error characteristics of the 16-level instrument, two basic requirements need to be satisfied. These are as follows:

- (a) The periodic waveform should have negligible distortion. It should also not have a d.c. component.
- (b) The r.m.s. value of the input should be measured accurately.

The function generator selected has very low distortion (.05% measured). The d.c. level output can be adjusted to a minimum for maximum a.c. output (\ll 1% of full scale peak output voltage).

Fig. 42. shows the circuit used for the measurements. The r.m.s. value of the input waveform is measured by a thermal transfer standard. The d.c. voltage required by the thermal standard is obtained from a low ripple, stabilised power supply unit, the d.c. voltage being measured by the differential voltmeter to the accuracy of 0.2%. The thermal standard is accurate to within 0.04% for frequencies above 5 Hz. Thus using this method periodic voltages can be set an accuracy better than ¼%.

5.3. Measurement of error e_n

1. Sine Wave

It has been seen that if the ratio f/p is very small and if measurements are made in the "one cycle" mode then the only error arising

is e_n . The error e_1 will be negligible in practice.

The ratio f/p is set to $\frac{1}{5000}$. The a.c. voltage is varied in suitable steps. For each a.c. input the reading $\sum_{r=1}^{n-1} rC_r$ is recorded several times, their mean value being used to calculate the error. Fig 33. shows the graph of e_n versus position of the peak of the input.

2. Triangular Wave

The error in this case is very small and cannot be measured unless the $\sum_{r=1}^{n-1} rC_r$ weighted-feed binary counter is modified to indicate the states of the intermediate binaries. In this way, fractions of a count can be measured. This is the order of magnitude of errors for triangular wave inputs. As overall error measurements were to be made, which would include e_n , this modification was not carried out.

5.4. Measurement of error e_p

As can be seen from the theoretical results of e_p , this error is very small for both periodic inputs considered. In order to obtain any accuracy in measurement of this error, it is necessary that all other errors are made extremely small. If the 'one cycle mode' is used then e_n is zero. If in addition the input peak is set at a value for which e_n is also zero, it would be expected that error e_p could then be measured successfully. However the fluctuations of the function generator must be taken into account. Fig. No.34 shows the variation of e_n above a zero e_n point. Thus if signal amplitude fluctuates by as little as 5 mV (i.e. .05% of full scale value) then the error e_n will completely swamp e_p . Thus any accuracy in measurement of e_p is

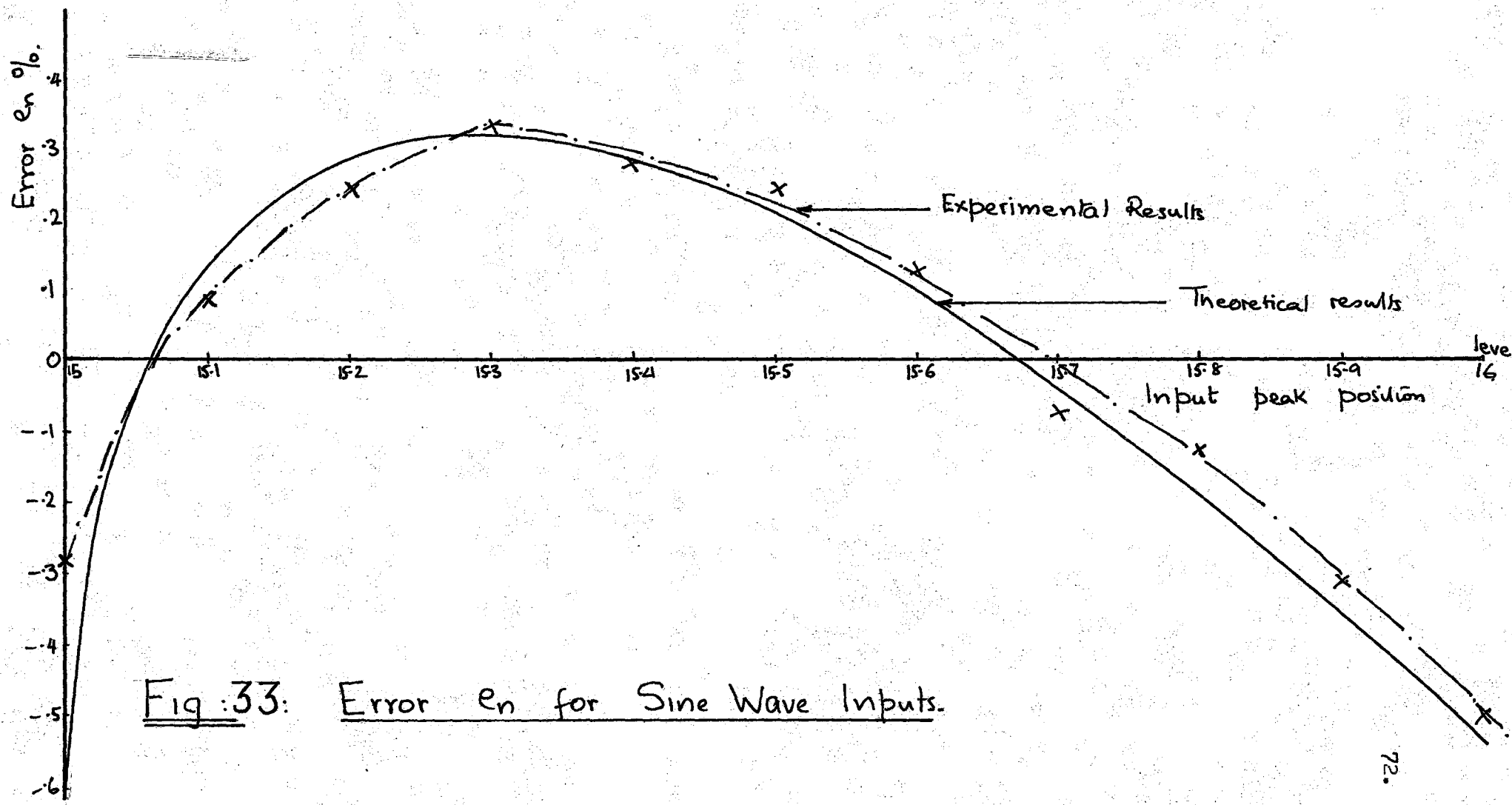


Fig:33: Error e_n for Sine Wave Inputs.

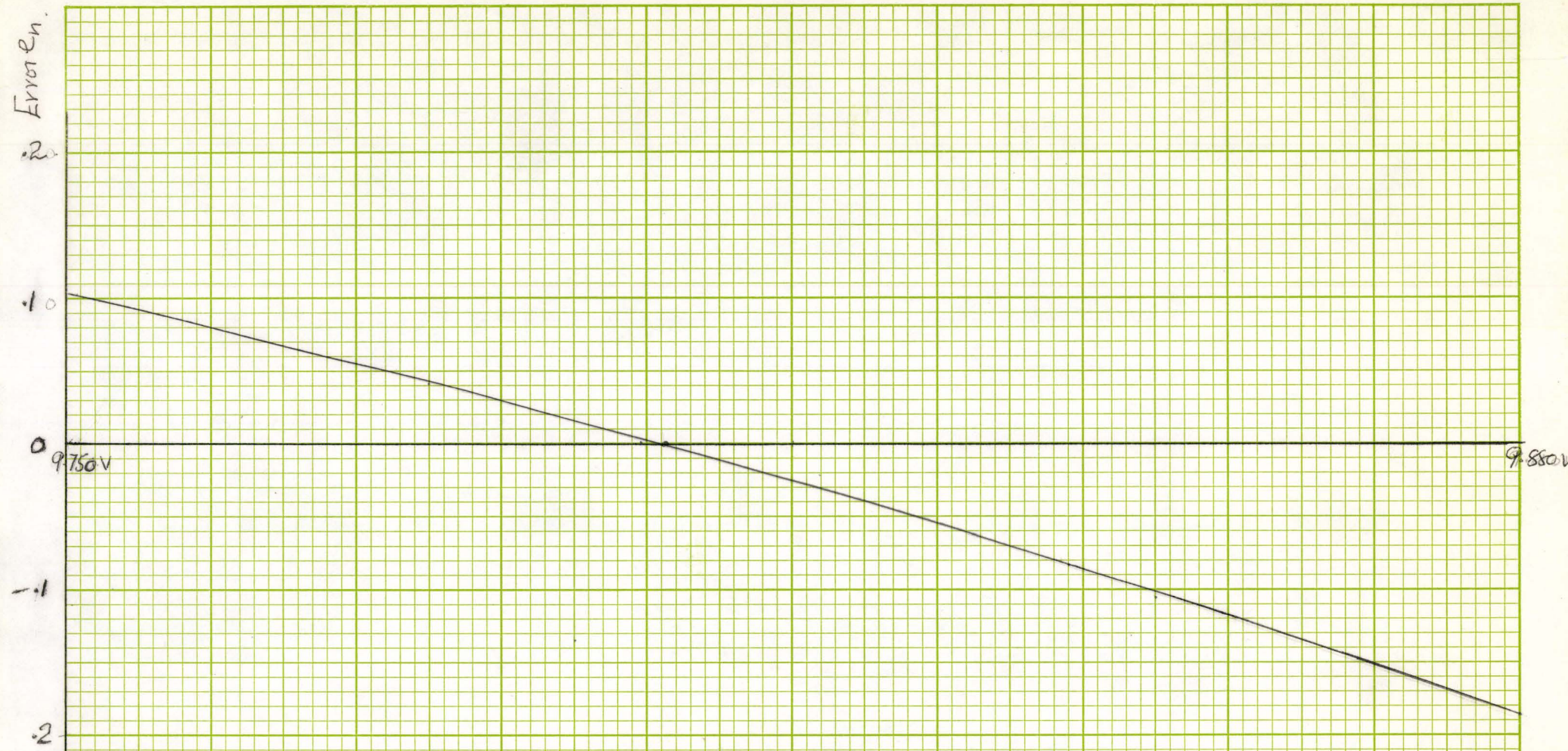


Fig: 34: Variation of e_n about a $e_n=0$ point

72a.

very difficult to achieve.

5.5. Overall error measurements

1. One cycle mode:

If e_1 is small then the overall error is $e_n + e_p$. The total number of samples taken is $C_o = p/f$. Therefore if p/f is small then the number of samples taken will also be small. As fractions of a count in $\sum_{r=1}^{n-1} rC_r$ readings are neglected, the error measurement accuracy for small C_o is poor. Also it is a requirement of a sampling process that the number of samples taken be large if the observed value is to be taken as a time measure with any confidence. In the one cycle mode this requires that f/p be made very small. This in turn however makes e_p negligible compared to e_n . Hence the error in this mode of operation is simply e_n . The error e_n has been measured for voltage peaks between the 15th and 16th levels (See Fig. 33).

2. Self-timed mode: Periodic wave inputs.

The instrument is arranged to stop when $C_o = 10000$. The measurements were made for sine wave and triangular wave inputs.

(a) Input waveform peak between the 15th and 16th levels.

Ten equally spaced positions are taken in this level interval. It is assumed that the peak of the input wave may occupy any of these positions. The r.m.s. values corresponding to these positions are calculated for both waveforms. The input r.m.s. voltage is set to one of these values. Readings of $\sum_{r=1}^{n-1} rC_r$ register are recorded for several measurements (e.g. 50). The procedure is repeated for other r.m.s. inputs. A frequency histogram of the

error ($e_n + e_p + e_\alpha$) is plotted from these observations.

Fig. 37, 40 show the histograms for the two waveforms, together with the theoretical distributions.

(b) Peak between 8th - 16th and 12th - 16th levels.

The procedure is identical to that above except that now equally spaced positions are taken between the 8th and 16th levels and between the 12th and 16th levels. The frequency histograms of the errors are shown in Fig. 36, 38, 39. The theoretical distributions are also shown in these graphs.

Self timed Mode: Normal distribution Noise.

A L.P. filter with cut off at 1 KHz is used to band-limit the noise. As the FET gates introduce heavy distortion for voltages exceeding 10 V, it is clear that the highest noise r.m.s. voltage which can be measured is about 3V. The true r.m.s. meter has thermocouples with square-law characteristics. A d.c. analogue of the input voltage is thus available. The meter used produces a + 1V d.c. for full scale deflection. As noise is a fluctuating voltage the meter pointer will respond to these fluctuations, thus making accurate direct observations impossible. Instead the d.c. output is averaged by using a long-time-constant R.C. circuit. The averaging time is 1000 sec. or 10T where T is the time constant of the R.C circuit. The circuit used is shown in Fig. 43. The circuit is calibrated for each range. Prior to commencement of measurement, the capacitor is discharged.

The sampling clock rate was set at 2 KHz i.e. the Nyquist rate corresponding to the noise input. The 16 level instrument was arranged

to stop the measurement process when $C_o = 10^6$. Thus the measuring time is 500 sec. giving a 99.73% confidence e_T , due to finite time of measurement, of less than $\frac{1}{4}$ %. For each setting of the input several measurements were made and their mean value was used to calculate the total error. Fig. 41, shows the graph of error versus standard deviation of the input noise.

5.6. Amplitude Probability distribution

As no weighted inputs are involved, it is expected that probability measurements will be more accurate than the mean square measurements. A sine wave of 10V peak (7.07^V r.m.s.) was used as input. Results given in Table IV, show that there is excellent agreement between the theoretical and measured probability distributions.

Total Number of Samples = 430.

$$s/p = \frac{1}{300}$$

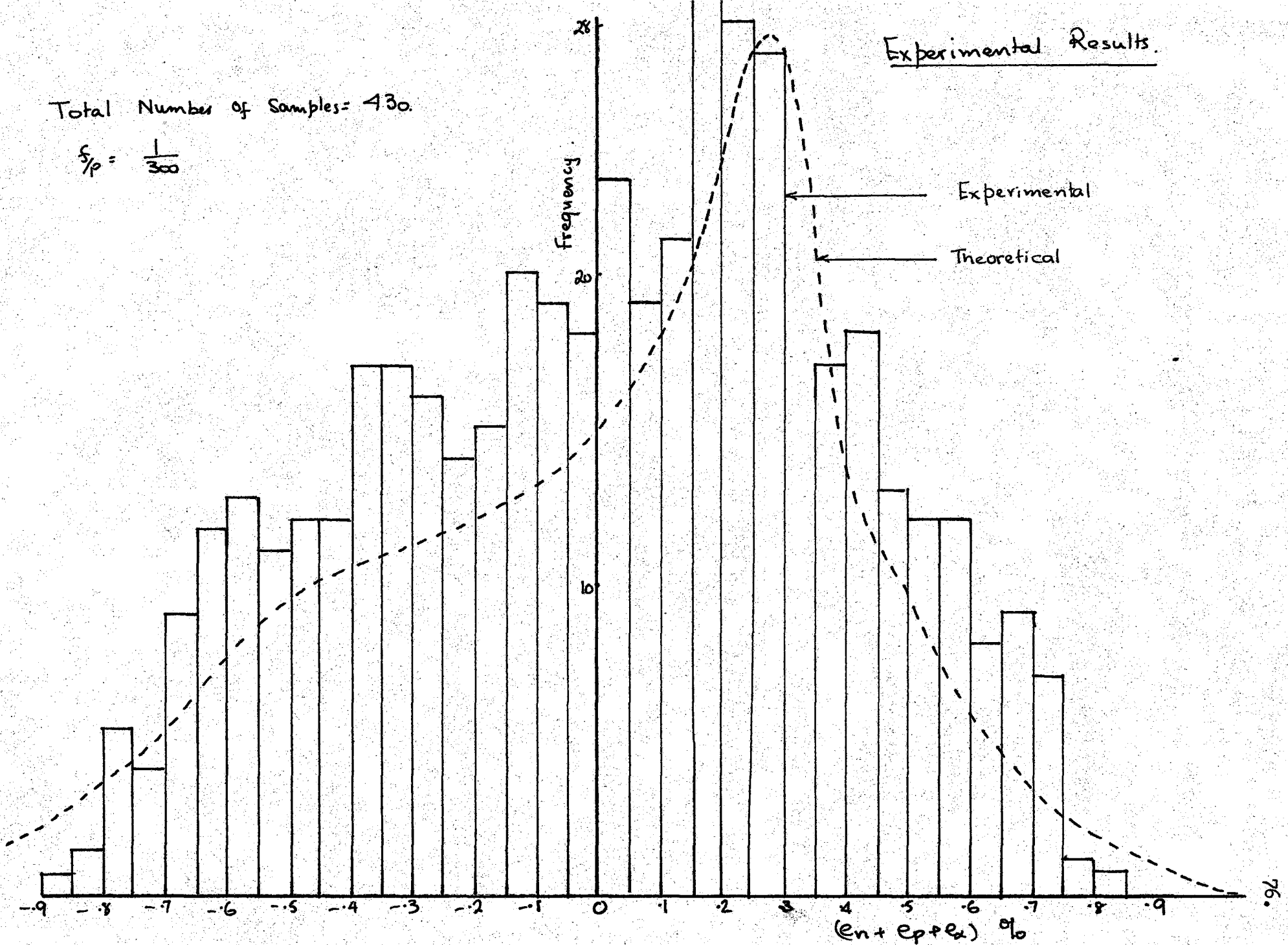


Fig: 35: Frequency Histogram of $(e_n + e_p + e_x)$: Sine Wave Input Peak between 8th - 16th levels

Experimental Results.

Total Number of samples = 275.

$$f/p = \frac{1}{300}$$

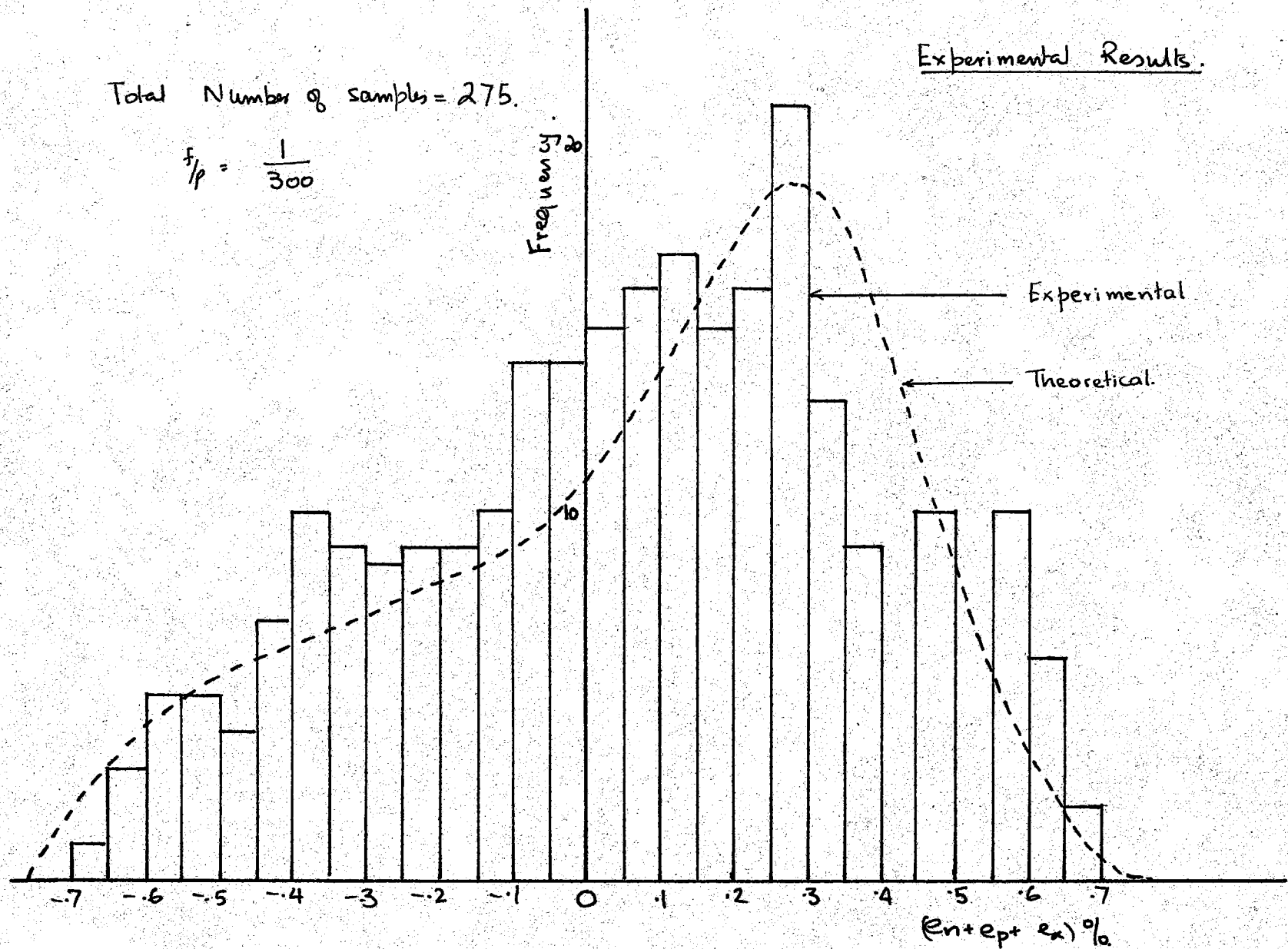


Fig:36: Frequency Histogram of $(e_n + e_p + e_x)$: Sine Wave Input peak between 12th-16th level

Experimental Results.

Total Number of Samples = 1000

$$f/p = \frac{1}{300}$$

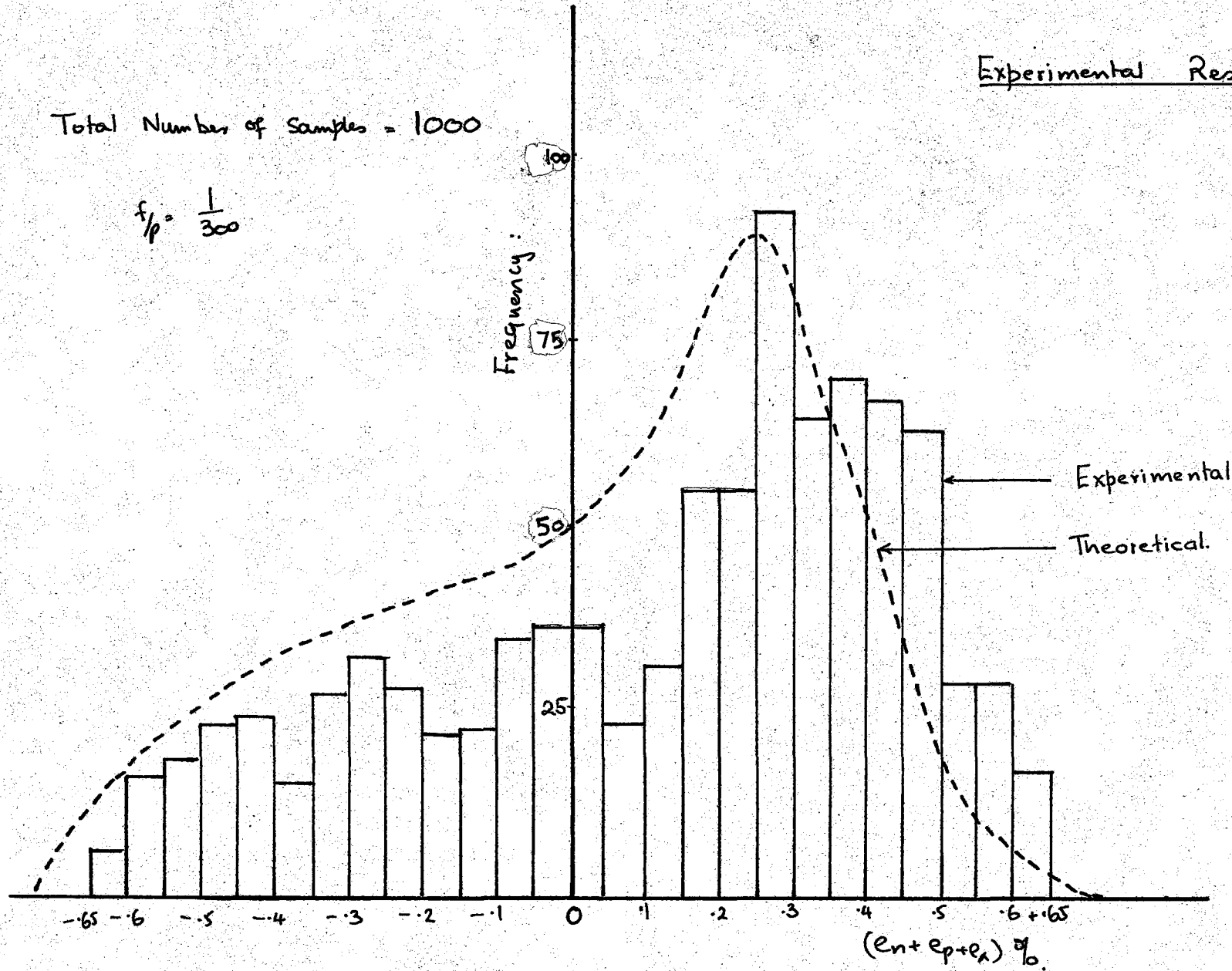


Fig :37: Frequency Histogram of $(e_n + e_p + e_a)$: Sine Wave Input peak between 15th-16th level

Total Number of Samples = 500
 $f/p = \frac{1}{300}$

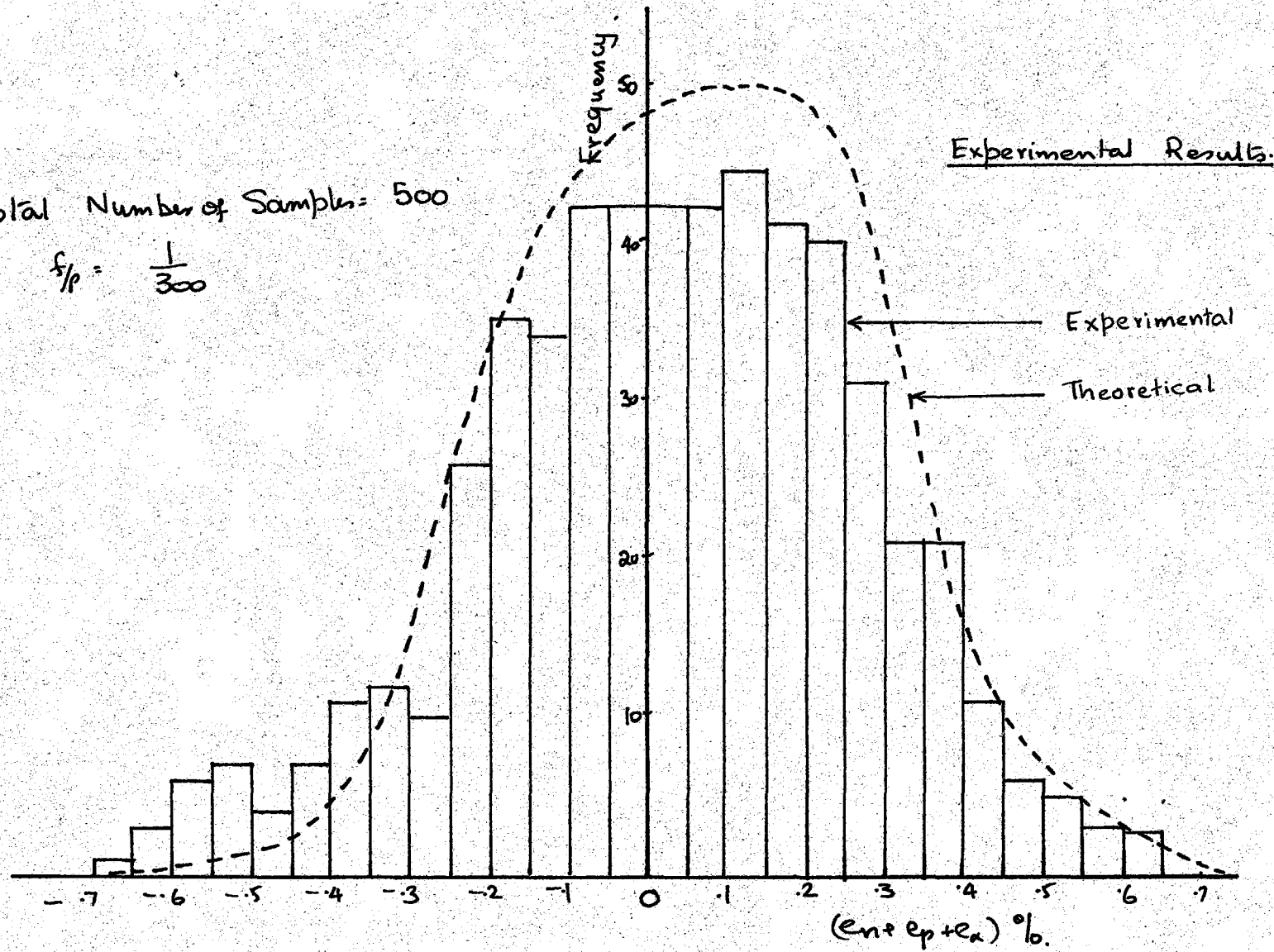


Fig. 38 : Frequency Histogram of $(e_n + e_p + e_a)$: Triangular Wave Input peak between 8th-16th levels.

Experimental Results.

Total Number of Samples = 250

$$f/p = \frac{1}{300}$$

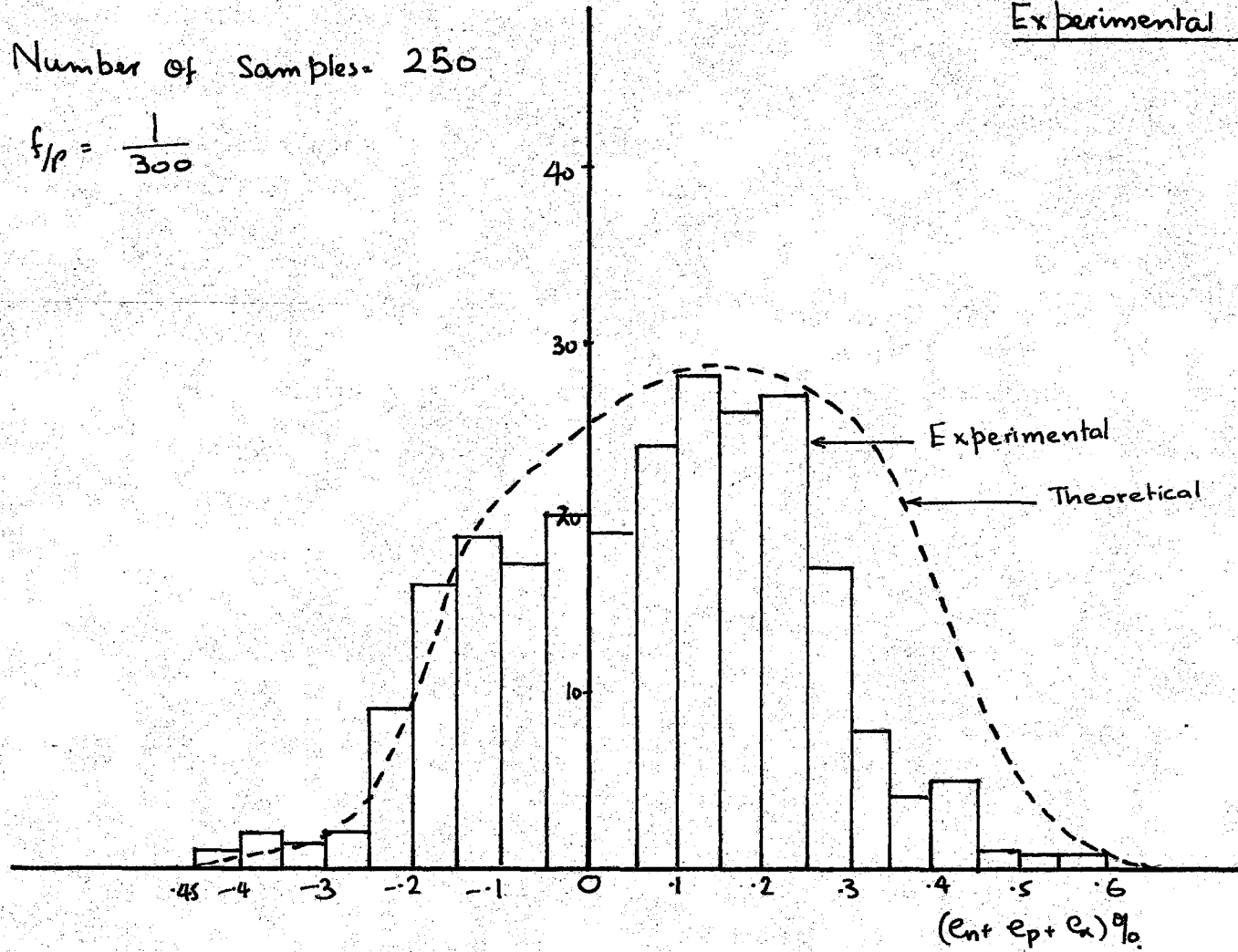


Fig:39: Frequency Histogram of $(e_n + e_p + e_x)$: Triangular Wave Input peak between 12th - 16th levels

Total Number of Samples 550

$$f/p = \frac{1}{300}$$

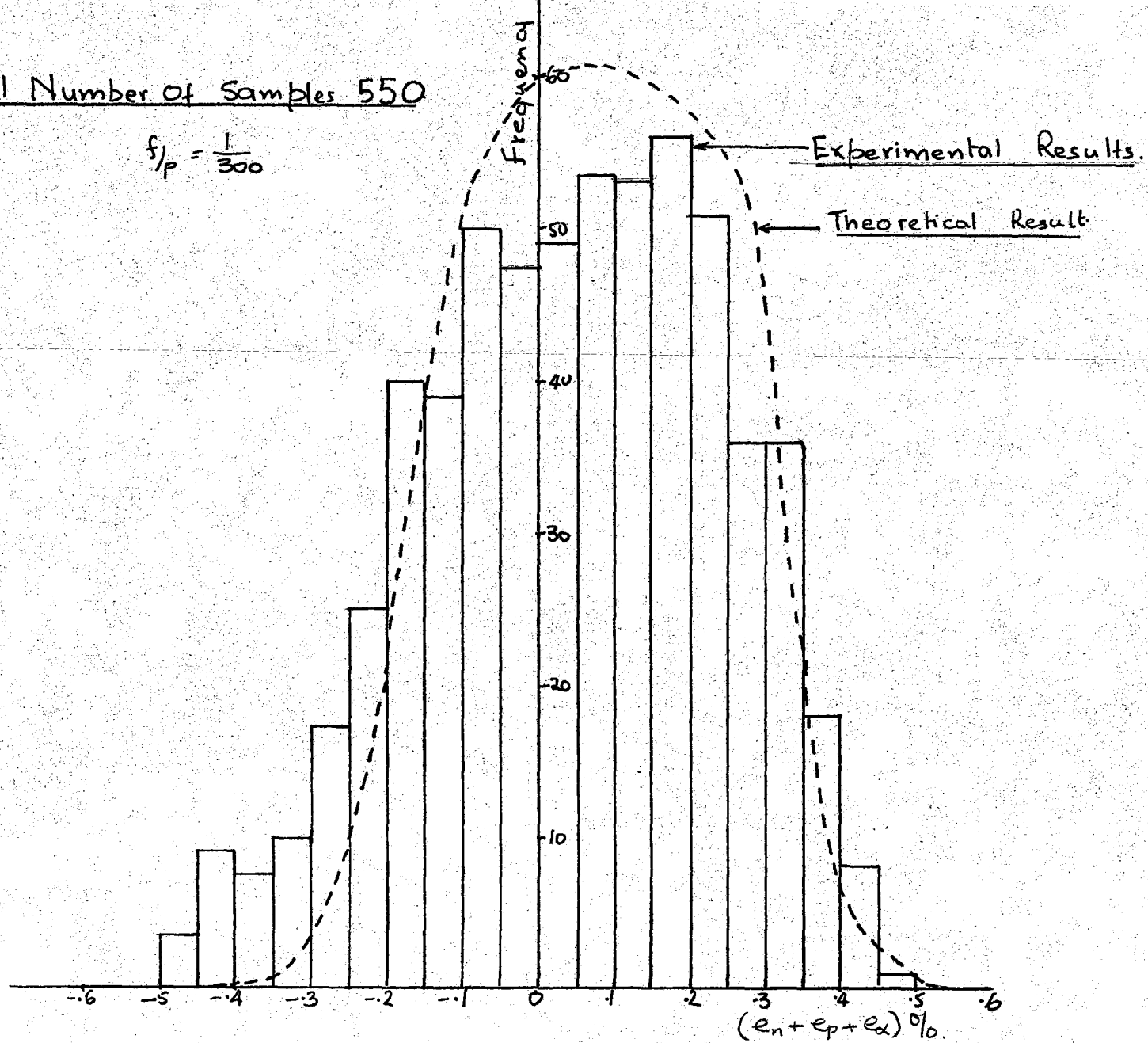


Fig:40 Frequency Histogram of ($e_n + e_p + e_a$): Triangular Wave Input peak between 15th-16th levels

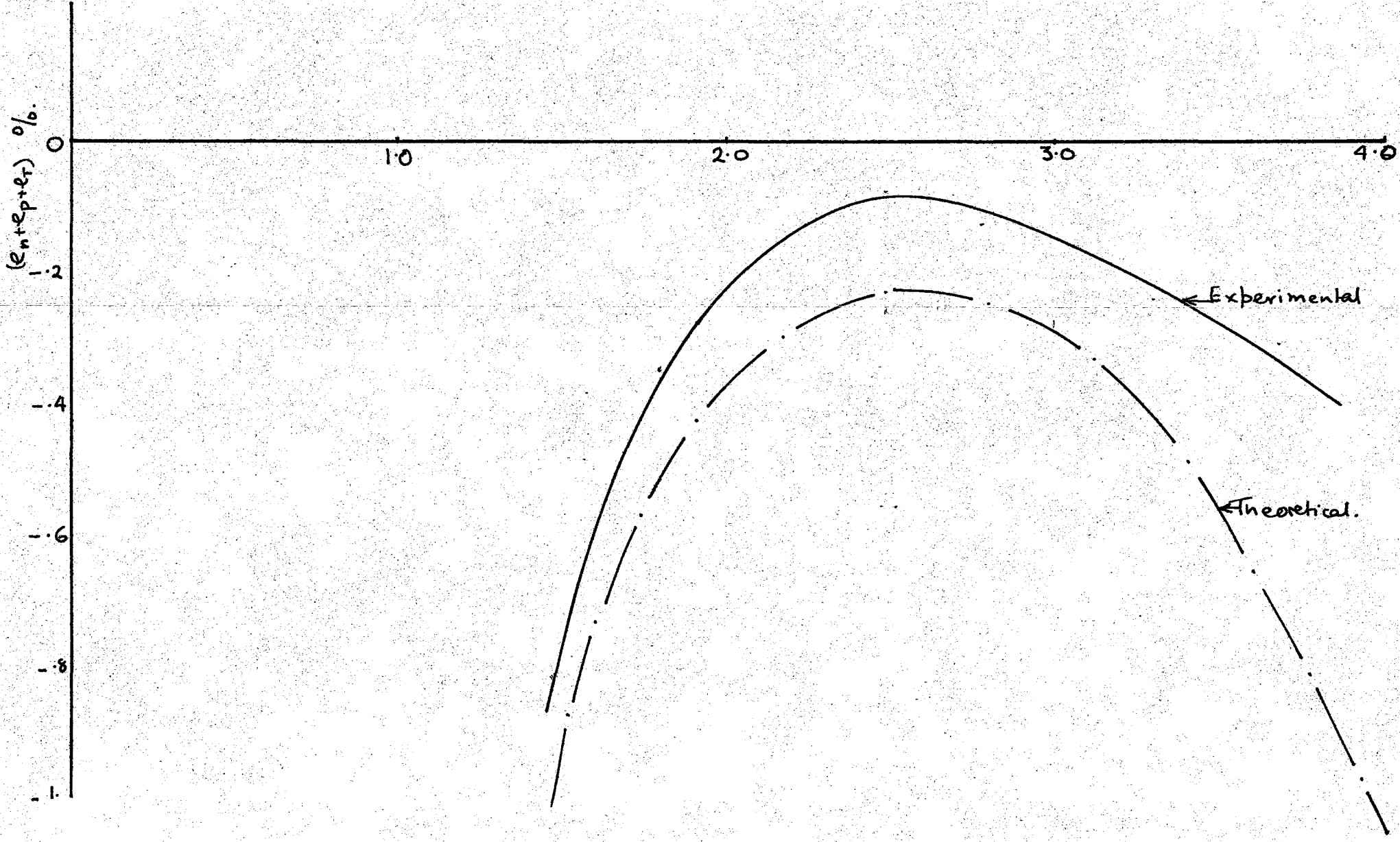


Fig: 41 : The total error results for Normal-distribution Noise.

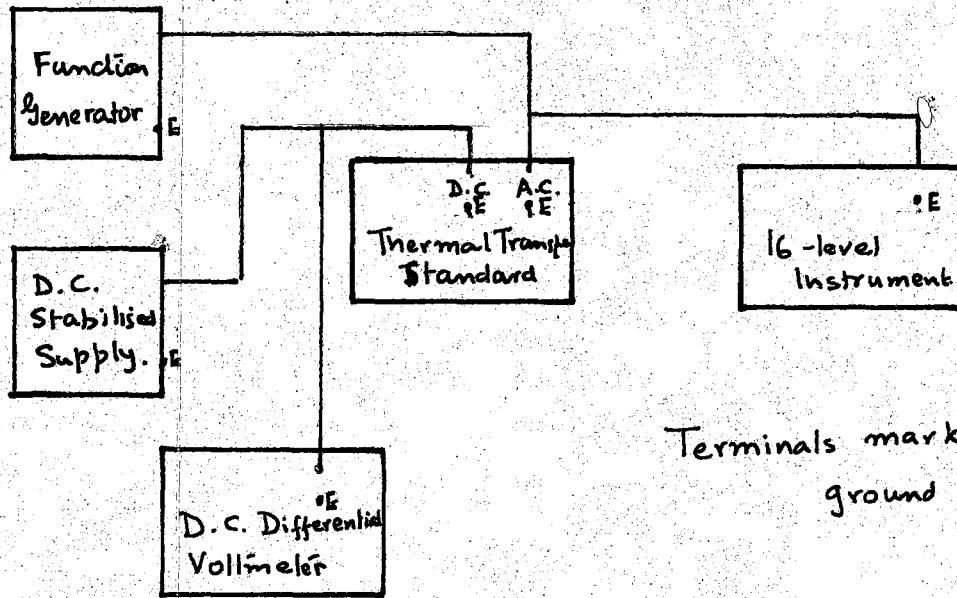


Fig : 42 : Circuit for error measurements Periodic Waves.

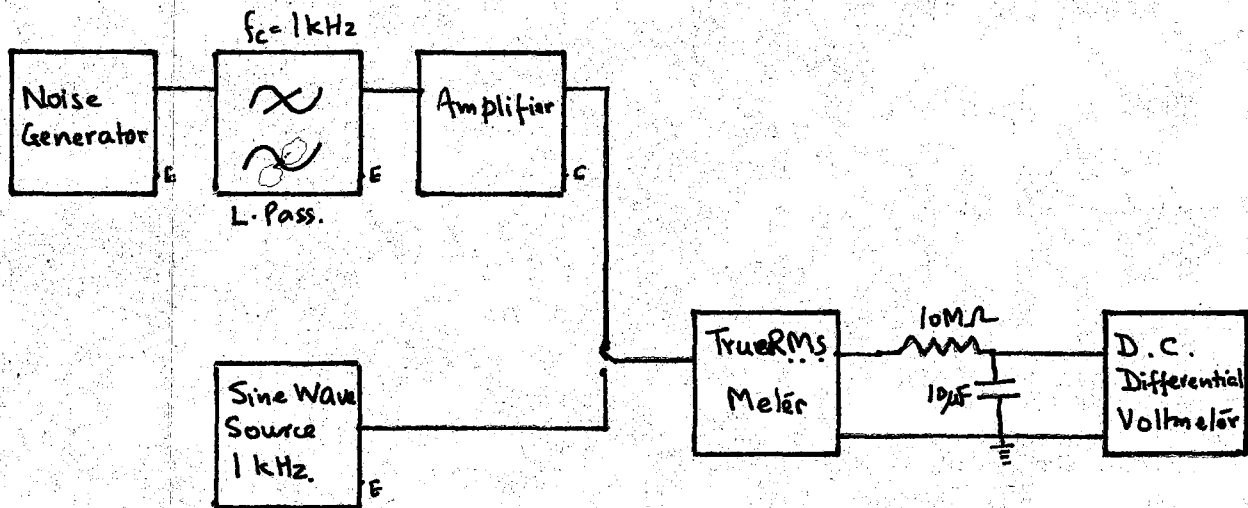


Fig : 43 : Circuit for error measurements: Noise Input.

T A B L E IV

Level Number	P(v) Measured	P(v) Theoretical	Difference
1	.961	.960	+.001
2	.920	.920	0
3	.880	.880	0
4	.839	.840	-.001
5	.797	.798	-.001
6	.757	.756	+.001
7	.713	.712	+.001
8	.668	.667	+.001
9	.621	.620	+.001
10	.571	.570	+.001
11	.519	.517	+.002
12	.461	.461	0
13	.398	.396	+.002
14	.323	.322	+.001
15	.228	.226	+.002
16	-	0	-

Sine Wave Amplitude Probability Distribution.

CHAPTER 6

DISCUSSION

The error analysis of the sampling instrument, is statistical in nature. In the "one cycle" mode when the ratio f/p is small, the only error of significance is the quantisation error e_n . Experimental measurements performed with sine wave input of peak value between the 15th and 16th levels show good agreement with the theoretical error curve. The maximum measured error in the mean square value was - 1.10%. Even if only half the levels are used, the error in mean square value does not exceed 2%. In practice however a scaler would be incorporated at the input so that a better use is made of the sixteen available levels.

The error due to finite sampling rate depends on f/p whereas the error due to a non-integral number of cycles of the input being sampled, depends on p/f . In the "one cycle" mode, the latter does not arise as sampling is for precisely one cycle. The ratio f/p may then be decreased so as to reduce the total error. In the self-timed mode, however, all three errors occur, and reducing f/p would reduce one error only to increase the other. The probability distribution for their sum has been calculated on the assumption that these errors are statistically independent. Although this is not strictly true in practice, the assumption simplifies the analysis considerably. Experimental and theoretical analyses made for a particular f/p show good agreement.

For normal distribution noise with highest frequency 1 KHz, r.m.s. values within 1V and 3.5V may be measured within an accuracy of 1%. The

error due to finite time of measurement is also present in this instrument. This is expected as such an error is inherent in measurement of random quantities.

In general therefore it may be concluded that the theoretical error analysis and the methods for calculation of overall characteristics of the sampling instrument are quite valid. The various errors are summarised in Table V. With proper choice of f/p the total error in mean square value can be kept well within 2% for a 16-level instrument.

The error due to level offset is difficult to evaluate as the offset voltage is not constant for all the levels. However level offsets are small and the error resulting is also small compared to other errors.

The limitation of the sampling instrument is the "aperture time". This was defined as the time required to determine the level of the input waveform at the sampling instant. This error depends on the method used for level determination. For the successive approximation method used here, the error becomes a function of the "critical decision" which in turn depends on the level being considered. Thus it is seen that errors due to aperture time are extremely complex. For an aperture time of 7 μ sec., a frequency of 2 KHz for the input signal may be considered as the upper limit of the instrument, before the errors due to aperture time become excessive. The aperture time can be reduced by various techniques e.g. by using a sample and hold circuit.

Error e %	Sine Wave Input	Triangular Wave Input	Normal distribution Noise
e_n Maximum	$-\frac{0.41}{(n-1)^{1.5}}$ large n	$\frac{1}{4n^2}$ large n	$\frac{1}{24V^2n^2}$ for small V and large n
e_p 99.73% confidence	$\pm \frac{6f}{np}$ for all filled levels	$\pm \frac{9f}{np}$ for all filled levels	$e_{p.av.} = \frac{1}{2n^2} \cdot \frac{f}{p} \cdot \frac{1}{V^2} \left\{ \frac{-1}{ne^{2V^2}} \frac{-1}{-e^{-2n^2V^2}} \right\}$
e_d Maximum	$\pm \frac{0.04}{q}$	$\pm \frac{0.048}{q}$	-
e_l Average	$< \delta E$	$< \frac{3}{2} \delta E$	$< \frac{\delta E}{V}$
e_T 99.73% confidence	-	-	$\frac{1.69}{\sqrt{f.T.}}$

TABLE V

Note: Errors in $\frac{1}{T} \int_0^T v^2 dt$ are twice the above errors.

Summary of Error Characteristics.

APPENDIX A

DETAILS OF THE D.E.C. MODULES

Power Supply Requirement: All modules except A 121.

+ 10V module pin A
- 15V module pin B
ground module pin C

A 121 FET gates

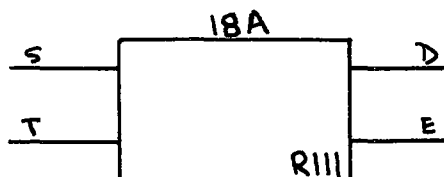
The supply voltage differential should not exceed 30V. Thus the following supplies are used in order to accommodate an input signal peak of 10V.

+ 10V module pin D
- 20V module pin E
ground module pin C

Frequency Range R series DC to 2 MHz

Logic Levels 1 state = - 3V
 0 state = 0V

Designations used in the circuit diagrams



1. Number inside block gives the module type number.

2. Letters beside the connecting lines are identifying letters of the connecting pins.
3. Number on top gives location of the module, with locations numbered from left to right. The subscript 'A' denotes top row while a 'B' denotes bottom row.

APPENDIX B

1. The error e_n

In general
$$e = \frac{V_1 - V}{V} \approx \frac{1}{2} \left\{ \left(\frac{V_1}{V} \right)^2 - 1 \right\}$$

$$e = \frac{1}{8n^2V^2} \left\{ 1 + 8 \sum_{r=1}^{n-1} r p_r \right\} - \frac{1}{2}$$

(a) Rectangular Wave: Peak at $(m - 1 + \epsilon)$

$$\text{R.M.S. normalised voltage} = \frac{m-1+\epsilon}{n}$$

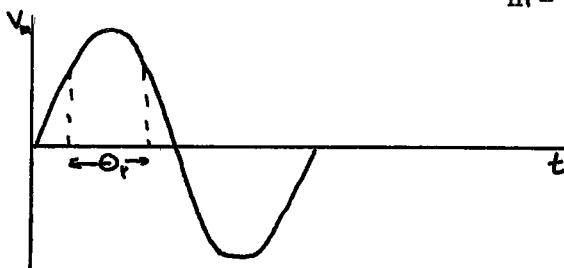
also $p_r = 1$

$$\therefore V_1 = \frac{2m-1}{2n}$$

$$\therefore e_n = \frac{1 - 2\epsilon}{2(m-1+\epsilon)}$$

(b) Sine Wave: Peak at $(m - 1 + \epsilon)$

$$\text{Normal voltage at } r^{\text{th}} \text{ level} = \frac{r}{m-1+\epsilon} = \text{Sin } \frac{\pi - \theta}{2}$$



As all values of θ between 0 & 2π are equally likely.

$$p(r) dv = p(\theta) d\theta = \frac{2d\theta}{2\pi} \text{ there being two values of}$$

for which the same voltage occurs.

\therefore Probability that voltage is above r^{th} level $= p_r = \frac{\Theta_r}{\pi}$

$$\therefore p_r = 1 - \frac{2}{\pi} \sin^{-1} \frac{r}{m-1+\epsilon} = \frac{2}{\pi} \cos^{-1} \frac{r}{m-1+\epsilon}$$

Normalised mean square of the input is $\frac{(m-1+\epsilon)^2}{2n^2}$

Hence
$$e_n = \frac{1}{4(m-1+\epsilon)^2} \left[1 + \frac{16}{\pi} \sum_{r=1}^{n-1} r \cos^{-1} \frac{r}{m-1+\epsilon} \right] - \frac{1}{2}$$

(c) Triangular Wave

As for sine wave but now

$$p_r = 1 - \frac{r}{m-1+\epsilon}$$

$$v^2 = \frac{1}{3} \left(\frac{m-1+\epsilon}{n} \right)^2$$

$$\therefore e_n = \frac{3n^2}{8n^2(m-1+\epsilon)^2} \left[1 + 8 \sum_{m=1}^{m-1} r \left(1 - \frac{r}{m-1+\epsilon} \right) \right] - \frac{1}{2}$$

using appropriate series e.g. $\sum_1^{m-1} r = \frac{m(m-1)}{2}$

$$\sum_1^{m-1} r^2 = \frac{m(m-1)(2m-1)}{6}$$

$$e_n = \frac{1 - m + 12m\epsilon(1-\epsilon) - \epsilon(2\epsilon-3)^2}{8(m-1+\epsilon)^3}$$

(d) Normal Wave and Normal distribution noise

As given in Chapter 3.

2. Probability distribution of e_n

Given a single valued function $e_n = f(\epsilon)$, to find $p(e_n)$ the probability density function of e_n

As all values of ϵ are equally likely in a range say 0 to Φ ,

$$p(\epsilon) d\epsilon = \frac{d\epsilon}{\Phi}$$

$p(e_n)de_n$ is the probability that $e_{n1} < e_n < e_n + de_n$ occurs

$$p(e_n)de_n = p(\epsilon) d\epsilon$$

$$\therefore p(e_n) = \frac{1}{\Phi} \frac{d\epsilon}{de_n}$$

As $\Phi = 1$

$$p(e_n) = \frac{1}{\left(\frac{de_n}{d\epsilon}\right)}$$

This is easily extended to cases where e_n is not singled-valued function of ϵ .

The equation for $p(e_n)$ gives a normalised density function as

$$\int_0^{\infty} p(e_n)de_n = 1 \text{ given that } \epsilon \text{ varies from 0 to 1.}$$

3. Error e_p due to finite sampling rate

Referring to section 33, the error in $\sum_{r=1}^{n-1} rC_r$ due to d_r and β_r at any one level r is

$$-d_r \tau (w_r - w_{r-1}) + \beta_r \tau (w_{r+1} - w_r) \text{ where } w_r \text{ is the weighting given to the } r^{\text{th}} \text{ level}$$

$$w_r = \sum_{i=1}^{r-1} i = \frac{r(r-1)}{2}$$

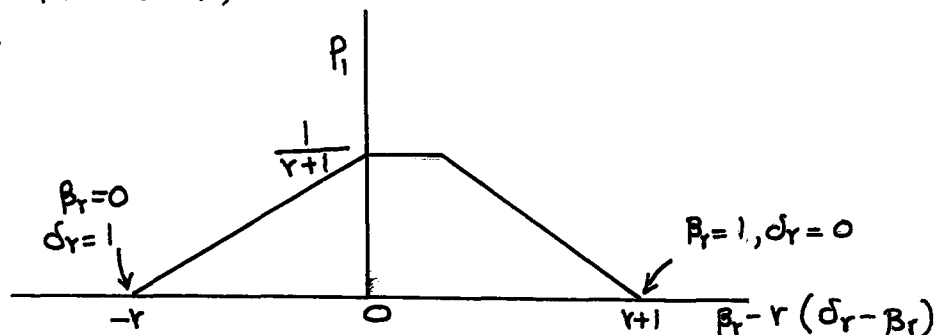
$$\begin{aligned} \text{The error is} \quad & -d_r \tau r + r \beta_r \tau + \beta_r \tau \\ & = \beta_r \tau (r+1) - r d_r \tau \end{aligned}$$

V_n^2 can be found. Thus

$$\text{Error in } V_n^2 C_0 = \frac{2}{n^2} \sum_{r=1}^{m-1} \left\{ -r \tau (d_r - \beta_r) + \beta_r \tau \right\}$$

$$\text{Error } e_p = \frac{1}{n^2} \frac{f}{P} \frac{1}{V_n^2} \sum_{r=1}^{m-1} \left\{ \beta_r - r(d_r - \beta_r) \right\}$$

Now all values of β_r and d_r are equally likely. For any level r , the probability distribution of β_r and d_r being known, the probability distribution of $\beta_r - r(d_r - \beta_r)$ is the convolution of two uniform distributions as shown below



The mean value of the above distribution is $\frac{1}{2}$ and the variance is $\frac{2r^2 + 2r + 1}{12}$

To find the error distribution taking all the levels used into

account, assume that the errors are statistically independent for the various levels. The Central Limit Theorem can be used to find the probability distribution for e_p . The theorem states that 'the distribution of the sum of independent variables approaches the Gaussian distribution'. The average and the variance of the Gaussian distribution are given by the sum of the individual average and variances respectively. Thus the error e_p will have a near Gaussian probability distribution with mean and variance given by :

$$\text{mean } \mu_{e_p} = \frac{1}{n^2} \frac{f}{p} \frac{1}{V_n^2} \frac{m-1}{2} \quad \text{if } m \text{ levels are filled.}$$

$$\text{Variance } \sigma_{e_p}^2 = \left\{ \frac{1}{n^2} \frac{f}{p} \frac{1}{V_n^2} \right\}^2 \sum_{r=1}^{m-1} \frac{2r^2+2r+1}{12}$$

$$\therefore \sigma_{e_p} \doteq \frac{1}{n} \frac{f}{p} \frac{1}{V_n^2} \sqrt{\frac{n}{18}} \quad \text{for } m = n \text{ and}$$

$$\text{for } n = 16 \quad \sigma_{e_p} \doteq \frac{1}{n} \frac{f}{p} \frac{1}{V_n^2}$$

The 99.73% confidence limit is given by:

$$\begin{array}{l} + \quad \frac{3}{n} \frac{f}{p} \frac{1}{V_n^2} \\ - \quad \frac{3}{n} \frac{f}{p} \frac{1}{V_n^2} \end{array}$$

Hence the mean error e_p for $m = n$ approaches

$$e_{p.av} = \frac{1}{2nV^2} \frac{f}{p}$$

The maximum possible e_p occurs when $\beta = 1$ $\delta = 0$ for all levels, a situation which is very unlikely to occur. The error in this case is for n levels,

$$e_{p.\max} = \frac{1}{n^2 V^2} \frac{f}{P} \sum_{r=1}^{n-1} r+1 \quad \doteq \frac{1}{2V_n^2} \frac{f}{P}$$

4. e_T for normal distribution noise

Van der Ziel has shown that

$$\gamma^2 = \frac{4}{t_i} \int_0^{\infty} \frac{\varphi^2(\tau)}{\varphi^2(0)} d\tau$$

where $\varphi(\tau)$ is the autocorrelation function of v the output of the L.P. filter.

Consider noise of power η W/ unit bandwidth being passed through an ideal L.P. filter with a response.

$$|H(j\omega)| = 1 \quad 0 \leq f \leq f_c$$

$$|H(j\omega)| = 0 \quad \text{elsewhere}$$

The output power spectrum, defined for positive frequencies only is

$$G'(w) = \eta/2 \quad 0 \leq f \leq f_c$$

$$= 0 \quad \text{elsewhere}$$

The autocorrelation function, by definition, is

$$\varphi(\tau) = \int_{-\infty}^{+\infty} G'(w) \cos(2\pi f t) df$$

$$= \int_{-\infty}^{+\infty} \frac{\eta}{2} \cos 2\pi f t. df$$

$$= \frac{\eta}{2} f_c \left[\frac{\sin 2\pi f_c \tau}{2\pi f_c \tau} \right]$$

$$\therefore \varphi(0) = \frac{\eta f_c}{2}$$

$$\therefore \gamma^2 = \frac{4}{t_i} \int_0^{\infty} \frac{\sin^2(2\pi f_c \tau)}{(2\pi f_c \tau)^2} d\tau$$

$$= \frac{4}{t_i} \frac{1}{2\pi f_c} \frac{\pi}{2}$$

$$= \frac{1}{f_c t_i}$$

APPENDIX C

The following programmes are included.

1. e_n & $\left(\frac{de_n}{d\epsilon}\right)$ for Sine Wave.
2. e_n & $\left(\frac{de_n}{d\epsilon}\right)$ for Triangular Wave.
3. e_n for Normal Distribution Noise.
4. F_s to evaluate e_1 for Sine Wave.

e_n SINE WAVE

```

$JOB          003514 MAJITHIA          100   010   030
$IBFTC
DOUBLE PRECISION SSI,SUM,X,X1,F(2001),SUM2,E(2001)
DIMENSION F1(1001),E1(1001)
50 READ(5,3) N,N2
3  FORMAT(2I5)
   IF(N.EQ.0)GO TO 100
   RN=N
   RN2=N2
   N2P =N2+1
   N1=N+1
   WRITE(6,4) N1,N2
4  FORMAT (18H1 SUMMATION FOR N=,I5,3X, 17HNUMBER OF STEPS =,I5//)
   L=1
   F(1)=0.0
   E(1)=0.0
   DO1 I=1,N2P
   L=L+1
   SI =I-1
   SI= SI/RN2
   SSI =(RN  +SI)**2
   SUM =0.0
   DO2 J=1,N
   RJ =J
   X =RJ/(SI +RN  )
   X1 =DSQRT (1.0 -X**2)
2  SUM  = SUM +2.0*RJ/3.14159 *DATAN(X1/X)
   F(L)=0.25/SSI -0.5 +2.0/SSI*SUM
   E(L)=(F(L)-F(L-1))*RN2
   E(L) = 1.0/E(L)
1  CONTINUE
   SUM2=0.0
   DO 110 L=2,N2P
   SUM2=SUM2+ABS((E(L)+E(L-1))*(F(L-1)-F(L)))/2.0
110 E1(L)=SUM2
   WRITE(6,112) SUM2
112 FORMAT (31H0 UNNORMALISED ERROR INTEGRAL =,E15.8)
   FMAX =0.0
   E1(1)=0.
   DO 11 L=1,N2P
   F1(L)=F(L)
   WRITE(6,10)F(L),E(L),E1(L)
10  FORMAT(3(E20.8,10X))
11  IF (ABS(F(L)).GT.FMAX) FMAX=ABS(F(L))
   FMIN =-FMAX

```

```
CALL PLOT 1 (F1,FMAX,FMIN,50.0,-5.,54 , 130 ,5)  
CALL PLOT1 (E1,EMAX,EMIN,50.0,-5.0,54,130,5)  
CALL PLOT 3(F1,E1,100,1.1,-1,FMAX,FMIN,48,100,4)  
GO TO 50  
100 CONTINUE  
CALL EXIT  
END
```

```
$ENTRY
```

```
14 40
```

```
15 40
```

```
$IBSYS
```

```
CD TOT 0077
```

e_n TRIANGULAR WAVE

```

$JOB          003514 MAJITHIA          100   010   030
$IBJOB        NODECK
$IBFTC

DOUBLE PRECISION SSI,Q,F(2001),SUM2,E(2001)
DIMENSION F1(1001),E1(1001)
50 READ(5,3) N,N2
3  FORMAT(2I5)
   IF (N.EQ.0) GO TO 100
   RN=N
   RN2=N2
   N2P =N2+1
   N1 = N+1
   WRITE (6,4) N1,N2
4  FORMAT (14H1 ERROR FOR N=,I5, 3X, 17HNUMBER OF STEPS =,I5//)
   L=1
   F(1) =0.0
   E(1) =0.0
   DO1 I=1,N2P
   L=L+1
   SI = I-1
   SI= SI/RN2
   SSI =(RN +SI)**3
   G=SI*(1.0-SI)*12.0
   Q= SI*(SI*2.0-3.0)**2
   F(L) = (-RN +RN*G +G -Q)/SSI*0.125
   E(L)=(F(L)-F(L-1))*RN2
   E(L) = 1.0/E(L)
1  CONTINUE
   SUM2=0.0
   DO 110 L=2,N2P
   SUM2=SUM2+ABS((E(L)+E(L-1))*(F(L-1)-F(L)))/2.0
110 E1(L)=SUM2
   WRITE (6,112) SUM2
112 FORMAT(31H0 UNNORMALISED ERROR INTEGRAL =,E25.8 )
   FMAX =0.0
   E1(1)=0.
   DO 11 L=1,N2P
   F1(L)=F(L)
   WRITE(6,10)F(L),E(L),E1(L)
10  FORMAT(3(E20.8,10X))
11  IF (ABS(F(L)).GT.FMAX) FMAX=ABS(F(L))
   FMIN =-FMAX

```

```
CALL PLOT 1 (F1,FMAX,FMIN,50.0,-5.0,54,130,5)  
CALL PLOT1 (E1,EMAX,EMIN,50.0,-5.0,54,130,5)  
CALL PLOT 3(F1,E1,100,1.1,-1,FMAX,FMIN,48,100,4)  
GO TO 50
```

```
100 CONTINUE  
CALL EXIT  
END
```

```
$ENTRY  
14 40  
15 40
```

```
$IBSYS
```

```
CD TOT 0074
```

e_n NORMAL DISTRIBUTION NOISE

```

$JOB          003514 MAJITHIA          100   010   030
$IBJOB        NODECK
$IBFTC
  1  READ (5,51) N, DV
  51  FORMAT (I5, F10.6)
      IF (N.EQ.0) GO TO 100
      RN =N
      N1=N-1
      WRITE (6,61) N
  61  FORMAT (14H1 ERROR FOR N=,I5//)
      V=0.0
  4   V= V+DV
      IF (V.GT.0.50) GO TO 1
      XR =0.0
      DO 2 J=1,N1
      RR=J
  2   XR =RR*ERF(RR/RN/V/SQRT(2.0)) +XR
      ENV =0.125/RN/RN/V/V*(1.0 +4.0*RN*(RN-1.0) -8.0*XR) -0.5
      WRITE (6,62) V,ENV
  62  FORMAT (F15.8 ,10X, E15.8)
      GO TO 4
  100 CONTINUE
      STOP
      END
$ENTRY
  8   0.01
  16  0.01
  32  0.01
  64  0.01
  128 0.01
  256 0.01
$IRSYS

```

CD TOT 0043

F_s TO EVALUATE e₁ SINE WAVE

\$JOB WATFOR 003514 MAJITHIA 100 010 030
 \$IBJOB
 \$IBFTC

```

50 READ (5,3) N
3  FORMAT (I5)
   IF (N.EQ.0) GO TO 100
   RN =N
   N1 =N+1
   RR =N1
   WRITE (6,4) N1
4  FORMAT (18H1 SUMMATION FOR N=, I5//)
   SUM =0.0
   DO 2 J=1,N
   RJ =J
   X =SQRT (1.0-(RJ/RR)**2)
   X1 =RJ/X
2  SUM = SUM +(1.2732/RR**2) *X1
   WRITE (6,62) SUM
62 6ORMAT (1H ,10X, E15.8 )
   GO TO 50
100 CONTINUE
   STOP
   END

```

\$ENTRY

7
8
9
10
11
12
13
14
15
16

\$IBSYS

CD TOT 0046

APPENDIX D

CONVOLUTION

1. Graphical Convolution

The convolution of $f(t)$ and $r(t)$ is given by

$$\begin{aligned} r(t) &= f(t) * h(t) \\ &= \int_0^{+\infty} f(\tau) h(t-\tau) d\tau \\ &= \int_0^t f(\tau) h(t-\tau) d\tau. \end{aligned} \quad \text{when } f(t) \text{ and } h(t) \text{ are causal.}$$

$$= \lim_{\Delta t \rightarrow 0} \sum_{\tau=0}^t f(\tau) h(t-\tau) \Delta \tau \quad \text{by definition of the integration process.}$$

The limits of the convolution $r(t)$ are from the sum of the lower limits of $f(t)$ and $h(t)$ to the sum of their upper limits. Thus for graphical convolution, the following details are pertinent:

- (a) Regard convolution as a product of two curves.
- (b) Invert one i.e. take its image about the vertical axis.
- (c) Shift this image through the second curve by constant amounts, working out the area at each instant. These areas represent the convolution.

2. Impulse train approximation for numerical convolution.

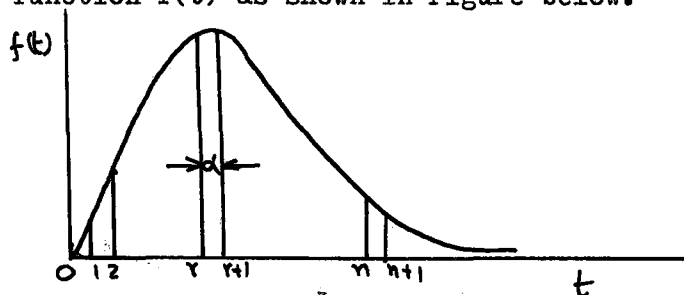
Theorem: Convolution of two impulse functions is also an impulse function.

$$\text{i.e.} \quad \delta(t-t_1) * \delta(t-t_2) = \delta(t-t_1-t_2)$$

$$\text{and also} \quad f(t-t_1) * \delta(t-t_2) = f(t-t_1-t_2)$$

The proof of the theorem is elementary.

Consider the function $f(t)$ as shown in Figure below.



The area is divided into a large number of strips. These strips are replaced by impulses. A narrow strip of area occupying the region $n\alpha < t < (n+1)\alpha$ may be approximated by an impulse of strength equal to the area of the strip and located at $n\alpha$. Thus the function $f(t)$ is replaced by a sequence of impulses located at $0, \alpha, 2\alpha, \dots$ etc, with the strength of the $(n+1)^{\text{th}}$ impulse being proportional to $f(n\alpha)$

$$\therefore f(t) \doteq \alpha f_0(t) \delta(t) + \alpha f(\alpha) \delta(t-\alpha) + \dots + \alpha f(n\alpha) \delta(t-n\alpha)$$

For numerical convolution both $f(t)$ and $h(t)$ are approximated by such sequences. Thus

$$h(t) \doteq \alpha h_0(t) \delta(t) + \alpha h(\alpha) \delta(t-\alpha) + \dots + \alpha h(n\alpha) \delta(t-n\alpha)$$

As the convolution between two impulses is an impulse function, the convolution between $f(t)$ and $h(t)$ is very simple to perform. It is readily seen that

$$\begin{aligned} f(t) * h(t) \Big|_{t=n\alpha} &= \alpha^2 \left\{ f_0 h_n + f_1 h_{n-1} + \dots + f_n h_0 \right\} \delta(t-n\alpha) \\ &= \alpha^2 \delta(t-n\alpha) \sum_{m=0}^n f_m h_{n-m} \end{aligned}$$

$$\text{where } f_m = f(m\alpha), h_m = h(m\alpha)$$

$$\text{also } r(t) = \alpha r_0 \delta(t) + \alpha r_1 \delta(t-\alpha) + \dots + \alpha r_n \delta(t-n\alpha)$$

If $r(t) = f(t) * h(t)$ then

$$r_0 = \alpha f_0 h_0, \quad r_1 = \alpha(f_0 h_1 + f_1 h_0) \text{ ----- and}$$

$$r_n = \sum_{m=0}^n f_m h_{n-m}$$

The most convenient method to obtain $\alpha^2 \sum_{m=1}^n f_m h_{n-m}$ is to write the impulse values on two strips of paper with the sequence $h(t)$ written in the reverse order. One strip is moved along the other, one number at a time, the result $\alpha^2 \sum_{m=0}^n f_m h_{n-m}$ being calculated at each instant. From these the values of r_n can be easily obtained.

A P P A R A T U S

Power Supply.

Function generator

A.C./ D.C. Differential Voltmeter John Fluke.

Thermal transfer meter. John Fluke.

True R.M.S. Meter. Hewlett Packard.

Electronic Voltmeter: Bruel and Kjoer Model, 2409.

Random Noise Generator: G.R. Company. Type 1390B

General Purpose Amplifier: Hewlett Packard.

L.P.Filter: G.R. Company. Type 830E

Pulse Generator: Philips Ltd. Type 5720.

B I B L I O G R A P H Y

1. Deist. F. and R. Kitai: Digital transfer Voltmeters: Principles and error characteristics. Proc. I.E.E. Vol. 110, No.10 October 1963.
 2. Braithwaite D: Ultra low-frequency digital analyser: Design and construction. M.Eng. Thesis McMaster University 1967.
 3. Digital Equipment Corporation: Digital Logic Handbook 1967 Edition.
 4. Schwartz M: Information Transmission, Modulation and Noise. Page. 338 - 449.
 5. Van der Ziel A: Noise. 1954 Prentice Hall. Page. 340
 6. Wax N: Selected papers on noise and stochastic processes. Dover Press.
 7. Terman F & Petit: Electronic Measurements. Page. 9 - 30.
 8. Sutcliffe H: Noise-spectrum measurement at subaudio frequencies. Proc. I.E.E. Vol. 112, No. 2. February 1965.
-